

UCSF

UC San Francisco Electronic Theses and Dissertations

Title

Rhythmic Action Synchronizes Memory Replay During Reinforcement Learning

Permalink

<https://escholarship.org/uc/item/10s205q3>

Author

Roumis, Demetris

Publication Date

2020

Peer reviewed|Thesis/dissertation

Rhythmic Action Synchronizes Memory Replay During Reinforcement Learning

by
Demetris Roumis

DISSERTATION

Submitted in partial satisfaction of the requirements for degree of
DOCTOR OF PHILOSOPHY

in

Neuroscience

in the

GRADUATE DIVISION

of the

UNIVERSITY OF CALIFORNIA, SAN FRANCISCO

Approved:

DocuSigned by:

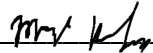


99D647545A30488...

Christoph Schreiner, MD, PhD

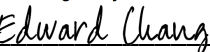
Chair

DocuSigned by:



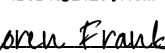
DocuSigned by:33...

Mazen Kheirbek



DocuSigned by:15...

Edward Chang



EF21CD5A6EE643A...

Loren Frank

Committee Members

Copyright 2020
by
Demetris Konstantinos Roumis

To my family

ACKNOWLEDGMENTS

Funding to support for this work was provided by the NIMH F31 Ruth L. Kirschstein National Research Service Award, UCSF Neuroscience Program, and Howard Hughes Medical Institute.

I would first like to express my gratitude to Dr. Loren Frank, my scientific advisor, for his continuous optimism, patience, and support of my research. I would also like to thank Christoph Schreiner, Mazen Khierbek, Michael Stryker, Phillip Sabes, and Edward Chang for their useful criticism and assistance along the way. My deep appreciation goes to all the current and former lab mates and collaborators from whom I've had the privilege to learn. Finally, I wish to thank my family and friends for their unwavering selfless encouragement.

“imagination is a necessary ingredient of perception itself”

- Immanuel Kant

Critique of Pure Reason A120

CONTRIBUTIONS

Anna Gillespie, Eric Denovellis, and David Kastner contributed data and results in the validation of technology development presented in **Fig. 2.1 [A-B]**.

Appendix A is reprinted largely as it appears in:

Roumis, D. K., & Frank, L. M. (2015). Hippocampal sharp-wave ripples in waking and sleeping states. *Curr Opin Neurobiol*, 35, 6-12. doi:10.1016/j.conb.2015.05.001

Rhythmic Action Synchronizes Memory Replay During Reinforcement Learning

Demetris Roumis

ABSTRACT

Our cognitive abilities - learning from the past, sensing the current environment, planning into the future, executing an action, and infusing value into an experience - all rely on precisely timed and widespread electrical communications across neural networks. The brain's hippocampal formation receives multimodal input, forges episodic associations, and predicts future state. Oscillating electrical bursts originating from the hippocampus, termed 'sharp-wave ripples' (**SWR**), often contain patterns of previously expressed neural spike sequences, and are necessary for certain forms of learning and memory. The discharge of SWR-replay resonates in remote parts of the brain and displays specific characteristics depending on a subject's state of awareness and sensory context. In the sleep state, when motoric repertoire is limited, waves of breathing synchronize neural activity in several regions of the brain, including SWRs of the hippocampus. During active sensation of the awake state, cyclic licking dynamically entrains taste-reward networks in subcortical and cortical areas throughout learning. However, the neural correlates linking oromotor movements in the active learning state to the memory system of the hippocampal formation have not yet been established. Given the recurrence of SWR-replay during rhythmic ingestion of reinforcement learning and the hierarchical coupling of orofacial behaviors, we hypothesized that repeated licking could provide the oscillatory framework to synchronize memory reactivation during active learning. We approach this question with new technology development to track licking events at a reward port (**P-event**) during behavior on a spatial alternation task. Additionally, we developed a modular brain implant to simultaneously record from hippocampal

area **CA1** and medial entorhinal cortex (**MEC**) - interconnected brain regions that are crucial to episodic memory processing. Along with the co-modulation of individual neurons by licking and SWRs, we provide the first evidence that SWRs detected in dorsal CA1 synchronize with the phase of P-event cycle during learning. Furthermore, we confirmed that SWRs occurring during licking bouts contain neural reactivation of active navigation and trigger enhanced ripple-frequency power in downstream MEC. These results connect movement with memory and may assist in addressing abnormal ingestion behaviors that negatively affect mental or physical health.

TABLE OF CONTENTS

INTRODUCTION.....	1
<i>References.....</i>	<i>5</i>
CHAPTER 1 : NEURAL REACTIVATION IS ENTRAINED WITH RHYTHMIC MOVEMENT	8
1.1 <i>Abstract.....</i>	<i>9</i>
1.2 <i>Introduction</i>	<i>10</i>
1.3 <i>Results</i>	<i>12</i>
1.4 <i>Discussion.....</i>	<i>17</i>
1.6 <i>Materials and Methods.....</i>	<i>23</i>
1.5 <i>Figures</i>	<i>31</i>
1.7 <i>Supplemental Figures.....</i>	<i>39</i>
1.8 <i>References.....</i>	<i>40</i>
CHAPTER 2 : MODULAR TOOLBOX FOR BEHAVIORAL ELECTROPHYSIOLOGY	50
2.1 <i>Abstract.....</i>	<i>51</i>
2.2 <i>Introduction</i>	<i>52</i>
2.3 <i>Results</i>	<i>54</i>
2.4 <i>Microdrive brain implant for chronic extracellular recordings in freely moving animals.....</i>	<i>55</i>
2.5 <i>Environmental Monitoring and Behavioral Control</i>	<i>64</i>
2.6 <i>Discussion.....</i>	<i>68</i>
2.7 <i>Figures</i>	<i>70</i>
2.8 <i>References.....</i>	<i>77</i>
CHAPTER 3 : CONCLUSION AND DISCUSSION	78
3.1. <i>Significance of Memory Reactivation Synchronization with Rhythmic Movement</i>	<i>79</i>
3.2 <i>Reafference and Corollary Discharge Underlying Replay-Movement Synchrony.....</i>	<i>81</i>
3.3 <i>Active sensing is associated with effective processing.....</i>	<i>83</i>
3.4 <i>Speculative Role of Synchrony Between Oromotor Phase and Memory Reactivation</i>	<i>84</i>
3.5 <i>References.....</i>	<i>86</i>

APPENDIX : HIPPOCAMPAL SHARP-WAVE RIPPLES IN WAKING AND SLEEPING STATES	92
<i>Abstract.....</i>	<i>93</i>
<i>Introduction</i>	<i>94</i>
<i>The Role of Awake SWR Replay.....</i>	<i>95</i>
<i>The Role of Sleep SWR Replay.....</i>	<i>97</i>
<i>The Fidelity of Replay</i>	<i>98</i>
<i>A Role for 'Noisy' Replay</i>	<i>100</i>
<i>Conclusion</i>	<i>101</i>
<i>Figures</i>	<i>103</i>
<i>References.....</i>	<i>105</i>

LIST OF FIGURES

Chapter 1

Figure 1.1 Spatial alternation task on the W-maze	31
Figure 1.2 Port-Crossings Capture a Consistent Phase of Movement During Lick Bursts	32
Figure 1.3 Electrophysiological and histological validation of recording sites.....	33
Figure 1.4 Rhythmic Bursts of Licking Entrain Sharp-Wave Ripple Events	34
Figure 1.5 Rhythmic Bursts of Licking Entrain Neural Reactivation.....	35
Figure 1.6 Licking modulates neural activity in the hippocampal formation	36
Figure 1.7 CA1 units co-modulated by sharp-wave ripple and port entry events.....	37
Figure 1.8 SWR-Triggered Ripple Power in MEC During Licking Bouts.....	38
Supplemental Figure 1.1 Behavioral Performance on W-task	39

Chapter 2

Figure 2.1 Validation of Microdrive Implant.....	70
Figure 2.2 Fabrication of the N-Trode Drive.....	71
Figure 2.3 Modular Guide-Cannula.....	72
Figure 2.4 Populating Electrode Interface Boards	73
Figure 2.5 Microdrive Assembly.....	74
Figure 2.6 Position tracking diode array	75
Figure 2.7 Entry Detection and Reward Delivery Port	76

Appendix

Figure A.1 SWR Reactivation of Spatial Sequences	103
Figure A.2 The quality of SWR replay of remote task trajectories is higher during awake than quiescent periods.....	104

INTRODUCTION

Association Formation in the Hippocampus

The hippocampal formation is essential for all aspects of spatial memory, including encoding, consolidation, and retrieval ([O'Keefe & Nadel, 1978](#); [Riedel et al., 1999](#)). Hippocampal pyramidal neurons that are active during a given experience are often referred to as 'place cells' because they get excited in a location-dependent manner - preferring specific 'place fields' as animals explore space. Plasticity mechanisms associate cells that have overlapping place fields, enhancing spatially continuous coactivity patterns during locomotion that remain heightened following navigation ([O'Neill, Senior, Allen, Huxter, & Csicsvari, 2008](#)). This post-experience reactivation of spatiotemporal trajectories may serve memory retrieval and consolidation by orchestrating the global reprocessing of episodic experience.

Sharp-Wave Ripple Reactivation

Sequences of simultaneously recorded place cells, whose collective place field assemblies reflect trajectories through space, are often reactivated in a time-compressed cascade during a hippocampal sharp-wave ripple (**SWR**). SWR events are brief (50–200 ms), high-frequency (150–250 Hz) fluctuations detected in local field potential (**LFP**), and most often occur during a pause in locomotion or slow-wave sleep. The timescale of SWRs aligns with the optimal window for inducing synaptic plasticity and, therefore, could influence the synaptic weights between coactive or induced activity patterns ([Buzsaki, 1989](#); [Marr, 1971](#)).

Respiration-locked oscillations entrain Sharp-Wave Ripples

Neural activity paced by high-frequency oscillations can spontaneously become nested in the phase of slow oscillations, potentially facilitating long-range communication of time-compressed

sequences, ([Hyafil, Giraud, Fontolan, & Gutkin, 2015](#)). Evidence from rodents ([Ito, 2014](#); [Y. Liu, McAfee, & Heck, 2017](#)) and humans ([Zelano, 2016](#)) support the notion that the slow phase of respiration provides an oscillatory scaffold to modulate the power of faster cognitive oscillations. These studies also provide evidence that such cross-frequency coupling can affect memory performance through a dual mechanism of respiratory entrainment by both olfactory input and brainstem output ([Fontanini & Bower, 2006](#)).

The brainstem's rhythmogenic preBötzinger Complex is an essential element producing the periodic drive for coupled orofacial behaviors ([Del Negro, Funk, & Feldman, 2018](#)). Many preBötzinger Complex targets discharge in phase with respiration. They could influence plasticity and SWR occurrence across the hippocampal network ([Hansen, 2017](#)), such as locus coeruleus ([Yackle, 2017](#)), thalamus ([Chen, Eldridge, & Wagner, 1992](#)), and basal forebrain ([Manns, Alonso, & Jones, 2003](#)). Indeed, the hippocampus exhibits respiration-locked oscillations ([Lockmann, Laplagne, Leao, & Tort, 2016](#); [Nguyen Chi, 2016](#); [Yanovsky, Ciatipis, Draguhn, Tort, & Brankack, 2014](#)), which could similarly be regulated by medial septum's disinhibitory pacing of the hippocampal-entorhinal network during periods of prominent theta oscillations. Additionally, a recent study found evidence that a corollary discharge from the brainstem can entrain SWR occurrence in sleep ([Karalis & Sirota, 2018](#)). However, there has been no research that has examined whether such SWR entrainment by oromotor behaviors applies in the awake, freely behaving animal, where the sensorimotor contextual complexity is higher and often coincides with reward signals.

Licking Induces Widespread Synchronization of Taste-Reward Network Over Learning

For a rat performing a reinforcement-based spatial memory task, like the one presented in this dissertation, rhythmic licking action coincides with positive valence reward signal and SWRs, which often contains reactivation of preceding experience. For awake rodents, licking shares a

similar frequency range (4-12 Hz) ([Travers, Dinardo, & Karimnamazi, 1997](#)) with other active sampling behaviors, including sniffing ([Kepecs, 2005](#)), visual saccades ([Kozma & Freeman, 2001](#)), and whisking ([Fanselow & Nicolelis, 1999](#)). Although substantially less focus has been given to licking, both sniffing and whisking have been shown to segment continuous sensory input into temporally discrete frames and synchronize activity across multiple regions in the brain ([Kleinfeld, Ahissar, & Diamond, 2006](#); [Nicolelis, Baccala, Lin, & Chapin, 1995](#)).

In one study connecting licking coherence and learning, Gutierrez and colleagues found that a population of neurons in the orbitofrontal cortex, insular cortex, amygdala, and nucleus accumbens tracked the oromotor rhythm of licking behavior, and showed synchronized spiking between neuron pairs from different regions ([Ranier Gutierrez, Simon, & Nicolelis, 2010](#)). Interestingly, the lick-synchronized neurons contained more information discriminating different tastants, a result that increased along with learning and performance. These results are in line with other findings of licking entrainment across several parts of the gustatory brain network, and altogether position rhythmic orofacial behavior as a global neural pacemaker ([Fonseca, de Lafuente, Simon, & Gutierrez, 2018](#); [Ranier Gutierrez & Simon, 2011](#); [Roussin, D'Agostino, Fooden, Victor, & Di Lorenzo, 2012](#); [Stapleton, MI, RI, Ma, & S.A, 2006](#)). This evidence implicates lick-spike coherence in the gating of feed-forward sensory input and motivates our investigation of orofacial synchronization in the feed-back memory system.

Overview of Dissertation

In this dissertation, I address oromotor influence on memory processing. To our knowledge, there has not been a link between voluntary motor movement and the occurrence of SWR-replay in the awake, learning state. In chapter 1, we show that a significant portion of single-unit activity in the hippocampal area **CA1** and medial entorhinal cortex (**MEC**) is synchronized with the licking cycle. Next, we show that SWR occurrence displays a licking phase preference, and that intra-licking

bout SWRs reactivate neural ensembles from locomotive periods. Finally, we show that the ripple-band power in MEC is enhanced at the time of hippocampal SWRs that occur during licking bouts, as compared to SWRs that arise outside of licking bouts. We believe this is the first report linking neural reactivation to rhythmic oromotor behavior in the context of learning. These findings fill a gap in knowledge that was primarily due to the technical challenges of simultaneously recording from MEC and CA1 from a freely moving animal learning a memory task. To accomplish this strategy, we designed a modular brain implant for dual-site neural recording, and a reward port with integrated sensors that monitored orofacial movement, as described in the second chapter., In Chapter 3, I discuss the significance of these findings. In the Appendix, we highlight the importance of sleep and awake state memory reactivation. Altogether, our results enhance our understanding of movement's impact on memory processing during reward-based learning.

References

- Buzsaki, G. (1989). Two-stage model of memory trace formation: a role for "noisy" brain states. *Neuroscience*, 31(3), 551-570.
- Chen, Z., Eldridge, F. L., & Wagner, P. G. (1992). Respiratory-associated thalamic activity is related to level of respiratory drive. *Respiration physiology*, 90(1), 99-113.
- Del Negro, C. A., Funk, G. D., & Feldman, J. L. (2018). Breathing matters. *Nature Reviews Neuroscience*, 19, 351-367.
- Fanselow, E. E., & Nicolelis, M. A. (1999). Behavioral modulation of tactile responses in the rat somatosensory system. *J Neurosci*, 19(17), 7603-7616.
- Fonseca, E., de Lafuente, V., Simon, S. A., & Gutierrez, R. (2018). Sucrose intensity coding and decision-making in rat gustatory cortices. *Elife*, 7, e41152.
- Fontanini, A., & Bower, J. M. (2006). Slow-waves in the olfactory system: an olfactory perspective on cortical rhythms. *Trends in Neurosciences*, 29, 429-437.
- Gutierrez, R., & Simon, S. A. (2011). Chemosensory processing in the taste-reward pathway. 26(4), 231-238. doi:10.1002/ffj.2050
- Gutierrez, R., Simon, S. A., & Nicolelis, M. A. (2010). Licking-induced synchrony in the taste-reward circuit improves cue discrimination during learning. *Journal of Neuroscience*, 30(1), 287-303.
- Hansen, N. (2017). The longevity of hippocampus-dependent memory is orchestrated by the locus coeruleus-noradrenergic system. *Neural Plast*, 2017, 2727602.
- Hyafil, A., Giraud, A. L., Fontolan, L., & Gutkin, B. (2015). Neural cross-frequency coupling: connecting architectures, mechanisms, and functions. *Trends Neurosci*, 38, 725-740.
- Ito, J. (2014). Whisker barrel cortex delta oscillations and gamma power in the awake mouse are linked to respiration. *Nature communications*, 5(3572).

- Karalis, N., & Sirota, A. (2018). Breathing coordinates limbic network dynamics underlying memory consolidation. *bioRxiv*, 392530. doi:10.1101/392530
- Kepecs, A. (2005). The Sniff as a Unit of Olfactory Processing. *31*(2), 167-179.
doi:10.1093/chemse/bjj016
- Kleinfeld, D., Ahissar, E., & Diamond, M. E. (2006). Active sensation: insights from the rodent vibrissa sensorimotor system. *Curr Opin Neurobiol*, *16*(4), 435-444. doi:10.1016/j.conb.2006.06.009
- Kozma, R., & Freeman, W. (2001). *Analysis of visual theta rhythm-experimental and theoretical evidence of visual sniffing*. Paper presented at the IJCNN'01. International Joint Conference on Neural Networks. Proceedings (Cat. No. 01CH37222).
- Liu, Y., McAfee, S. S., & Heck, D. H. (2017). Hippocampal sharp-wave ripples in awake mice are entrained by respiration. *Sci Rep*, *7*(1), 8950. doi:10.1038/s41598-017-09511-8
- Lockmann, A. L., Laplagne, D. A., Leao, R. N., & Tort, A. B. (2016). A Respiration-Coupled Rhythm in the Rat Hippocampus Independent of Theta and Slow Oscillations. *J Neurosci*, *36*(19), 5338-5352.
doi:10.1523/JNEUROSCI.3452-15.2016
- Manns, I. D., Alonso, A., & Jones, B. E. (2003). Rhythmically discharging basal forebrain units comprise cholinergic, GABAergic, and putative glutamatergic cells. *J Neurophysiol*, *89*(2), 1057-1066.
- Marr, D. (1971). Simple memory: a theory for archicortex. *Philos Trans R Soc Lond B Biol Sci*, *262*(841), 23-81.
- Nguyen Chi, V. (2016). Hippocampal respiration-driven rhythm distinct from theta Oscillations in awake mice. *Journal of Neuroscience*, *36*, 162-177.
- Nicolelis, M. A., Baccala, L. A., Lin, R., & Chapin, J. K. (1995). Sensorimotor encoding by synchronous neural ensemble activity at multiple levels of the somatosensory system. *Science*, *268*(5215), 1353-1358.
- O'Keefe, J., & Nadel, L. (1978). *The hippocampus as a cognitive map*. London: Oxford University Press.

- O'Neill, J., Senior, T. J., Allen, K., Huxter, J. R., & Csicsvari, J. (2008). Reactivation of experience-dependent cell assembly patterns in the hippocampus. *Nat Neurosci*, *11*(2), 209-215.
doi:10.1038/nn2037
- Riedel, G., Micheau, J., Lam, A. G., Roloff, E. L., Martin, S. J., Bridge, H., . . . Morris, R. G. (1999). Reversible neural inactivation reveals hippocampal participation in several memory processes. *Nat. Neurosci*, *2*(10), 898-905.
- Roussin, A. T., D'Agostino, A. E., Fooden, A. M., Victor, J. D., & Di Lorenzo, P. M. (2012). Taste Coding in the Nucleus of the Solitary Tract of the Awake, Freely Licking Rat. *J Neurosci*, *32*(31), 10494-10506.
doi:10.1523/jneurosci.1856-12.2012
- Stapleton, J. R. L., MI, W., RI, N., Ma, S., & S.A. (2006). Rapid taste responses in the gustatory cortex during licking. *J Neurosci*, *26*, 4126-4138.
- Travers, J. B., Dinardo, L. A., & Karimnamazi, H. (1997). Motor and premotor mechanisms of licking. *Neuroscience & Biobehavioral Reviews*, *21*(5), 631-647.
- Yackle, K. (2017). Breathing control center neurons that promote arousal in mice. *Science*, *355*, 1411-1415.
- Yanovsky, Y., Ciatipis, M., Draguhn, A., Tort, A. B., & Brankack, J. (2014). Slow oscillations in the mouse hippocampus entrained by nasal respiration. *J Neurosci*, *34*(17), 5949-5964.
doi:10.1523/JNEUROSCI.5287-13.2014
- Zelano, C. (2016). Nasal respiration entrains human limbic oscillations and modulates cognitive function. *Journal of Neuroscience*, *36*, 12448-12467.

Chapter 1 : Neural Reactivation is Entrained with Rhythmic Movement

1.1 Abstract

Cognition relies on precisely orchestrated electrical communication across the central nervous system. The brain's hippocampal formation receives multimodal sensory input, forges episodic associations, and forms a prediction of future state. Oscillating electrical bursts originating from the hippocampus, called sharp-wave ripples, emit patterns of previously expressed neural spike sequences, and are necessary for formation and expression of certain forms of memory. Although theta oscillations have been shown to regulate global communication during locomotion, little is known about the behavioral regulation of neural reactivation during reward ingestion period of reinforcement learning. We hypothesized that repeated licking during a period of learning could provide the oscillatory framework to synchronize neural reactivation. We approach this question by tracking licking events at a reward port during learning of a spatial alternation task, while simultaneously recording from interconnected brain regions that are crucial to episodic memory processing - hippocampal area CA1 and medial entorhinal cortex. Along with co-modulation of individual neurons by licking and sharp-wave ripples, we discovered that neural reactivation is synchronized with licking phase. By demonstrating that bursts of mnemonic information across the hippocampal formation are aligned with rhythmic licking signals, these results advance our understanding of the interaction between internal reactivation and externalized rhythmic activity.

1.2 Introduction

When an animal is locomoting, theta oscillations (4-12 Hz) in the hippocampus discretize place-selective neural sequences that precess in phase from one cycle to the next ([Burgess & O'Keefe, 2011](#); [J. O'Keefe, 1971](#); [O'Keefe & Recce, 1993](#)) while coordinating activity with extrahippocampal structures such as entorhinal and prefrontal cortex ([Buzsaki, 2002](#); [Fernandez-Ruiz et al., 2017](#); [Mizuseki, Sirota, Pastalkova, & Buzsaki, 2009](#)) ([Benchenane et al., 2010](#); [Siapas, Lubenov, & Wilson, 2005](#)). As locomotion halts, our memory and planning system irregularly emits a high-frequency (150-250 Hz) burst, termed 'sharp-wave ripple' (SWR), that permeates remote regions of the brain with spike patterns representing a trajectory of the past or possible future ([Axmacher, Elger, & Fell, 2008](#); [Yunzhe Liu, Dolan, Kurth-Nelson, & Behrens, 2019](#); [Logothetis, 2012](#); [Roumis & Frank, 2015](#); [Vaz, Wittig, Inati, & Zaghloul, 2020](#)). ([Buzsaki, 2015](#); [Wilson & McNaughton, 1993, 1994](#)).

The mechanism of phase coupling has been proposed to facilitate long-term plasticity, working memory, and coherence of brain communication ([Axmacher et al., 2010](#); [Hyafil et al., 2015](#); [Zheng & Zhang, 2015](#)). In different states of awareness, SWR occurrence can be phase-locked to near theta-range oscillations, such as centrifugal 'spindle' oscillations (~10Hz) in sleep ([Siapas & Wilson, 1998](#)) which correlate with cortical dendritic activity resulting in long-term modification of synaptic efficacy ([Geva-Sagiv & Nir, 2019](#); [Seibt et al., 2017](#)), as well as phasic respiration (2-4 Hz) in both sleep and head-fixed awake states ([Karalis & Sirota, 2018](#); [Y. Liu et al., 2017](#); [Molle & Benoit, 2019](#)).

The rhythmogenic brainstem that paces breathing also orchestrates other orofacial actions like sniffing, whisking, and licking ([Del Negro et al., 2018](#); [Jeffrey D Moore, Kleinfeld, & Wang, 2014](#); [Welzl & Bureš, 1977](#); [Yackle, 2017](#)). The commencement of cyclic licking triggers a transient surge in neuromodulatory discharge ([Coddington & Dudman, 2018](#)), and for rodents engaged in learning, this chemically catalyzed period is coincident with outcome discovery following reward-seeking behavior. In this context, the movement associated with reward ingestion is often overlooked and mischaracterized as ‘immobility,’ but the oromotor system remains mobile and cyclic within the range of locomotive theta. Strikingly, over the course of learning to discriminate sensory cues, cyclic licking sharpens spike-timing precision and entrains neural activity across the brain’s taste-reward network ([Ranier Gutierrez et al., 2010](#)). This taste-reward network includes the amygdala which regulates information exchange at the rhinal interface of the hippocampus and neocortex ([Paz, Pelletier, Bauer, & Pare, 2006](#)), along with the nucleus accumbens, of whose direct connections with the hippocampus are required for successful recall of spatial-reward associations ([Trouche et al., 2019](#)).

Although concerted sensorimotor inputs can affect the phase of hippocampal theta and facilitate association encoding ([Arshamian, Iravani, Majid, & Lundstrom, 2018](#); [Fell & Axmacher, 2011](#); [Jutras, Fries, & Buffalo, 2013](#); [Zelano, 2016](#)), the coordination of licking during reinforcement learning with hippocampal SWR replay has remained unknown. Here we address the hypothesis of rhythmic licking entrainment of memory reactivation. To this end, we simultaneously record neural ensembles in hippocampal area CA1 and medial entorhinal cortex (MEC), along with detection of reward port entry events (P-events). We identified a phasic coupling between SWR reactivation and cyclic reward ingestion. Rhythmic licking is may therefore act as a facilitator of synchrony between movement, memory, and reward systems.

1.3 Results

Memory-guided spatial learning

Commonly, spatial memory testing registers an animal's response through entry into a limited set of specific locations, motivated by their natural appetitive behavior. To investigate the role of licking in organizing neuronal dynamics in CA1 and MEC, we engaged rats in a reinforcement learning hippocampal-dependent paradigm ([Kim & Frank, 2009](#))([L. M. Frank, E. N. Brown, & M. Wilson, 2000a](#)) that elicits behaviorally relevant changes in the hippocampal-entorhinal network ([Carr, Jadhav, & Frank, 2011](#); [Frank et al., 2000a](#); [Karlsson & Frank, 2009](#); [Kay et al., 2016](#); [Singer & Frank, 2009](#)). In this paradigm, animals learn through trial and error to navigate in a specific sequence to three reward-ports positioned at the ends of a “W”-shaped spatial alternation task (W-task) (**Fig. 1.1 [A-B]**). The rewarded sequence is a visit to the center port, followed by a visit to the less recently visited outer port (**Fig. 1.1[A]**). On visits to a port that deviates from this sequence, food was simply withheld so that the only cue the animals had of an incorrect outcome was the absence of reward delivery. In extension to the W-task paradigm, the animals foraged for scattered food during “open-field” epochs (**Fig. 1.1 [B]**). Following a period of learning, subject performance became stable (**Fig. 1.1 [C]**, **Fig. S1.1 [B]**).

Capturing cyclical licking movement

To detect port penetration events (**P-events**) and control reinforcement, we designed a device encasing an infrared photosensor with a liquid delivery system that was used to discharge sweetened evaporated milk in a flow constrained by the narrow trough access point cross-section (**Fig. 1.2 [A-C]**). We sought to test that P-events detected by this device could signal a specific phase of the head movement during cycles of licking bouts. We video-recorded from a camera

positioned to capture a close-up perspective on animal behavior at a reward port (**Fig. 1.2 [D]**). We selected five head features (eye, ear, nose, tongue, and jaw), then trained and applied a model to accurately reconstruct their position over time (**Fig. 1.2 [E]**, see Methods). We then derived the primary oscillatory phase of each tracked feature and tested for the head-movement phase-consistency of P-events. We found that the P-events were tightly clustered by the feature movement phase and captured the vast majority of visually confirmed movement cycles. These results established that P-events could be used as an indicator of a lick movement phase.

Recording neural activity from CA1 and MEC in freely behaving

Next, we set out to record electrophysiologically from individual neurons expressing activity patterns associated with memory processing. To this end, we designed a microdrive array of independently moving electrode bundles (**n-trodes**) coupled with a modular guide-cannula that had been adapted for the specific brain regions of interest. After pretraining, we implanted several subjects using this chronic microdrive assembly (**Fig. 1.3 [A]**). Following recovery and n-trode positioning, we recorded from CA1 and MEC as animals performed for several days on the memory task paradigm (**Fig. 1.1 [A-B]**). Recording locations of n-trodes directed at CA1 and MEC were histologically verified (**Fig 1.3 [B-E]**), along with the reference electrodes in corpus callosum.

Sharp wave ripples are synchronized with orofacial movement phase

Given previous observations of phase-locking between breathing and the occurrence of SWRs, and the coupling of breathing with licking, we hypothesized that SWR onset during licking bouts would be coordinated with the licking movement phase. We first examined the onset timing of SWR events, detected as brief bursts in ripple-band (**Fig. 1.4 [A-B]**), relative to the timing of, and phase between, P-events. We found phase preference for SWR events, with the mean resultant

vector angle of the preferred phase relatively consistent across animals (**Fig. 1.4 [C]**). Further confirming this periodic coupling, we found significant non-uniformity in the cross-correlation of the two events (**Fig. 1.4 [D]**). Additionally, we confirmed that this phase-locking exists across consecutive sessions (**Fig. 1.4 [E-F]**). For the first time, these results provide evidence that sensorimotor activity of freely moving animals could provide the oscillatory scaffold for population processing of memory.

Memory reactivation during licking bouts selectively occurs with SWRs

We next asked whether the detected SWR events during licking bouts indeed contained reactivation of neural spike patterns. Previous studies investigating breathing and SWRs did not confirm whether the detected SWR events contained replayed population activity patterns, as only a portion of SWR events coincides with reactivation. To address this, we computed the similarity of spike patterns in each moment during reward ingestion to the patterns observed while the animal was actively navigating through space ($> 4\text{cm/s}$; see Methods). Our method is based on previous work showing reactivation of awake experience during SWRs ([Peyrache, Khamassi, Benchenane, Wiener, & Battaglia, 2009b](#); [Rothschild, Eban, & Frank, 2017](#)). We found that the reactivation measure increased coincident with awake state intra-licking bout and extra-licking bout SWRs, but not during licking bouts in the absence of SWRs (**Fig. 1.5 [A, C, E]**). Additionally, since replayed patterns can consist of several spatial motifs, we computed this reactivation measure for the first few principal components of the population activity (see Methods). We found a consistent enhancement of reactivation for only SWR-times (**Fig. 1.5 [B, D, F]**). These results demonstrate that structured neural patterns reactivate during SWRs that occur within licking bout periods.

Lick-modulation of single-unit activity in CA1 and MEC

Having found evidence for neural activity pattern reactivation, we next investigated the nature of the underlying P-event cycle phase preference of single units. We sorted clips of neural action potential waveforms (see Methods) and analyzed spiking per putative single-unit (**Fig 1.6 [A]**). To determine whether single-units were modulated by the phase of head movement during licking bursts, we measured the phase clustering of spike timing relative to the proportion of time elapsed between P-events. We found that 40% of CA1 units and MEC units showed significant phase modulation, compared to a phase-shuffled distribution (**Fig 1.6 [E, I]**). Notably, significantly P-event phase-entrained neurons were found at all P-cycle angles (**Fig 1.6 [B-D, F-H]**). The fraction of modulated cells was significantly larger than was expected by pure chance, demonstrating a diverse and widespread synchronization of individual units to an awake orofacial behavior expressed during a learning task.

Co-modulation of single CA1 units by port entry events and sharp-wave ripples

A remaining question is whether the units that participate in SWR events are also modulated directly by the licking phase, and how this co-modulation is manifested during coincident events. As populations of neurons in the hippocampal formation have been found with multiplexed encoding of spatial and contextual features ([L. M. Frank, E. N. Brown, & M. A. Wilson, 2000b](#); [Hardcastle, Maheswaranathan, Ganguli, & Giocomo, 2017](#); [Salz et al., 2016](#)), and because previously examined regions in the taste-reward network have shown both tuned to specific sensory cues and to oromotor behavior ([Ranier Gutierrez et al., 2010](#)), we predicted that licking-tuned cells were also engaged by SWRs. To this end, we examined spike rasters and peri-event time histogram, aligning the spike timing relative to P-events and SWRs. We found that many P-

event modulated CA1 neurons were also SWR-modulated (**Fig1.7 [A-H]**). These results demonstrate a layered encoding of sensorimotor and memory-related information.

SWRs during licking-bouts trigger ripple-power enhancement in downstream MEC

Sharp-wave ripples containing packets of sequence replay originate in the hippocampus ([Buzsaki, 2015](#)) and propagate to connected brain regions. As the anatomically densest input and output target of the hippocampus, the entorhinal cortex is best positioned to examine the inter-areal communication with the hippocampus. Since the licking movement entrains neural activity in each individual region (**Fig 1.6**), we sought to investigate the relative strength of inter-regional communication across conditions within and outside of licking-bouts. We first assessed the patterned synaptic input to each location through the examination of the local field potential (**LFP**) (1-400 Hz). We created complex-morlet wavelets to transform the LFP time-series into a time and frequency indexed signal (**Fig 1.8**). Aligned to all P-events, we found an ~8 Hz fluctuation across many frequency bands in both CA1 and MEC, indicative of widespread synchronization of synaptic activation during licking bouts (**Fig. 1.8 [A, D]**). Next, we examined the power in the ripple-band in MEC and CA1 during the time of SWRs that occurred either during to licking bouts (intra-P-event; **Fig. 1.8 [C, F]**) and those that did not occur near in time to any licking (extra P-event; **Fig. 1.8 [B, E]**). We found that CA1-SWR times during licking bouts had enhanced ripple-band power in MEC, along with an enhancement in the ~8Hz range that continued beyond the SWR event (**Fig 1.8 [F]**). These results suggest that the licking action could facilitate replay information across brain regions, and perhaps facilitate sequences of concurrent SWR events ([Davidson, Kloosterman, & Wilson, 2009](#)), which has been shown to enhance learning ([Fernandez-Ruiz et al., 2019](#)).

1.4 Discussion

Understanding how oromotor activity interacts with memory replay is critical to our knowledge of how the internal state interacts with externalized behavior. In the present investigation, we identified that hippocampal SWR-replay during learning was phase-locked to the licking cycle. Our findings demonstrate that orofacial rhythmic movement can provide an oscillatory scaffold for neural activity amid active memory processing. The results also confirm that SWRs occurring during licking bouts contain reactivated sequences and may trigger enhanced ripple-band activity in MEC. These findings establish that endogenously emanating memory replay is gated by externally manifested sensorimotor inputs and sets the stage for further testing of the embodied affordances on constructive mnemonics that are vital to the sustenance of the subject.

Single-unit activity in CA1 and MEC is modulated by the phase of licking and SWRs

Licking-modulated neural activity in different brain regions has previously been identified ([Ranier Gutierrez et al., 2010](#)) including the insular cortex which is involved in interoception ([Accolla & Carleton, 2008](#); [Katz, Simon, & Nicolelis, 2001](#); [Livneh et al., 2020](#)) and the reward-action network consisting of the orbitofrontal cortex ([E. T. Rolls, 2007](#); [Tremblay & Schultz, 1999](#)), amygdala ([Pecina & Berridge, 2005](#); [Schoenbaum, Chiba, & Gallagher, 1998](#)), and nucleus accumbens ([Mogenson, Jones, & Yim, 1980](#)). To this picture, we add that individual neurons in area CA1 and MEC were modulated by the phase of licking. The distribution of preferred phases for individual units spanned the licking cycle, indicating a diverse responsivity to the sensorimotor input. We speculate that this diversity of phase preference is indicative of a traveling wave of activation or reflective of the multiplicity of anatomical pathways, leading to timing delays or sign changes between the orofacial source and hippocampal formation. The diversity of lick phase tuning that we observe is consistent with the heterogeneity of lick phase profiles of observed within other

limbic structures ([Ranier Gutierrez et al., 2010](#)). We also found that the engagement of unit activity by SWRs and by licking was multiplexed within a subpopulation of neurons. This demonstrated a direct integration of feed-back and feed-forward processes and confirms that the underlying components engaged during SWRs are also synchronized with the taste-reward network ([Ranier Gutierrez et al., 2010](#)).

SWR reactivation during reinforcement learning is entrained to cyclic ingestion of reward

Previous studies have shown learning-related lick-entrainment of sensorimotor regions that receive hippocampal projections ([Ranier Gutierrez et al., 2010](#)), the coupling of licking with breathing ([Welzl & Bureš, 1977](#)), and entrainment of SWRs to breathing in sleep and head-fixed awake states ([Karalis & Sirota, 2018](#); [Y. Liu et al., 2017](#)). Our findings extend these results in several important ways. First, the demonstration of licking-entrainment of SWRs presents a candidate mechanism for the dynamics of gustatory spike-timing lick-entrainment over learning and behavioral states ([Ranier Gutierrez et al., 2010](#)). Second, previous investigations ([Karalis & Sirota, 2018](#); [Y. Liu et al., 2017](#)) linking oromotor behavior to SWRs had not examined whether the detected SWRs were part of a subset which contains reactivation of active experience. Therefore, we describe novel evidence that neural ensembles expressed during locomotion are reactivated during SWRs that occurred during licking bouts, thereby establishing a link between reward-related memory and movement in reinforcement learning.

Ripple power synchronization between hippocampus and entorhinal cortex

Finally, we found that ripple-band power in MEC at the time of SWRs was enhanced for intra-licking bout SWRs. This evidence supports the notion that synchronized sensorimotor oscillation (4-12 Hz) operating at behavioral timescales may serve as a mechanism to facilitate information

transmission of higher frequency (150-250 Hz) SWR-replay packets required for practical neural computation and synaptic plasticity, thus integrating taste-reward signaling with memory processing.

Synchrony Between Oromotor Phase and Memory Reactivation

Does oromotor entrainment influence behavior that relates to hippocampal function? Recording from intracranial electroencephalogram in humans, it has been shown that local field potential in the hippocampus, amygdala, and piriform cortex are all entrained to respiration, and that performance on a memory recall task is sensitive to the phase of nasal breathing when the stimulus is initially presented ([Zelano, 2016](#)). Complementary to our claim that rhythmic licking bouts are privileged periods regarding the efficiency of reactivated information flow, these results show that in humans, the efficacy of encoding sensory stimuli is predicted by an externally identifiable phase of orofacial behavior.

Consistent with several reports of licking-related activity across the brain ([R. Gutierrez, Carmena, Nicolelis, & Simon, 2006](#); [Nishijo, Uwano, Tamura, & Ono, 1998](#); [T. Yamamoto, Matsuo, Kiyomitsu, & Kitamura, 1988](#)), a study in rodents discovered that proficiency in solving reinforcement-based associative cue learning required licking-induced synchrony across neural ensembles of the frontal cortex, insular cortex, nucleus accumbens, and amygdala ([Ranier Gutierrez et al., 2010](#)). The authors attributed the increase in spike-timing precision over learning to lick-coherency, as the cue-selective neurons that most effectively discriminated stimulus identity were most coherent with licking. Moreover, they found that lick-phase-locking was context-specific, showing that neural activity is perceptually relevant, and not merely an exhaust fume of oromotor behavior.

Neural activity across many regions have been shown to couple with hippocampal activity bursts like SWRs, including both primary and associative cortices ([R. Gutierrez et al., 2006](#); [Jadhav, Rothschild, Roumis, & Frank, 2016](#); [Peyrache, Khamassi, Benchenane, Wiener, & Battaglia, 2009a](#); [Wang & Ikemoto, 2016](#); [Wierzynski, Lubenov, Gu, & Siapas, 2009](#); [Wilber, Skelin, Wu, & McNaughton, 2017](#)) ([Ji & Wilson, 2007](#); [Rothschild et al., 2017](#); [Sirota, Csicsvari, Buhl, & Buzsaki, 2003](#)), as well as subcortical regions including ventral striatum ([Lansink et al., 2008](#)), ventral tegmental area ([Gomperts, Kloosterman, & Wilson, 2015](#)), basolateral amygdala ([Girardeau, Inema, & Buzsaki, 2017](#)), and thalamic nuclei ([Lara-Vásquez, Espinosa, Durán, Stockle, & Fuentealba, 2016](#); [Yang, Logothetis, & Eschenko, 2019](#)). It has been proposed that hippocampal SWRs are part of the update mechanism or teaching signal employed during learning that modifies the connectivity between coincident neural circuits, and we speculate that this encoding is orchestrated by active sensing.

In addition to effecting change in synaptic networks, extensive evidence exists that active sensing involving expectation and volition changes the sensory response in licking ([Mayrhofer et al., 2019](#); [Wilkins & Bernstein, 2006](#)), somatosensory ([Krupa, Wiest, Shuler, Laubach, & Nicolelis, 2004](#)), auditory ([Eliades & Wang, 2008](#)), and olfactory ([Fuentes, Aguilar, Aylwin, & Maldonado, 2008](#)) modalities. This is consistent with the increased delay of identification in experiments employing passive reward delivery via an intraoral cannula ([Katz et al., 2001](#)), compared to active sensing state ([Poulet & Petersen, 2008](#)). Additionally, evidence shows that sniffing-induced theta oscillations enhance discrimination by ensuring spike time precision in the olfactory system ([Schaefer, Angelo, Spors, & Margrie, 2006](#)). We suggest that the act of licking induces synchrony of the reward, sensorimotor, and memory systems.

Conclusions and Future Directions

Altogether our efforts represent an advancement in understanding how the orofacial movement for active sampling and reward ingestion can synchronize with mechanisms of association formation. In addition to licking being a behavior used to monitor animal models of disorders such as mental illness ([Galistu et al., 2011](#); [Hartfield, Moore, & Clifton, 2003](#); [Schepisi et al., 2014](#)) and aging ([Zhang, Bethel, Smittkamp, & Stanford, 2008](#)), our results could facilitate future work to address critical questions in compulsive consumption of diet-induced obesity, eating disorders, and alcohol ([Barkley-Levenson & Crabbe, 2012, 2015](#); [Robinson & McCool, 2015](#)) or drug addiction ([Eastwood, Barkley-Levenson, & Phillips, 2014](#)).

In the research setting, our results suggest that more considerable attention be paid to head movements during periods of reduced locomotive velocity, which are often categorized as 'immobile.' This terminology of the spatial memory-task behavioral state is used as a convenient simplification; however, given the pervasive impact on memory networks currently presented, the appropriate experimental design must be employed to avoid misinterpretation of neural activity.

Beyond experimental diligence, the evidence of enhanced learning and dopaminergic signaling during active vs. passive states of sensing ([Graham, Sun, & Hill, 2014](#); [Ranier Gutierrez et al., 2010](#); [Lutas et al., 2019](#)) motivates a tantalizing future study into the replay propensity across conditions of reward reception. Additionally, our findings do not at this time dissociate putative interneuron from principal neuron subtypes, which we believe the diversity of licking responses will be readily dissociable, given many differences, including firing rate and waveform shape ([Fox & Ranck, 1981](#)). Furthermore, a remaining question is whether the licking movement influences

hippocampal activity through sensory efference or motor efference. Lastly, higher density sampling of MEC will allow for distinguishing between superficial (layers 2/3) and deep (layers 5/6) responses, which have distinct cytoarchitecture, projection patterns, and gene expression patterns([Burgalossi, 2011](#); [Canto, Wouterlood, & Witter, 2008](#); [Kobro-Flatmoen & Witter, 2019](#); [Ramsden, Sürmeli, McDonagh, & Nolan, 2015](#); [Witter, Doan, Jacobsen, Nilssen, & Ohara, 2017](#)). Altogether, we propose that cyclic licking is well suited to support coordination of reward intake with mnemonic processing, resulting in oromotor-facilitated learning. We believe this work will facilitate the efforts to understand and address the physiological dynamics underlining adverse consumption in diet-induced obesity and eating disorders.

1.6 Materials and Methods

Subjects

All experimental procedures were conducted in accordance with guidelines from the University of California San Francisco Institutional Animal Care and Use Committee and US National Institutes of Health. Four or more animals is the minimum number of subjects established as necessary to yield sufficient statistical power in analyses common to our investigation. Data used for the present report were collected from seven Long-Evans male rats, sourced from Charles River Laboratories at weights of 400-550 g and 6-8 months of age. Experimental animals were housed with additional animals with a 12-hour light cycle and had ad libitum access to rat chow (LabDiet 5001) until the pre-training began, at which point they were single-housed, and food-restricted gradually to stabilize their weight to 85% of their baseline weight. After pretraining and surgery, animals were entered our experimental recording protocol, at which time they weighed between 500-600 g and were 9-12 months of age.

Pre-training

Subjects were food deprived to 85% of their baseline body weight, then pre-trained to spatially alternate between reward ports at the ends of a 1 m long linear track, for which they received the liquid reward (evaporated milk plus 5% sucrose). The animals quickly became familiar with the reward port dispensing mechanism, and after the animals reached consistency on this linear alternation task (~30 rewards per 5 minutes for consecutive days), they were put back on standard ad libitum rat chow access for several days before implantation.

Microdrive

Custom microdrive implants were designed (Autodesk Inventor) and constructed, with designs and instructions freely available online ([Demetris, 2017](#)). Each microdrive contained 28-30 independently moveable bundles of 4 or 8 electrodes (n-trode). The body of the microdrive was 3D-printed with PolyJetHD Blue or White (Stratasys Ltd.). A custom 3D printed protective housing encased the microdrive body, head-stage, and n-trode shuttles. The dual-site guide cannula was designed using CAD software and created using a combination of 3D printing of castable wax and metal casting to reproducibly create a modular, high-strength, high-resolution, reusable, and biocompatible stainless steel cannula. The electrode bundles were made of either gold-plated 12.7 μm nichrome (Sandvik) or unplated 20 μm tungsten (California Fine Wire), with a final impedance of ~200-500 kOhms.

Surgery

Anesthesia was induced with isoflurane, then a cocktail of ketamine, xylazine, and atropine was administered while isoflurane remained at minimal levels. A ground screw was inserted in the skull above the left cerebellum as a global reference. The microdrive was stereotaxically implanted over the right hemisphere such that the center of each cannula was targeted to the following coordinates relative to the animal's Bregma: MEC: AP -9.1 mm, ML 5.6 mm; CA1: AP -3.6 mm, ML 2.2 mm. The oblong MEC cannula was longer in the medial-lateral axis and tilted 10° laterally. Once the cannulae were in place over the pial surface, Gelfoam soaked in artificial cerebral spinal fluid was placed between the outer cannulae diameter and the inner craniectomy bone surface, then top-coated with silicone gel (Dow-Corning 3-4680) and finally secured to the skull using 4-META/MMA-TBB ([Matsumura & Nakabayashi, 1988](#)) (C&B Metabond). Dental

acrylic was used to reinforce the integrity of the exposed 30 G tubing. The total surgery time for each implant was less than 4 hours.

Adjusting n-trode position

After 5-7 days of recovery following surgery, subjects were once again food-deprived to 85% of their baseline weight and reacclimated to the linear track and reward ports. Over 2-4 weeks post-surgery, n-trodes were advanced toward the principal cell layers of dorsal CA1 and all layers of MEC. At least one n-trode from each cannula was positioned in corpus callosum as a reference to subtract non-spiking common noise and signal from the rest. Before implantation, MEC n-trodes target depths were determined by stereotaxically aligning to a target sagittal range lateral to the midline. Once the W-task began, there were minimal adjustments made to the n-trode position. If any further n-trode repositioning occurred in between recording periods, it was done 18 hours before the next recording and was typically less than ~25 μm .

Behavior

For the first 4-12 days of recording, subjects were run on two 20-minute W-task epochs, during which they were required through trial and error to learn the alternation sequence of visits to the reward ports. The rewarded sequence was a visit to the center arm, followed by the less recently visited outer arm. The subjects were always rewarded at the center arm following an outer arm visit. Accurate visits were rewarded with sweetened evaporated milk (~100 μl) after a 1-second delay, while inaccurate visits received no milk. Custom 3D printed reward ports positioned at the three termination points of the W track arms detected port entry with an infrared light beam break. The reward was automatically delivered through the reward port feeding trough by syringe pumps

(OEM syringe pumps, Braintree Scientific) attached to food-grade plastic tubing. The animal's departure from the reward port was self-paced.

Five of the seven subjects were run on a variant of the previously described W-task ([Karlsson & Frank, 2009](#)) where for the last 3-4 days of recording, the second W-track each day was a novel W-maze positioned behind an opaque wall, and at a 90-degree angle relative to the first W-maze. All W-task epochs were flanked by 20-minute rest-box epochs. Each recording day concluded with two 20-minute open foraging (open-field) epochs, also flanked by 10 - 20-minute rest box epochs. Animals on the open-field environment were free to move through the square environment with raised sides and spent most of the time collecting small crumbles of food particles (a curated assortment of crumbled Reese's Pieces, Fruit Loops, imported chocolate sprinkles, and finely grated parmesan cheese) scattered randomly in advance by the experimenter. Most animals showed a preference for Reese's Pieces (observation, data not presented).

The W-shaped tracks consisted of three 75 x 7 cm arms with 3 cm high walls, separated 36 cm apart, and connected by a straight path at one end. The resting box measured 25 x 35 x 50 cm with an open top. One wall was latched and hinged to open to place or retrieve the subject and remained closed during rest box epochs. The open-field measured 48 x 48 x 18 inches with an open top. It also had one drawbridge-style wall that opened to facilitate subject placement and retrieval by the experimenter at the beginning and end of foraging epochs. Subjects had custom PCB ring array with colored lights attached to the top of the implant housing, allowing the position to be extracted from video recorded by a camera mounted to the ceiling.

Electrophysiological acquisition

All electrophysiological data were sampled and saved at 30 kHz on a 320-channel head-stage using Trodes software package (SpikeGadgets LLC). Spike data were recorded relative to the reference n-trode and digitally filtered 600 – 6,000 Hz (2-pole Bessel for high and low-pass). Local field potentials were sampled at 1.5 kHz and digitally filtered 1 - 400 Hz. Analyzed LFP is relative to the reference n-trode. Overhead video of the experimental environment was collected at ~30 Hz, and the position was semi-automatically reconstructed by tracking the array of diodes secured above the subjects' head using online and offline tracking provided by Trodes.

Data processing

Data processing was performed using custom JavaScript, Python, and Matlab (MathWorks) code, along with open source packages, as noted below.

Recording site identification

At the end of the experiment, subjects were anesthetized with isoflurane, and a small electrolytic lesion was made at each recording site (30 μ A of positive current for 3 seconds, on 2 channels of each n-trode). After 24 hours of recovery, the subjects were euthanized with pentobarbital and perfused transcardially with PBS followed by 4% paraformaldehyde in 0.1M PB. The skull was manually cleared of muscle then allowed to postfix in 4% paraformaldehyde, 0.1M PB for 24 hours. Finally, the n-trodes were retracted, and the brain was removed from the skull and cryoprotected in 30% sucrose in PBS. Subject brains were embedded in OCT compound and sectioned in the sagittal plane at 50 μ m thickness with a cryostat. Sections were blocked (5% donkey serum in 0.3% Triton-X in TBS, used for all incubations) for 1 hr, incubated with

parvalbumin antibody overnight, washed, and subsequently incubated with fluorescent secondary antibody (1:400) (Alexa 568, Life Technologies). Then sections were mounted with fluorescent Nissl reagent NeuroTrace Blue (1:200) (Life Technologies, N-21479). Recording sites were reconstructed using a rat atlas and electrophysiological markers. Recording sites were designated within a region if the lesion or end of the n-trode track overlapped with the cytoarchitectural zone characteristic of each area.

Reward port movement tracking

While subjects alternated between two reward ports, a high-angle oblique video camera recorded a close-up of licking bouts at ~125 frames/s. An open-source software package (DeepLabCut) ([Mathis et al., 2018](#)) was used to track the nose, eye, ear, jaw, and tongue features, which included manual labeling of a subset of frames before training a model.

Unit spike clustering

Spike sorting was performed using ISO split algorithm and verified with manual curation in Mountainsort and Mountainview software ([Chung et al., 2017](#); [Magland & Barnett, 2016](#)). Units were clustered within epochs but drift-tracked across all valid task, sleep, forage epochs. Clustering was performed using an event detection threshold set to 3, and valid single units scored isolation > 0.95, noise overlap < 0.03. Only units with at least 100 spikes were included in the current analysis.

SWR-detection

One electrode per CA1 n-trode was chosen and band-pass filtered (150-250 Hz) to create 'ripple-band' filtered trace. Then the amplitudes for the CA1 n-trodes were individually squared, summed across, smoothed with a Gaussian kernel ($\sigma = 4$ ms), and the square root of the smoothed sum was analyzed as the power envelope to detect threshold excursions greater than 2 s.d. of the mean power that lasted at least 15 ms. The envelope threshold crossing was designated as the SWR start time. The entire SWR event was defined from the time of baseline crossing before the threshold crossing until the envelope no longer exceeded the baseline value. SWRs occurring when subjects' head speed was >4 cm/s were excluded.

Port entry event cycle phase modulation of spiking and SWR occurrence

For each cluster's spikes that occurred between two port-entry events during a lick burst, the time duration between the first lick to each spike was taken in proportion to the full inter-lick interval (ILI), making the range of possible values between 0 and 1. The distribution was then transformed as the proportion of 0 to 2π , in order to convert into polar coordinates. The phase modulation score then followed a method previously described ([Karalis & Sirota, 2018](#)). Briefly, the strength of phase modulation was defined as the log of the Rayleigh Z metric ($\ln(R^2/n)$). Spike proportions of inter-lick intervals was shuffled for each cluster and the phase modulation score recomputed, and repeated 1000 times to create a shuffled distribution from which the 95% threshold of shuffled values was used as a significance test. This threshold value matched the values used by previous studies employing this phase modulation score. The analysis for the lick phase modulation of SWR was similar to phase modulation analysis of unit spiking.

Sharp-wave ripple and port entry event cross-correlation

For each recording day, the cross-correlation between port-entry events and SWR start times were calculated in 10 ms bins at up to 0.5-second lag. Each cross-correlation histogram was first normalized by the square root of the product of the number of events. To z-score the cross-correlation histogram, the SWR times were circularly shuffled 1000 times by a random amount within the 1 second window to create 100 shuffled cross-correlation histograms. Each real and shuffled cross-correlation histogram was smoothed with a 20 ms s.d., 160 ms wide Gaussian. The real cross-correlation values were then z-scored relative to the distribution of shuffled values within each bin. We averaged the cross-correlation z-score 20ms centered on 0-lag to get an approximate 0-lag value.

Reactivation Strength

For a given W-task epoch, spike trains from multiple, simultaneously recorded cells when the animal's velocity was $> 4\text{cm/s}$ were binned at 100 ms and z-transformed. The correlation matrix of the binned spike trains was then computed and diagonalized. The spike trains from a 2 second window around each event (intra-lick bout SWR, extra-lick bout SWR, and P-event) were then binned and z-transformed. Note that detected events were all from when the animal was $< 4\text{ cm/s}$. A measure of instantaneous similarity, termed reactivation strength ([Peyrache, Benchenane, Khamassi, Wiener, & Battaglia, 2010](#); [Peyrache et al., 2009a](#)), of the event-centered spiking activity at each time bin (population vector) with the locomotive eigenvalue was then computed.

1.5 Figures

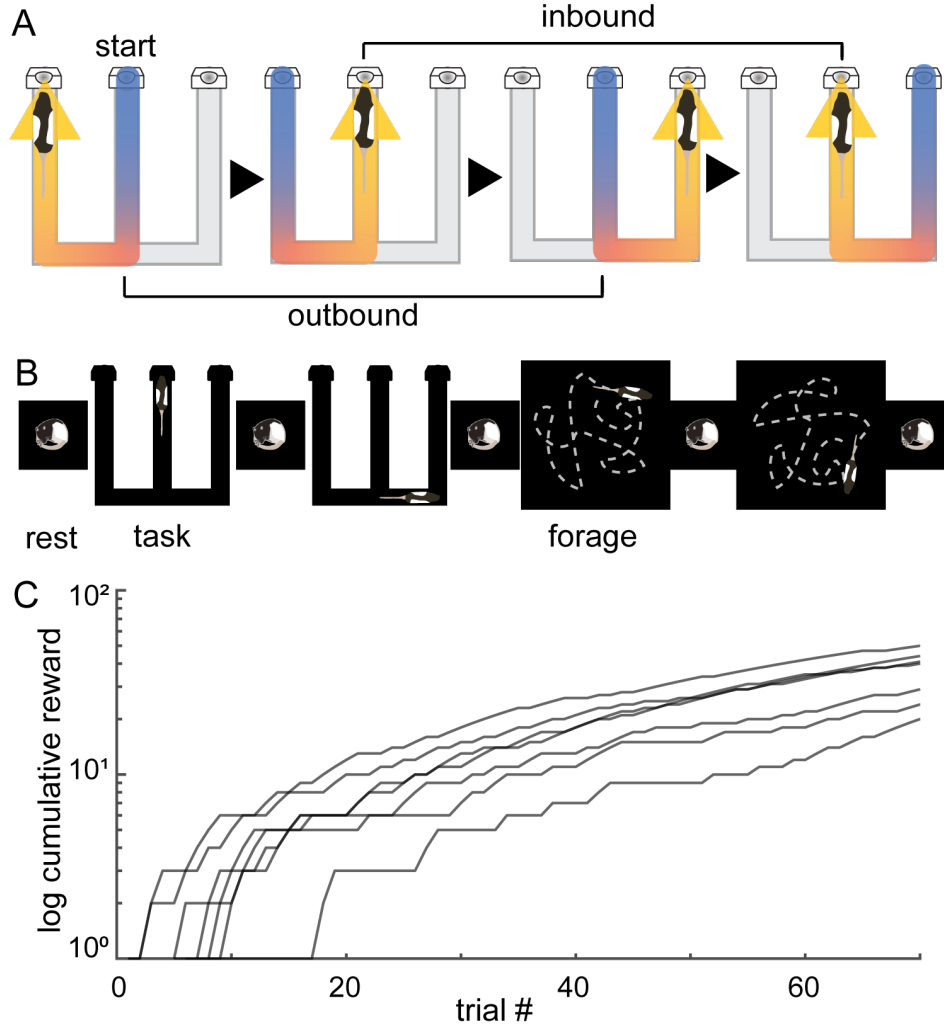


Figure 1.1 | Spatial alternation task on the W-maze

(A) Schematic of rewarded behavior on the spatial alternation W-maze task. Ports located at the termination of the center and outer arms registered arrivals and dispensed sweetened milk as reward. Rewarded performance is as shown in sequence – center arm port dispensed reward if preceded by either outer arm visit, and outer arm ports dispensed reward if preceded by, first, a visit to the other outer arm, and then to the center arm. (B) Rest-box epochs flank spatial alternation task on the W-shaped maze and epochs spent freely foraging on an open-field environment. (C) Log cumulative reward for all animals on the W-maze task as a function of trial. One trace per animal.

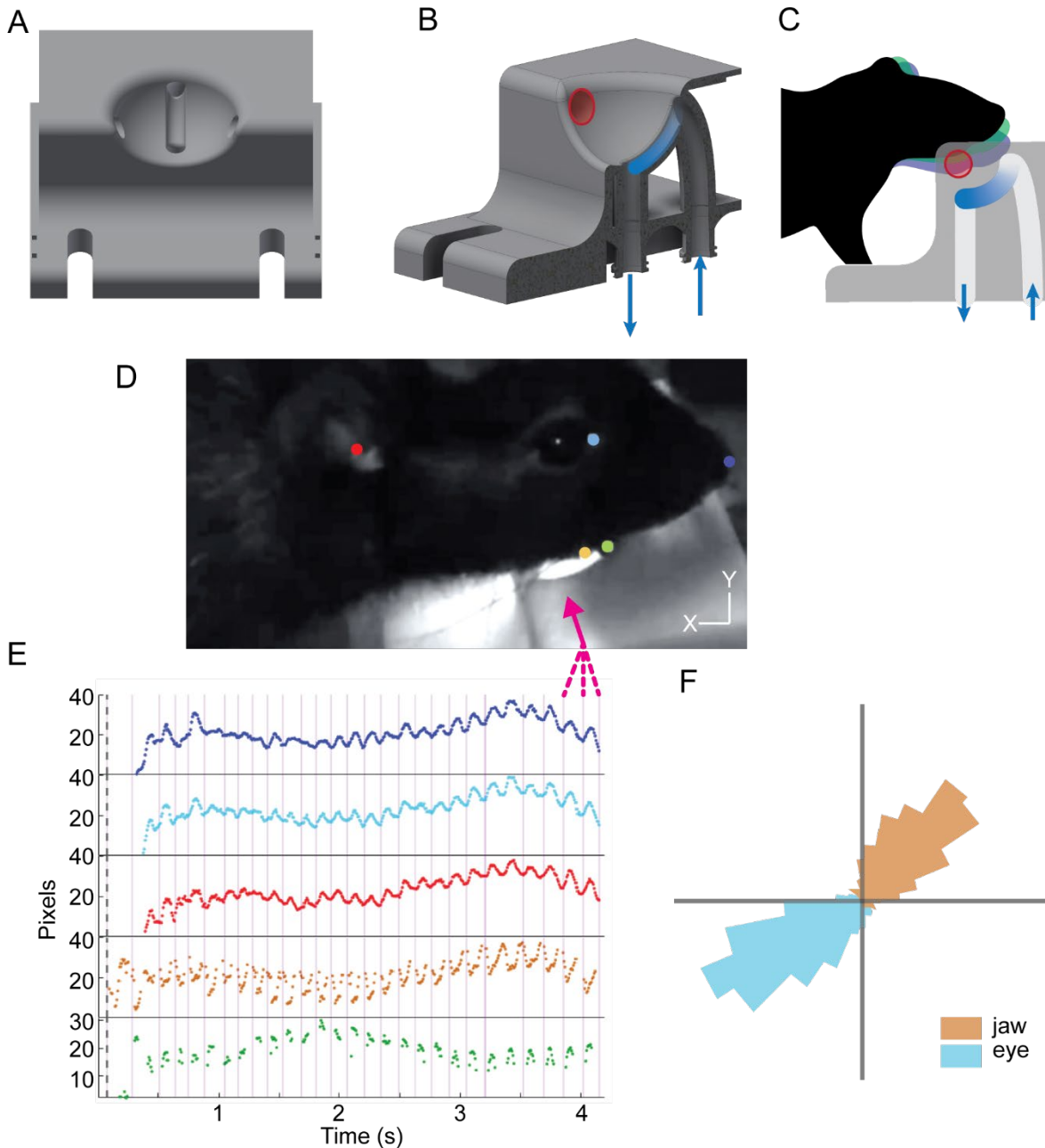


Figure 1.2 | Port-Crossings Capture a Consistent Phase of Movement During Lick Bursts

(A) Rendering of the port from top-front perspective. (B) Section of the port showing the input and output (blue arrows) piping of the milk and the exposed trough where the subject could access the reward. The red circle marks one side of the infrared light sensor which was triggered on each port entry (P-event). (C) Side profile of the reward port with the rat's schematized movement during licking bouts. (D) Video frame showing tracked markers on animal's ear, eye, nose, tongue, and jaw. (E) Example of a lick burst showing y-axis (tongue: x-axis) pixel position of tracked markers. The vertical pink lines indicate the time of P-events. The vertical dotted gray line is the time of reward pump delivery onset. (F) Polar histogram of the tracked phases of the jaw and eye at the time of P-events.

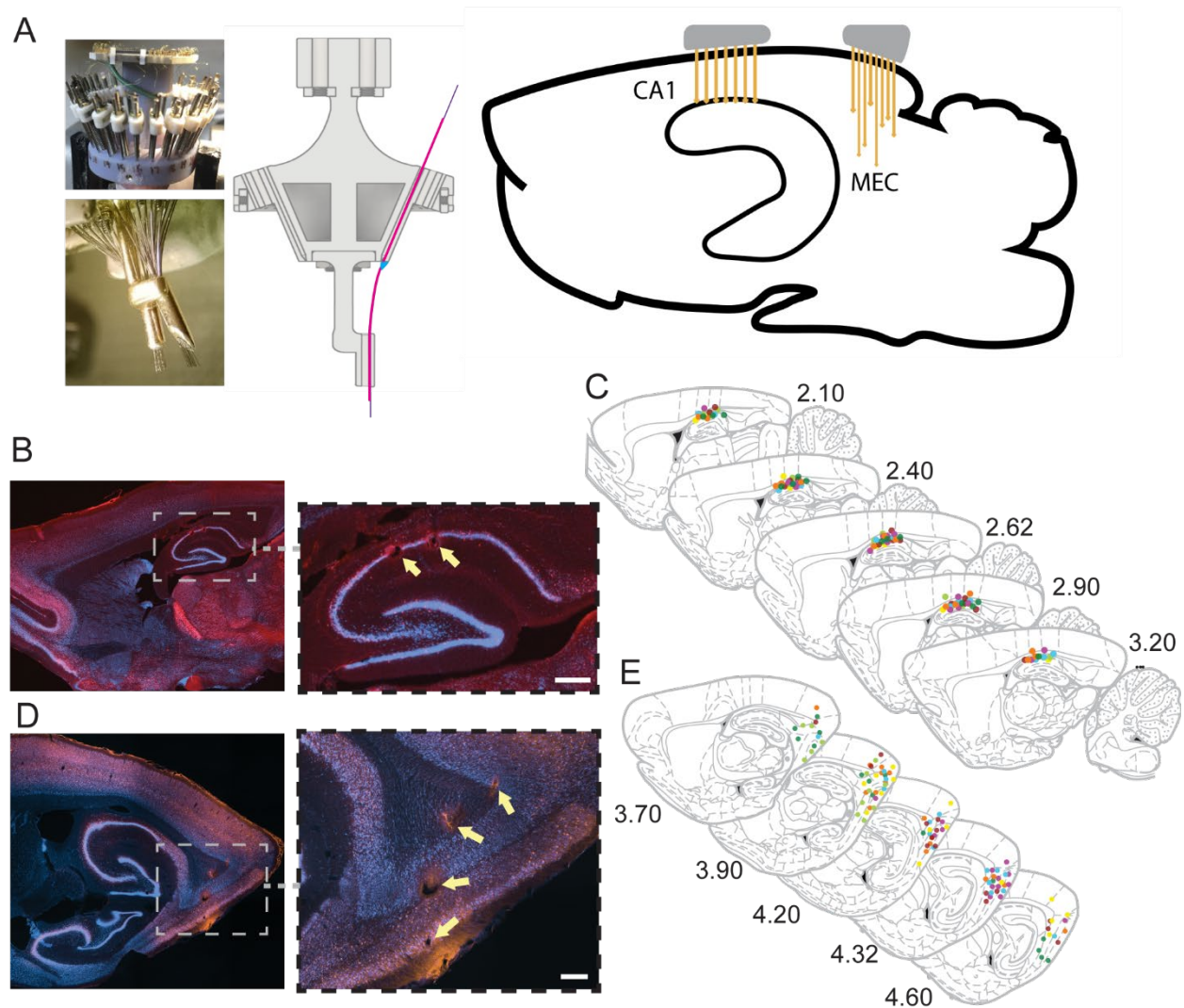


Figure 1.3 | Electrophysiological and histological validation of recording sites

(A) (Left) Pictures of a completed microdrive assembly, prior to implantation, from the top and bottom perspective. (Middle and Right) Schematic showing the microdrive assembly, guide-cannula, and electrode bundle tracks penetrating the brain. Note that the MEC tracks were further lateral than the hippocampal tracks, schematic is purely for illustration of relative anterior/posterior positioning. **(B)** Sagittal, dual fluorophore tagged histological section through dorsal hippocampus showing electrolytic lesions at recording sites in CA1 (yellow arrows), including expanded inset on right. Parvalbumin is stained red, Neurotrace stained neuronal cell bodies blue. scale bar: 500 μ m **(C)** Sagittal summary schematic of final recording depth of all electrodes emanating from the hippocampal-directed guide-cannula for all subjects. Locations have been aligned to the nearest representative section adapted from a rat brain atlas (Paxinos, 2007). **(D)** Histological section showing MEC-directed cannula tracks, with close-up inset on the right. Note that only the ventral two yellow arrows are recordings in MEC. **(E)** Summary schematic of all final recording sites of MEC-directed electrode bundles. Locations outside of MEC were not included in further analysis.

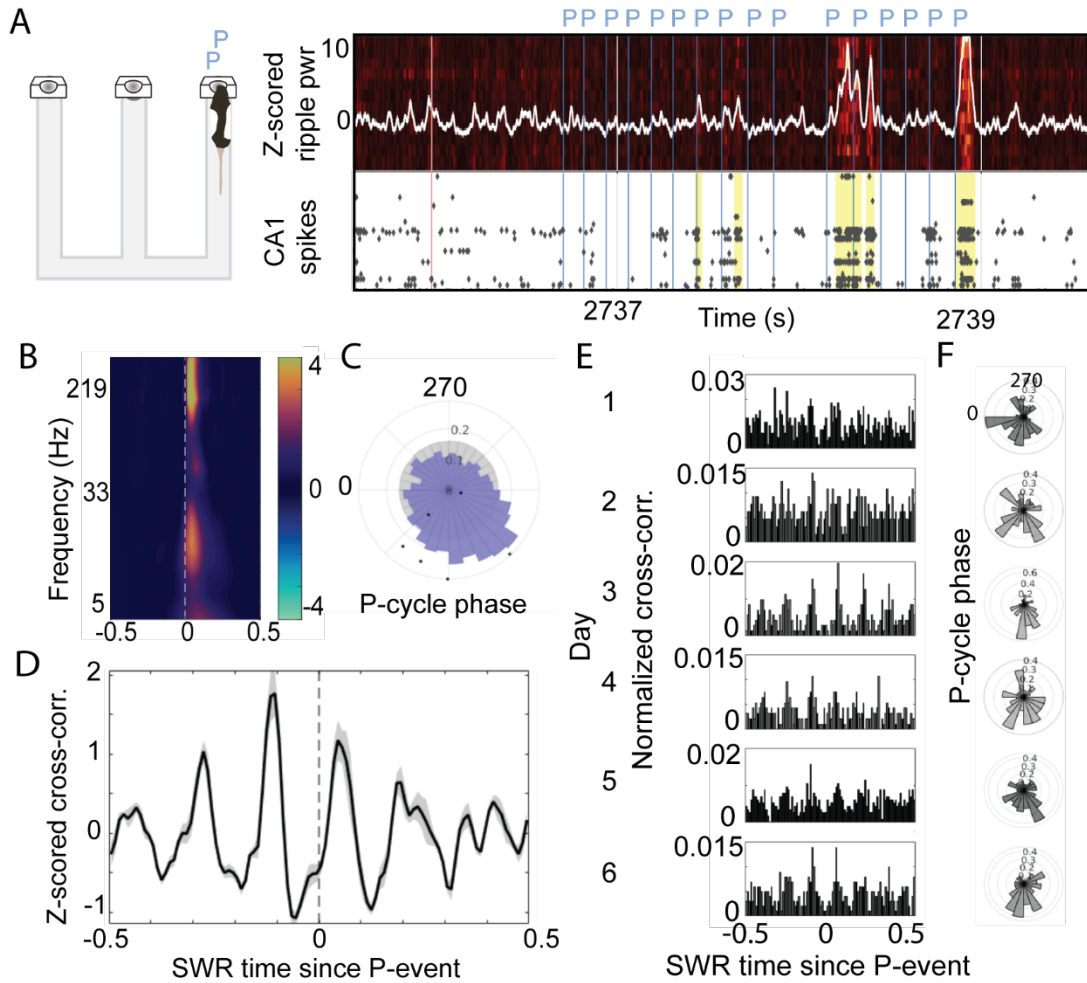


Figure 1.4 | Rhythmic Bursts of Licking Entrain Sharp-Wave Ripple Events

(A) Example data showing SWR events highlighted as yellow vertical lines and P-events as blue vertical lines. Combined ripple-band (150-250 Hz) power for all CA1 sites (white trace) overlaid on ripple-band power for individual (row wise) CA1 sites in this subject (heatmap). Schematic animal positioned at a reward port is to the left. (B) SWR-triggered LFP spectrogram in CA1. (C) Polar histogram of SWR occurrence relative to P-cycle phase for all animals (purple; grey: shuffled). Black dots show mean resultant vector for individual animals. (D) Z-normalized cross-correlation of SWR onset relative to the time of P-events for one animal. (E) Peri-P-event histogram of SWR onset, with each row per day for one animal. (F) Polar histogram of corresponding SWR times relative to the phase of P-event cycle, per day.

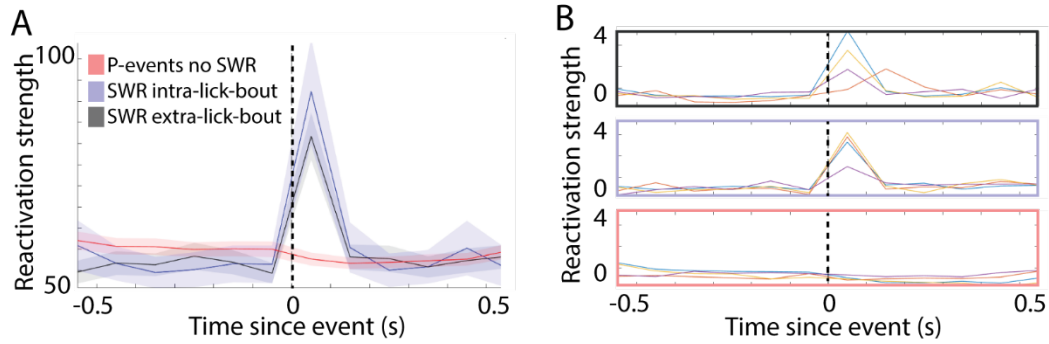


Figure 1.5 | Rhythmic Bursts of Licking Entrain Neural Reactivation

(A) Binned (100ms) time-series of reactivation strength (see Methods) for one subject. grey solid line is mean reactivation strength centered on SWR's that occurred outside of detected licking bouts. Purple is mean reactivation strength centered on SWR's that occurred within detected licking bouts. Red is mean reactivation strength centered on P-events that occurred within detected licking bouts. Shaded area denotes sem. Note the increase in reactivation strength during SWRs, but not XP events **(B)** Mean reactivation strength for the top four principal components of extra-lick-bout SWRs (top), intra-lick-bout SWRs (center), and P-events events (bottom).

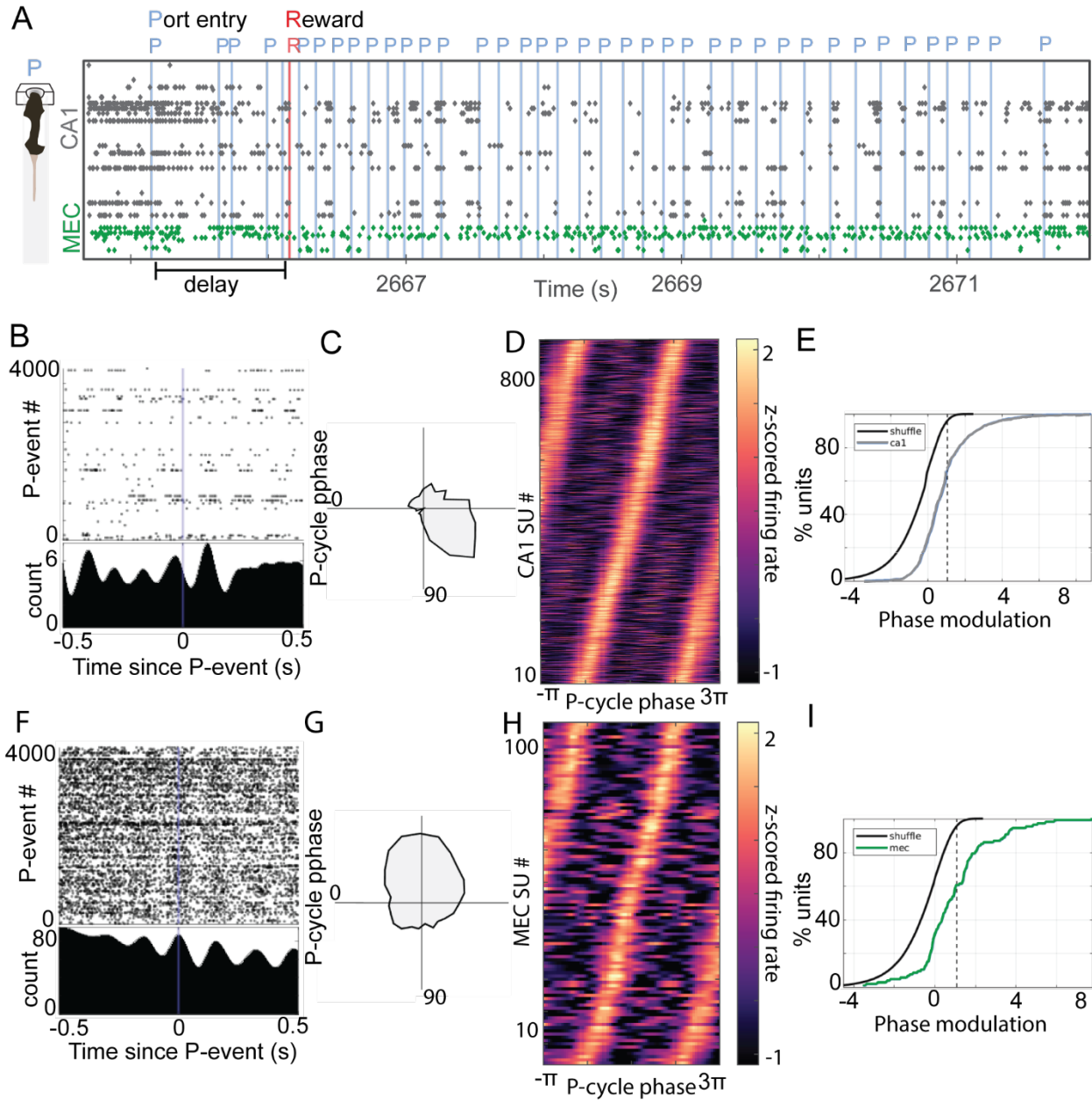


Figure 1.6 | Licking modulates neural activity in the hippocampal formation

(A) Example time-series data segment during a licking burst. Port entry events (P, vertical blue lines) are overlaid on neural spiking data from CA1 (grey) and MEC (green). Schematized animal positioned at a reward port is to the left. (B) Spike-raster and peri-event time histograms aligned to the detection of port-entry event for a CA1. (C) Polar histogram of P-phase spiking for unit shown in B. (D) Z-normalized firing rate per unit (row) over two full P-event cycles. (E) Cumulative percent of units by phase modulation score. Vertical dotted line denotes 95% threshold of phase-shuffled phase-modulation score distribution. (F-I) Plotting conventions as in B-E, but for MEC.

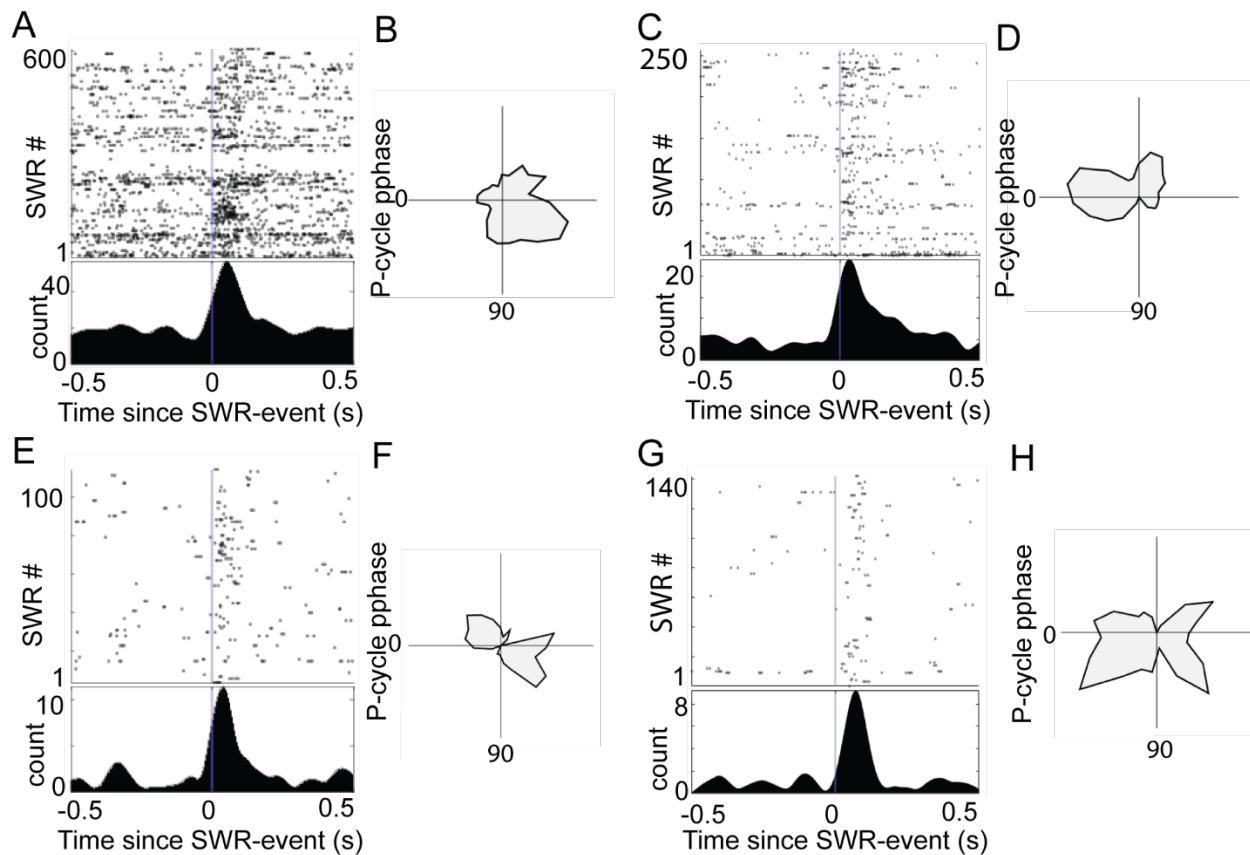


Figure 1.7 | CA1 units co-modulated by sharp-wave ripple and port entry events

(A) SWR-aligned spike raster and peri event time histogram for one CA1 unit. Note that the 4-8 Hz rhythmicity preceding the SWR-modulation. (B) Spike phase histogram for the same CA1 unit as in A, centered on port entry events. (C) A second example of a CA1 unit, but in a different animal, showing co-modulation by SWR and (D) P-event phase. (E) An example CA1 unit in a third animal, also showing co-modulation by SWR and (F) P-event phase. (G-H) A second unit from same animal as in C-D, showing SWR modulation, but with an overall lower firing rate.

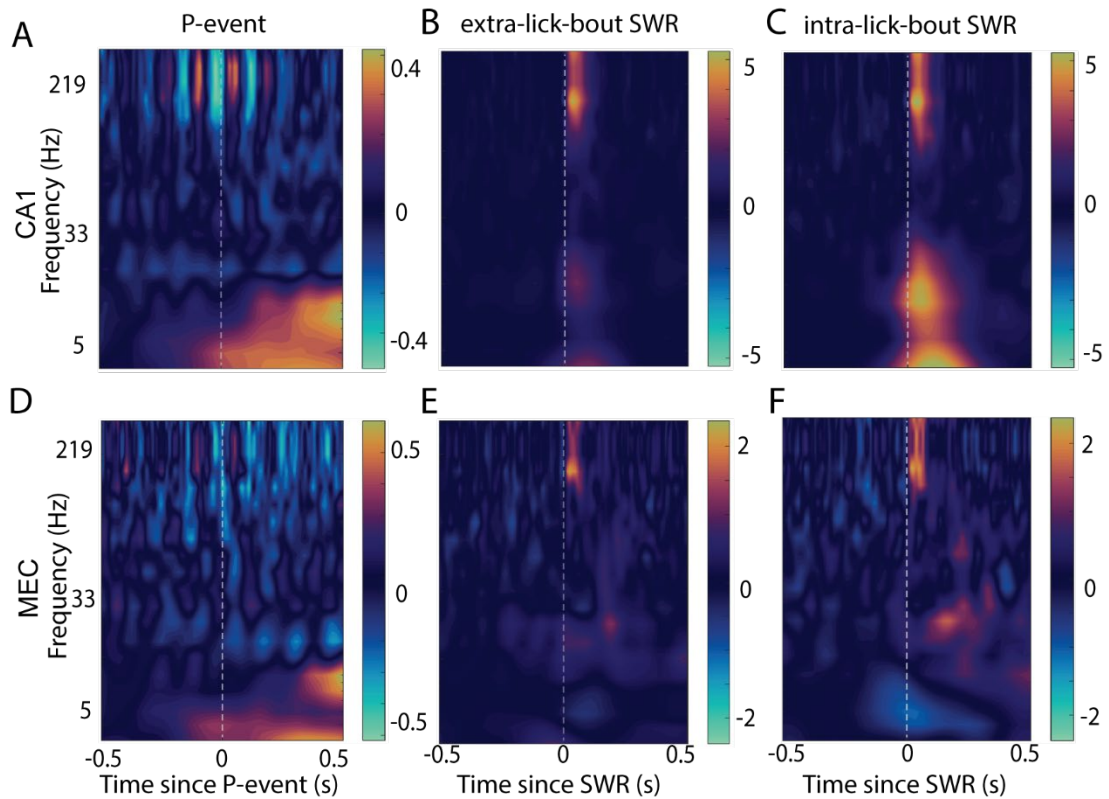
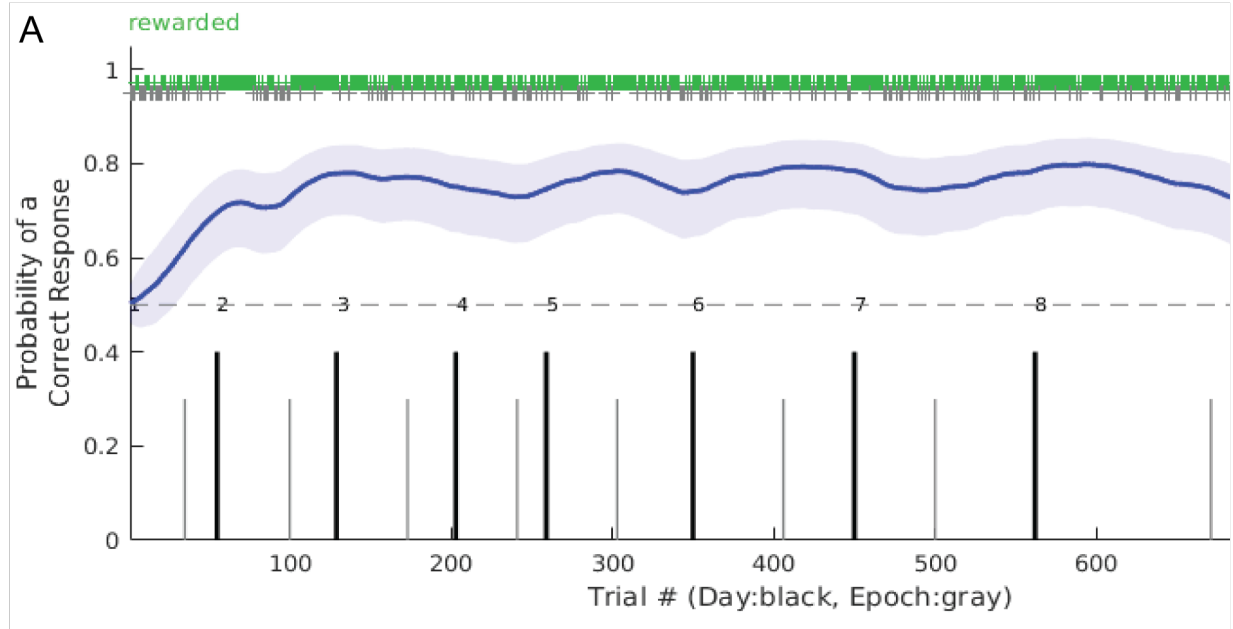


Figure 1.8 | SWR-Triggered Ripple Power in MEC During Licking Bouts

(A) Mean P-event centered LFP from CA1 recording sites in one subject over all W-maze epochs. (B) Hippocampal SWR-triggered spectrogram from CA1 n-trodes during times when the animal was not engaged in licking. (C) Hippocampal SWR-triggered spectrogram from CA1 n-trodes during times when the animal was engaged in licking. (D) Spectrogram from MEC n-trodes triggered by P-events. (E) Hippocampal SWR-triggered spectrogram from MEC n-trodes during times when the animal was not engaged in licking. (F) Hippocampal SWR-triggered spectrogram from MEC n-trodes during times when the animal was engaged in licking.

1.7 Supplemental Figures



Supplemental Figure 1.1 | Behavioral Performance on W-task

(A) Dynamic analysis of learning to estimated probability of an accurate trial for one animal over several days. Rewarded trials are marked with a green tick at the top, and unrewarded trials in grey. Solid blue line indicates the mode of the probability distribution, and the shaded region indicates the 90% confidence interval. Grey vertical lines mark epoch boundaries, black lines mark the start of each day, and the horizontal dotted line indicates chance performance (0.5).

1.8 References

- Accolla, R., & Carleton, A. (2008). Internal body state influences topographical plasticity of sensory representations in the. In *rat gustatory cortex. Proc Natl Acad Sci U S A* 105 (pp. 4010-4015).
- Arshamian, A., Iravani, B., Majid, A., & Lundstrom, J. N. (2018). Respiration modulates olfactory memory consolidation in humans. *J Neurosci*, 38(10286), 10294.
- Axmacher, N., Elger, C. E., & Fell, J. (2008). Ripples in the medial temporal lobe are relevant for human memory consolidation. *Brain*, 131(Pt 7), 1806-1817. doi:10.1093/brain/awn103
- Axmacher, N., Henseler, M. M., Jensen, O., Weinreich, I., Elger, C. E., & Fell, J. (2010). Cross-frequency coupling supports multi-item working memory in the human hippocampus. *Proc Natl Acad Sci USA*, 107(7), 3228-3233. doi:10.1073/pnas.0911531107
- Barkley-Levenson, A. M., & Crabbe, J. C. (2012). Ethanol drinking microstructure of a high drinking in the dark selected mouse line. *Alcohol Clin Exp Res*, 36, 1330-1339.
- Barkley-Levenson, A. M., & Crabbe, J. C. (2015). Distinct ethanol drinking microstructures in two replicate lines of mice selected for drinking to intoxication. *Genes Brain Behav*, 14, 398-410.
- Benchenane, K., Peyrache, A., Khamassi, M., Tierney, P. L., Gioanni, Y., Battaglia, F. P., & Wiener, S. I. (2010). Coherent Theta Oscillations and Reorganization of Spike Timing in the Hippocampal-Prefrontal Network upon Learning. *Neuron*, 66(6), 921-936. doi:10.1016/j.neuron.2010.05.013
- Burgalossi, A. (2011). Microcircuits of functionally identified neurons in the rat medial entorhinal cortex. *Neuron*, 70, 773-786. doi:10.1016/j.neuron.2011.04.003
- Burgess, N., & O'Keefe, J. (2011). Models of place and grid cell firing and theta rhythmicity. *Curr. Opin. Neurobiol.*, 21(5), 734-744. doi:10.1016/j.conb.2011.07.002
- Buzsaki, G. (2002). Theta oscillations in the hippocampus. *Neuron*, 33(3), 325-340.

- Buzsaki, G. (2015). Hippocampal sharp wave-ripple: A cognitive biomarker for episodic memory and planning. *Hippocampus*, *25*(10), 1073-1188.
- Canto, C. B., Wouterlood, F. G., & Witter, M. P. (2008). What does the anatomical organization of the entorhinal cortex tell us? *Neural Plast.*, *2008*, 381243. doi:10.1155/2008/381243
10.1155/2008/381243.
- Carr, M. F., Jadhav, S. P., & Frank, L. M. (2011). Hippocampal replay in the awake state: a potential substrate for memory consolidation and retrieval. *Nat Neurosci*, *14*(2), 147-153.
- Chung, J. E., Magland, J. F., Barnett, A. H., Tolosa, V. M., Tooker, A. C., Lee, K. Y., . . . Greengard, L. F. (2017). A Fully Automated Approach to Spike Sorting. *Neuron*, *95*(6), 1381-1394.e1386.
doi:10.1016/j.neuron.2017.08.030
- Coddington, L. T., & Dudman, J. T. (2018). The timing of action determines reward prediction signals in identified midbrain dopamine neurons. *Nat. Neurosci.*, *21*(11), 1563-1573. doi:10.1038/s41593-018-0245-7
- Davidson, T. J., Kloosterman, F., & Wilson, M. A. (2009). Hippocampal replay of extended experience. *Neuron*, *63*(4), 497-507.
- Del Negro, C. A., Funk, G. D., & Feldman, J. L. (2018). Breathing matters. *Nature Reviews Neuroscience*, *19*, 351-367.
- Demetris, R. (2017). *electrophysiology toolbox*.
- Eastwood, E. C., Barkley-Levenson, A. M., & Phillips, T. J. (2014). Methamphetamine drinking microstructure in mice bred to drink high or low amounts of methamphetamine. *Behav Brain Res*, *272*, 111-120.
- Eliades, S. J., & Wang, X. (2008). Neural substrates of vocalization feedback monitoring in primate auditory cortex. *Nature*, *453*(7198), 1102-1106. doi:10.1038/nature06910

- Fell, J., & Axmacher, N. (2011). The role of phase synchronization in memory processes. *Nat Rev Neurosci*, 12(2), 105-118. doi:nrn2979 [pii]
10.1038/nrn2979
- Fernandez-Ruiz, A., Oliva, A., Fermino de Oliveira, E., Rocha-Almeida, F., Tingley, D., & Buzsaki, G. (2019). Long-duration hippocampal sharp wave ripples improve memory. *Science*, 364(6445), 1082-1086. doi:10.1126/science.aax0758
- Fernandez-Ruiz, A., Oliva, A., Nagy, G. A., Maurer, A. P., Berenyi, A., & Buzsaki, G. (2017). Entorhinal-CA3 Dual-Input Control of Spike Timing in the Hippocampus by Theta-Gamma Coupling. *Neuron*, 93(5), 1213-1226 e1215. doi:10.1016/j.neuron.2017.02.017
- Fox, S. E., & Ranck, J. B., Jr. (1981). Electrophysiological characteristics of hippocampal complex-spike cells and theta cells. *Exp Brain Res*, 41(3-4), 399-410.
- Frank, L. M., Brown, E. N., & Wilson, M. (2000a). Trajectory encoding in the hippocampus and entorhinal cortex. *Neuron*, 27(1), 169-178.
- Frank, L. M., Brown, E. N., & Wilson, M. A. (2000b). Trajectory encoding in the hippocampus and entorhinal cortex. *Neuron*, 27, 169-178.
- Fuentes, R. A., Aguilar, M. I., Aylwin, M. L., & Maldonado, P. E. (2008). Neuronal activity of mitral-tufted cells in awake rats during passive and active odorant stimulation. *J Neurophysiol*, 100, 422-430.
- Galistu, A., Modde, C., Pireddu, M. C., Franconi, F., Serra, G., & D'Aquila, P. S. (2011). Clozapine increases reward evaluation but not overall ingestive behaviour in rats licking for sucrose. *Psychopharmacology (Berl)*, 216, 411-420.
- Geva-Sagiv, M., & Nir, Y. (2019). Local Sleep Oscillations: Implications for Memory Consolidation. *Frontiers in Neuroscience*, 13. doi:10.3389/fnins.2019.00813
- Girardeau, G., Inema, I., & Buzsaki, G. (2017). Reactivations of emotional memory in the hippocampus-amygdala system during sleep. *Nat Neurosci*, 20(11), 1634-1642. doi:10.1038/nn.4637

- Gomperts, S. N., Kloosterman, F., & Wilson, M. A. (2015). VTA neurons coordinate with the hippocampal reactivation of spatial experience. *Elife*, *4*. doi:10.7554/eLife.05360
- Graham, D. M., Sun, C., & Hill, D. L. (2014). Temporal Signatures of Taste Quality Driven by Active Sensing. *Journal of Neuroscience*, *34*(22), 7398-7411. doi:10.1523/jneurosci.0213-14.2014
- Gutierrez, R., Carmena, J. M., Nicolelis, M. A., & Simon, S. A. (2006). Orbitofrontal ensemble activity monitors licking and distinguishes among natural rewards. *J Neurophysiol*, *95*(119–133).
- Gutierrez, R., Simon, S. A., & Nicolelis, M. A. (2010). Licking-induced synchrony in the taste–reward circuit improves cue discrimination during learning. *Journal of Neuroscience*, *30*(1), 287-303.
- Hardcastle, K., Maheswaranathan, N., Ganguli, S., & Giocomo, L. M. (2017). A Multiplexed, Heterogeneous, and Adaptive Code for Navigation in Medial Entorhinal Cortex. *Neuron*, *94*(2), 375-387. doi:10.1016/j.neuron.2017.03.025
- Hartfield, A. W., Moore, N. A., & Clifton, P. G. (2003). Effects of clozapine, olanzapine and haloperidol on the microstructure of ingestive behaviour in the rat. *Psychopharmacology (Berl)*, *167*, 115-122.
- Hyafil, A., Giraud, A. L., Fontolan, L., & Gutkin, B. (2015). Neural cross-frequency coupling: connecting architectures, mechanisms, and functions. *Trends Neurosci*, *38*, 725-740.
- J. O'Keefe, J. D. (1971). The hippocampus as a spatial map. Preliminary evidence from unit activity in the freely-moving rat. *Brain Research*, *34*(1), 171-175.
- Jadhav, S. P., Rothschild, G., Roumis, D. K., & Frank, L. M. (2016). Coordinated Excitation and Inhibition of Prefrontal Ensembles during Awake Hippocampal Sharp-Wave Ripple Events. *Neuron*, *90*(1), 113-127. doi:10.1016/j.neuron.2016.02.010
- Ji, D., & Wilson, M. A. (2007). Coordinated memory replay in the visual cortex and hippocampus during sleep. *Nat Neurosci*, *10*(1), 100-107.

- Jutras, M. J., Fries, P., & Buffalo, E. A. (2013). Oscillatory activity in the monkey hippocampus during visual exploration and memory formation. *Proc Natl Acad Sci USA*, *110*(32), 13144-13149. doi:10.1073/pnas.1302351110
- Karalis, N., & Sirota, A. (2018). Breathing coordinates limbic network dynamics underlying memory consolidation. *bioRxiv*, 392530. doi:10.1101/392530
- Karlsson, M. P., & Frank, L. M. (2009). Awake replay of remote experiences in the hippocampus. *Nat Neurosci*, *12*(7), 913-918.
- Katz, D. B., Simon, S. A., & Nicolelis, M. A. (2001). Dynamic and multimodal responses of gustatory cortical neurons in awake rats. *J Neurosci*, *21*, 4478-4489.
- Kay, K., Sosa, M., Chung, J. E., Karlsson, M. P., Larkin, M. C., & Frank, L. M. (2016). A hippocampal network for spatial coding during immobility and sleep. *Nature*, *531*(7593), 185-190.
- Kobro-Flatmoen, A., & Witter, M. P. (2019). Neuronal chemo-architecture of the entorhinal cortex: A comparative review. *European Journal of Neuroscience*, *50*(10), 3627-3662.
- Krupa, D. J., Wiest, M. C., Shuler, M. G., Laubach, M., & Nicolelis, M. A. (2004). Layer-specific somatosensory cortical activation during active tactile discrimination. *Science*, *304*(5679), 1989-1992. doi:10.1126/science.1093318
- Lansink, C. S., Goltstein, P. M., Lankelma, J. V., Joosten, R. N., McNaughton, B. L., & Pennartz, C. M. (2008). Preferential reactivation of motivationally relevant information in the ventral striatum. *J. Neurosci.*, *28*(25), 6372-6382. doi:10.1523/JNEUROSCI.1054-08.2008
- Lara-Vásquez, A., Espinosa, N., Durán, E., Stockle, M., & Fuentealba, P. (2016). Midline thalamic neurons are differentially engaged during hippocampus network oscillations. *Sci Rep*, *6*(1), 1-16.
- Liu, Y., Dolan, R. J., Kurth-Nelson, Z., & Behrens, T. E. (2019). Human replay spontaneously reorganizes experience. *Cell*, *178*(3), 640-652. e614.

- Liu, Y., McAfee, S. S., & Heck, D. H. (2017). Hippocampal sharp-wave ripples in awake mice are entrained by respiration. *Sci Rep*, 7(1), 8950. doi:10.1038/s41598-017-09511-8
- Livneh, Y., Sugden, A. U., Madara, J. C., Essner, R. A., Flores, V. I., Sugden, L. A., . . . Andermann, M. L. (2020). Estimation of Current and Future Physiological States in Insular Cortex. *Neuron*.
- Logothetis, N. K. (2012). Hippocampal-cortical interaction during periods of subcortical silence. *Nature*, 491, 547-553.
- Lutas, A., Kucukdereli, H., Alturkistani, O., Carty, C., Sugden, A. U., Fernando, K., . . . Andermann, M. L. (2019). State-specific gating of salient cues by midbrain dopaminergic input to basal amygdala. *Nature neuroscience*, 1-14.
- Magland, J. F., & Barnett, A. H. (2016). Unimodal clustering using isotonic regression: ISO-SPLIT. *arXiv*, 1508.04841v04842. doi:1508.04841v2
- Mathis, A., Mamidanna, P., Cury, K. M., Abe, T., Murthy, V. N., Mathis, M. W., & Bethge, M. (2018). DeepLabCut: markerless pose estimation of user-defined body parts with deep learning. *Nature neuroscience*, 21(9), 1281-1289. doi:10.1038/s41593-018-0209-y
- Matsumura, H., & Nakabayashi, N. (1988). Adhesive 4-META/MMA-TBB opaque resin with poly(methyl methacrylate)-coated titanium dioxide. *J Dent Res*, 67(1), 29-32. doi:10.1177/00220345880670010501
- Mayrhofer, J. M., El-Boustani, S., Foustoukos, G., Auffret, M., Tamura, K., & Petersen, C. C. H. (2019). Distinct Contributions of Whisker Sensory Cortex and Tongue-Jaw Motor Cortex in a Goal-Directed Sensorimotor Transformation. *Neuron*. doi:10.1016/j.neuron.2019.07.008
- Mizuseki, K., Sirota, A., Pastalkova, E., & Buzsaki, G. (2009). Theta oscillations provide temporal windows for local circuit computation in the entorhinal-hippocampal loop. *Neuron*, 64(2), 267-280.
- Mogenson, G. J., Jones, D. L., & Yim, C. Y. (1980). From motivation to action: functional interface between the limbic system and the motor system. *Prog Neurobiol*, 14(69–97).

- Molle, L., & Benoit, C.-É. (2019). The Respiratory Modulation of Memory. *J. Neurosci.*, *39*(30), 5836-5838. doi:10.1523/JNEUROSCI.0224-19.2019
- Moore, J. D., Kleinfeld, D., & Wang, F. (2014). How the brainstem controls orofacial behaviors comprised of rhythmic actions. *Trends in Neurosciences*, *37*(7), 370-380.
- Nishijo, H., Uwano, T., Tamura, R., & Ono, T. (1998). Gustatory and multimodal neuronal responses in the amygdala during licking and discrimination of sensory stimuli in awake rats. *J Neurophysiol*, *79*, 21-36.
- O'Keefe, J., & Recce, M. L. (1993). Phase relationship between hippocampal place units and the EEG theta rhythm. *Hippocampus*, *3*(3), 317-330.
- Paz, R., Pelletier, J. G., Bauer, E. P., & Pare, D. (2006). Emotional enhancement of memory via amygdala-driven facilitation of rhinal interactions. *Nat. Neurosci.*, *9*(10), 1321-1329. doi:10.1038/nn1771
- Pecina, S., & Berridge, K. C. (2005). Hedonic hot spot in nucleus accumbens shell: where do μ -opioids cause increased hedonic impact of sweetness? *J Neurosci*, *25*, 11777-11786.
- Peyrache, A., Benchenane, K., Khamassi, M., Wiener, S. I., & Battaglia, F. P. (2010). Principal component analysis of ensemble recordings reveals cell assemblies at high temporal resolution. *J.Comput.Neurosci.*, *29*(1-2), 309-325.
- Peyrache, A., Khamassi, M., Benchenane, K., Wiener, S. I., & Battaglia, F. P. (2009a). Replay of rule-learning related neural patterns in the prefrontal cortex during sleep. *Nat.Neurosci.*, *12*(7), 919-926.
- Peyrache, A., Khamassi, M., Benchenane, K., Wiener, S. I., & Battaglia, F. P. (2009b). Replay of rule-learning related neural patterns in the prefrontal cortex during sleep. *Nat Neurosci*, *12*, 919-926.
- Poulet, J. F., & Petersen, C. C. (2008). Internal brain state regulates membrane potential synchrony in barrel cortex of behaving mice. *Nature*, *454*(7206), 881-885. doi:10.1038/nature07150

- Ramsden, H. L., Sürmeli, G., McDonagh, S. G., & Nolan, M. F. (2015). Laminar and dorsoventral molecular organization of the medial entorhinal cortex revealed by large-scale anatomical analysis of gene expression. *PLoS computational biology*, *11*(1), e1004032-e1004032.
doi:10.1371/journal.pcbi.1004032
- Robinson, S. L., & McCool, B. A. (2015). Microstructural analysis of rat ethanol and water drinking patterns using a modified operant self-administration model. *Physiol Behav*, *149*, 119-130.
- Rolls, E. T. (2007). Sensory processing in the brain related to the control. In *of food intake. Proc Nutr Soc* *66* (Vol. 96).
- Rothschild, G., Eban, E., & Frank, L. M. (2017). A cortical-hippocampal-cortical loop of information processing during memory consolidation. *Nat Neurosci*, *20*(2), 251-259. doi:10.1038/nn.4457
- Roumis, D. K., & Frank, L. M. (2015). Hippocampal sharp-wave ripples in waking and sleeping states. *Curr Opin Neurobiol*, *35*, 6-12. doi:10.1016/j.conb.2015.05.001
- Salz, D. M., Tiganj, Z., Khasnabish, S., Kohley, A., Sheehan, D., Howard, M. W., & Eichenbaum, H. (2016). Time Cells in Hippocampal Area CA3. *36*(28), 7476-7484. doi:10.1523/jneurosci.0087-16.2016
- Schaefer, A. T., Angelo, K., Spors, H., & Margrie, T. W. (2006). Neuronal oscillations enhance stimulus discrimination by ensuring action potential precision. *PLoS Biol*, *4*, 163.
- Schepisi, C., Cianci, S., Bedse, G., Fu, J., Gaetani, S., & Nencini, P. (2014). Differences in the structure of drinking, cart expression and dopamine turnover between polydipsic and non polydipsic rats in the quinpirole model of psychotic polydipsia. *Psychopharmacology (Berl)*, *231*(19), 3889-3897.
- Schoenbaum, G., Chiba, A. A., & Gallagher, M. (1998). Orbitofrontal cortex and basolateral amygdala encode expected outcomes during learning. *Nat Neurosci*, *1*(2), 155-159.
- Seibt, J., Richard, C. J., Sigl-Glöckner, J., Takahashi, N., Kaplan, D. I., Doron, G., . . . Larkum, M. E. (2017). Cortical dendritic activity correlates with spindle-rich oscillations during sleep in rodents. *Nature communications*, *8*(1), 1-13.

- Siapas, A. G., Lubenov, E. V., & Wilson, M. A. (2005). Prefrontal phase locking to hippocampal theta oscillations. *Neuron*, *46*(1), 141-151.
- Siapas, A. G., & Wilson, M. A. (1998). Coordinated interactions between hippocampal ripples and cortical spindles during slow-wave sleep. *Neuron*, *21*(5), 1123-1128.
- Singer, A. C., & Frank, L. M. (2009). Rewarded outcomes enhance reactivation of experience in the hippocampus. *Neuron*, *64*(6), 910-921.
- Sirota, A., Csicsvari, J., Buhl, D., & Buzsaki, G. (2003). Communication between neocortex and hippocampus during sleep in rodents. *Proc Natl Acad Sci USA*, *100*(4), 2065--2069.
- Tremblay, L., & Schultz, W. (1999). Relative reward preference in primate orbitofrontal cortex. *Nature*, *398*(6729), 704-708.
- Trouche, S., Koren, V., Doig, N. M., Ellender, T. J., El-Gaby, M., Lopes-Dos-Santos, V., . . . Dupret, D. (2019). A Hippocampus-Accumbens Tripartite Neuronal Motif Guides Appetitive Memory in Space. *Cell*, *176*(6), 1393-1406. doi:10.1016/j.cell.2018.12.037
- Vaz, A. P., Wittig, J. H., Inati, S. K., & Zaghoul, K. A. (2020). Replay of cortical spiking sequences during human memory retrieval. *Science*, *367*(6482), 1131-1134.
- Wang, D. V., & Ikemoto, S. (2016). Coordinated Interaction between Hippocampal Sharp-Wave Ripples and Anterior Cingulate Unit Activity. *J Neurosci*, *36*(41), 10663-10672.
doi:10.1523/JNEUROSCI.1042-16.2016
- Welzl, H., & Bureš, J. (1977). Lick-synchronized breathing in rats. *Physiology & behavior*, *18*(4), 751-753.
- Wierzynski, C. M., Lubenov, E. V., Gu, M., & Siapas, A. G. (2009). State-dependent spike-timing relationships between hippocampal and prefrontal circuits during sleep. *Neuron*, *61*(4), 587-596.
- Wilber, A. A., Skelin, I., Wu, W., & McNaughton, B. L. (2017). Laminar Organization of Encoding and Memory Reactivation in the Parietal Cortex. *Neuron*, *95*(6), 1406-1419 e1405.
doi:10.1016/j.neuron.2017.08.033

- Wilkins, E. E., & Bernstein, I. L. (2006). Conditioning method determines patterns of c-fos expression following novel taste-illness pairing. *Behav Brain Res*, *169*, 93-97.
- Wilson, M. A., & McNaughton, B. L. (1993). Dynamics of the hippocampal ensemble code for space. *Science*, *261*(5124), 1055-1058.
- Wilson, M. A., & McNaughton, B. L. (1994). Reactivation of hippocampal ensemble memories during sleep. *Science*, *265*(5172), 676-679.
- Witter, M. P., Doan, T. P., Jacobsen, B., Nilssen, E. S., & Ohara, S. (2017). Architecture of the entorhinal cortex a review of entorhinal anatomy in rodents with some comparative notes. *Frontiers in systems neuroscience*, *11*, 46.
- Yackle, K. (2017). Breathing control center neurons that promote arousal in mice. *Science*, *355*, 1411-1415.
- Yamamoto, T., Matsuo, R., Kiyomitsu, Y., & Kitamura, R. (1988). Sensory inputs from the oral region to the cerebral cortex in behaving rats: an analysis of unit responses in cortical somatosensory and taste areas during ingestive behavior. *J Neurophysiol*, *60*, 1303-1321.
- Yang, M., Logothetis, N. K., & Eschenko, O. (2019). Occurrence of hippocampal ripples is associated with activity suppression in the mediodorsal thalamic nucleus. *Journal of Neuroscience*, *39*(3), 434-444.
- Zelano, C. (2016). Nasal respiration entrains human limbic oscillations and modulates cognitive function. *Journal of Neuroscience*, *36*, 12448-12467.
- Zhang, H., Bethel, C. S., Smittkamp, S. E., & Stanford, J. A. (2008). Age-related changes in orolingual motor function in F344 vs F344/BN rats. *Physiol Behav*, *93*(3), 461-466.
- Zheng, C., & Zhang, T. (2015). Synaptic plasticity-related neural oscillations on hippocampus–prefrontal cortex pathway in depression. *Neuroscience*, *292*, 170-180.

Chapter 2 : Modular Toolbox for Behavioral Electrophysiology

2.1 Abstract

In order to measure spike-scale dynamics, the zeros and ones of electrical brain activity, bundles of conductive threads are positioned near the neural source of interest. From research in animal models, including that of mental disorders, it is increasingly evident that decoding cognitive state requires single-cell to multi-population levels of functional network dissection. Methods of simultaneously listening to many cells in multiple circuits over the timescale of learning are essential to make significant inroads with neurological therapies. While electrophysiology has enjoyed development over many decades, it remains a challenge to scale the electrophysiological recordings with independently targetable electrodes to the multi-population level for a period of learning. For instance, the device needs not to encumber behavior, and the recordings must be stable enough to detect single-unit spiking across multiple circuits while animals actively move around for hours at a time. Additionally, experiments in small animals almost exclusively require multiple subjects and consistency of protocol across an entire cohort of animals requires extreme precision at maximal efficiency. Otherwise, excessive divergence in methodology will either render the data unusable or force the use of more than the minimal number of animal lives. This underscores how technology development that reduces approach variability and maximizes population sampling can directly minimize animal sacrifice and support reproducible science. Presently, we describe the context, process, and validation of our electrophysiological and behavioral recording system, featuring an independently moveable array of electrode bundles for recording from multiple regions of the brain, as well as a reward control and oromotor behavior tracking device. This technology development and approach has now been validated by many researchers over a period of 3 years using an array of behavioral paradigms and targeting of different brain regions. Altogether, the key improvements discussed here increase efficiency and reduce experimental variability, allowing for recording from populations of single units from the multiple areas in the behaving rat with high signal quality.

2.2 Introduction

Although many new techniques for recording from the neural activity are being developed, including those employing optical or laminar probes, drivable electrode arrays continue to be a primary electrophysiological technique. In part, this is because they are relatively inexpensive and have a rich history of probing brain structures that lay deep below the cranial surface without having to resect or demonstrably damage overlying neural tissue ([Aharoni, Khakh, Silva, & Golshani, 2019](#); [Andermann et al., 2013](#); [Ghosh et al., 2011](#)). Additionally, the microdrive approach allows for the indefinite capacity to adjust the recording location of each individual electrode bundle at any point in an experiment while remaining flexible enough not to damage surrounding tissue during animal movement. This allows for either increasing the number of neurons recorded or continuing to follow the same neurons in the face of an inevitable gradual recording position drift.

Like the present report, previous drive designs utilized an array of rotating threaded rod components to enable the independent linear translation of the rod-coupled electrode bundles. However, these other approaches have differed in the specific mode of operation, choosing either hand-crafted shuttles affixed to guide pins, 3D printed shuttle guides ([Blair, 2015](#); "[Halo-18 Microdrive . Neuralynx,](#)"; [Jakob Voigts, Newman, Wilson, & Harnett, 2019](#); [J. Yamamoto & Wilson, 2008](#)), or a combination of 3d printed body with a fixed shuttle spring ([J. Voigts, Siegle, Pritchett, & Moore, 2013](#)). Our approach to the moveable drive leverages the higher precision and lower cost of manufacturing inherent in injection molding, compared to other additive manufacturing processes. Likewise, for other components, we matched manufacturing technology to the specific constraints and tolerances while minimizing costs.

Recent designs for microdrive arrays have utilized 3D-printed components, validating it as the foundational technology to produce the core microdrive body component. Likewise, we used computer-aided design software (Adobe Autodesk Inventor, Fusion 360) to make 3D-printable components for microdrive body, housing, position tracking adapter, and reward port body. Additionally, we use printed circuit board design software (Eagle) to make an electrode interface board, position tracking board, and reward port circuit board. Finally, we exploited recent technological developments in metal casting and 3D modeling to create a modular guide cannula that mates with the microdrive body and can be adapted to target any combination of brain regions.

Our toolbox allows for the reduction in mechanical variability and manual assembly involved in otherwise hand-crafting many additional components, as was the state of affairs in our lab before these developments. In addition to 3D-printing, we exploit multiple technologies to accommodate specific design constraints of different components. Towards validation of our approach, we show results of successful recording from various brain regions, on multiple memory task environments, and decoding of spatial information from spiking in the hippocampus. We have released the toolbox, including design files and part ordering information online at <https://github.com/droumis/physiology>.

2.3 Results

Each major component of the toolbox is described below with information about component context, design decisions, materials, and equipment, along with step-by-step procedures. First, the electrophysiological and behavioral validation of the toolbox is presented. Then, the protocol describes the microdrive assembly, including electrode shuttles, electrode interface board, microdrive body, modular cannula, and housing. The last protocol section covers environmental monitoring and behavioral control with the position tracking diode array and the reward port.

Validation of Technology Development

The tools presented here have been tested by a multitude of researchers targeting many brain regions on various behavioral tasks. Despite other protocols focusing on arbitrary thresholds for size, weight, shape, and precision, we approached definitive validation of the microdrive design through evidence of whether behavioral learning patterns were altered by the presence of the device. To this end, we used a 6-arm, automated variant of the spatial alternation task, in which animals first were rewarded at any reward well, then the contingency changed to where only a certain sequence of three arms was rewarded. Finally, an additional contingency of a different set of three arms was rewarded, requiring animals to recognize and adjust to the changing task demands ([Kastner et al., 2019](#)). This task is sensitive to different behavioral strategies, and as such, is ideal for monitoring extended behavioral learning. We found that animals implanted with this protocol's microdrive were indistinguishable in their learning and performance, as measured by reward probability([Kastner et al., 2019](#)). These results demonstrate that investigations utilizing our microdrive design are applicable to normal behavior and do not encumber the relevant behavior.

Next, we investigated whether the recording quality was high enough to detect known features of neural activity. First, we pooled all the spike waveforms from each hippocampal area CA1 electrode bundle in an awake, behaving rat and then decoded spatial location during detected sharp-wave ripples, looking for the existence reactivated spatial trajectories, which we readily found (**Fig. 2.1 [B]**). Finally, we clustered spiking from CA1 and medial entorhinal cortex (MEC) and confirmed place cell units in CA1 with phase precession (**Fig. 2.1 [C]**), along with grid cell firing in MEC (**Fig. 2.1 [D]**). These results provide evidence for the integrity, signal quality, and behavioral compatibility of our toolbox.

2.4 Microdrive brain implant for chronic extracellular recordings in freely moving animals

2.4.1 Electrode Drive

Context

The purpose of the drive component in a microdrive assembly is to adjust the position of the shuttle-coupled electrode bundle (**Fig. 2.2 [A]**). The primary force is caused by the manual rotation of a custom circular nut with a retaining collar that is embedded within an injection molded shell by casted Metabond. This mechanism provides a controlled thrust in short increments, translating radial spin into linear translation by radially stabilizing the shuttle component with guide pins. The inner of the two metal tube travels with the shuttle and is directly coupled to the n-trode, while the outer guide pin remains in place.

The primary novel part of this work is the design, testing, and validation of the shuttle shell system. Before this work, drives in our lab were constructed by the time-intensive layering of dental acrylic around a circular nut and metal tubes. This was tedious because multiple layers of acrylic needed

to dry, and challenging because the nut had to be rotated inside the drying acrylic at precisely the right moment. Turning the nut too early would create a space around the nut, which could cause vibrations to move the electrode in the brain and severely reduce the sufficient recording time and stability. Rotating the nut too late would crack the fragile acrylic, which would manifest in unpredictable changes during an experiment, or catastrophic loss of the recording site. Additionally, the dental acrylic shuttles required extensive sanding to reduce the size and form the final shape. The presently described protocol automates the shuttle formation and removes the need for precise timing in the drying of adhesive.

Procedure

1. For each n-trode drive, prepare
 - a. 4cm 23G tubing
 - b. 3.5cm 23G tubing. Ream ends with a needle and ensure a 30G wire or tube can easily thread. Roughly score the outside end, up to ~10mm, with a Dremel.
 - c. 4cm 0-80 threaded rod. Notch 10mm of one end halfway through and make a rounded point on the other end. Check that a circular nut can translate from the sharp end to below the notch without a change in resistance.
2. Clean shell by rotating a 23g needle through the 23G holes, starting from the bottom.
3. Screw the nut onto the rod with the two teeth facing notch, flat lip facing pointed end (**Fig. 2.2 [B]**). Apply lube to the nut.
4. Slide a shell up the rod and encase the nut. The base lip of the nut should sit flush within the bottom seat of the shell, and the top teeth of the nut should begin just below the top surface of the shell (**Fig. 2.2 [C]**).
5. Repeat steps 2-4 for remaining drives.

6. Place a drop of cold and fresh Metabond into each shell window (**Fig. 2,2 [D]**). Turn each nut halfway, then apply another drop if necessary. Ideally, Metabond will be flush with outside of shell.
7. Let fully curate for ~1hr.
8. Release the nut from the Metabond by first unscrewing the entire shuttle from the rod, then use a flathead screwdriver to turn the nut teeth. The nut should now turn smoothly within the shuttle.
9. If the nut is too tight after Metabond is cured, add more lube to any exposed part of the nut and spin with hand drill until looser.
10. Ensure the tube is parallel with the rod, then use pliers to put a 3.5cm 23g tube into the inner hole of the shuttle, leaving ~2-4mm of the roughened end sticking above the shuttle surface. Apply thick superglue around the exposed roughened 23g and onto the depression on the shuttle (**Fig. 2.2 [E]**).
11. Insert the longer 23g tube into the outer shuttle hole.
12. Test that the shuttle can travel smoothly down the rod, bringing along the inner tube (**Fig. 2.2 [F]**).

2.4.2 Modular guide cannula

Context

The purpose of the guide-cannula is to direct the electrodes into the brain region of interest. Previously, directing electrodes to multiple brain regions was error-prone because of the difficulties inherent in hand-manufacturing various approach angles and adapting cannula tips to the dimensions of the uneven cranial surface. Additionally, depending on the distance between brain regions and the approach strategy, having multiple bundles of n-trode tubes could put excessive force on the cannula mold, formerly made of hand-layered dental acrylic, that the

targeting could be displaced and warped over time, causing unexpected and brain recording. This could cost months of time and work to detect and correct.

To address these issues, I designed a novel guide cannula system that is machine-fabricated and directly mates with the microdrive body. The primary innovative aspect of this system is the modularity to adapt to any recording target, while keeping the microdrive coupling alignment consistent and fixed (**Fig. 2.3 [A]**). These developments allow for reproducible and simultaneous targeting of multiple brain regions necessary for investigating neural networks at a systems level.

Procedure

1. Determine the position, angle, and dimensions for each cannula. Test injections of a colored dye can help determine implant coordinates.
2. Use these parameters to adapt the guide-cannula template in CAD software.
3. Place order for modified guide-cannula design to be 3D printed in high-definition castable wax and metal cast in stainless steel, see ordering details in the repository.
4. Use a drill to thin the chamfer of cannulae tips (**Fig. 2.3 [B-C]**). This reduces the required craniectomy diameter during surgery while remaining within the design constraints of the manufacturer.
5. Use 4 x 0-80 screws and matching nuts to secure the cannula to the microdrive (**Fig. 2.3 [D-F]**).

2.4.3 Electrode Interface Board

Context

The electrode interface board (EIB) is an accessible head-stage breakout to the electrode wires (**Fig 2.4 [A]**). I designed an EIB that mates with the microdrive body and the head-stage offered by the SpikeGadgets company. The mechanism of electrode attachment is by insertion into a via, or plated through-hole, of soft gold, and subsequent pinning using micro-serrated small gold pins supplied by the Neuralynx company, as is shared with other microdrive protocols. When pressed into an electrode-loaded EIB via, these pins strip the insulation of the electrode wire and hold the exposed wire against the deposited soft gold via. Because of the fragility of the electrode wires, considerable trial and error was required before finding a suitable PCB fabrication pipeline and parameter set. Notably, the EIB must be made with special request 99.9% gold plating (Grade A: Hardness range is 70 Knoop). Additionally, the screw holes on the EIB must be countersink milled to retain a flush surface for the head-stage and extender board to attach. Below, I detail the steps of populating the EIB with connectors.

Procedure

1. Apply a thin layer of superglue along the center of the EIB connector pad, avoiding contact with metal traces (**Fig. 2.4 [B]**).
2. Place connector on pad without spreading glue onto connector feet or metal trace pads. Ensure alignment between all pads and connector feet. Let the glue completely dry before proceeding.
3. Apply flux to all connector feet and EIB pads.
4. Use a small amount of solder to secure corners of connector feet to pads (**Fig. 2.4 [C]**).

5. Apply additional solder to remaining feet/pad interfaces, starting from one end and lightly dragging the soldering iron across all contacts. The solder should distribute to all contact points (**Fig. 2.4 [D]**).
6. Apply a very thin layer of superglue to insulate the contacts (**Fig. 2.4 [E]**).
7. Test alignment of connectors by plugging in head-stage
8. With a multimeter, test all connector lines with EIB electrode via, including all neighboring pairs for shorts. Use solder wick to remove any excess solder causing shorts between neighboring contacts.

2.4.4 Microdrive body fabrication

Context

The purpose of the microdrive body is to hold the individual drives together with the guide-cannula and EIB. The previous iteration of the microdrive body was attached to head-stage and guide-cannula through the time-intensive and error-prone manual layering of dental acrylic. Additionally, the protective casing for the previous microdrive was constructed from a surgical glove box cardboard that was loosely taped together. Critical improvements to the microdrive design include built-in mating with the novel modular guide-cannula, attachment points for the novel and robust protective casing, and attachment points for the EIB. The protocol below describes the process of joining together all the components of this new microdrive assembly.

Procedure

1. Create the skull-attached part of the ground wire by soldering a 2" insulated cable to the two threads closest to the head of a bone screw. This may require liberal use of flux. Solder the other end to a 2 x 2 male Mill-max connector (**Fig. 2.5 [A]**).
2. Create the microdrive-attached part of a ground wire by soldering a 2" insulated cable to a 2 x 2 female Mill-max connector, leaving the other end bare (**Fig. 2.5 [B]**).
3. Drill a small hole through the side of the microdrive body. Avoid puncturing any drive holes. Thread the open end of the braided ground wire through the hole.
4. Solder this wire to the ground via on the EIB and glue the female Mill-max to the outer side of the microdrive body.
5. Insert two 0-80 threaded rods through the smaller two holes on the top of the microdrive head (**Fig. 2.5 [C]**). The threaded rod reinforces the full length of the neck of the microdrive. Cut the top of the threaded rod until flush with the top of the microdrive head.
6. Insert two 2-56 nuts under the head of the drive (**Fig. 2.5 [D]**). These will secure the EIB to the microdrive body. Glue the nuts in place without compromising the threads.
7. Screw the EIB to the head of the drive using countersink screws.
8. Load four 0-80 nuts into the side compartments of the microdrive (**Fig. 2.5 [E]**). These will secure the housing to the drive body.
9. For each n-trode, prepare one:
 - a. ~9cm of 5.5mil steel wire. Ensure the ends are not crimped.
 - b. ~8cm of 30G hypodermic stainless-steel tubing. Ensure the ends are not crimped.
10. Thread each 5.5mil wire into a 30G tube. Then thread each 5.5mil-loaded 30G through one of the guide-cannula holes from the bottom. Continue threading through the microdrive body (**Fig. 2.5 [F]**). Use a drop of superglue at the interface of the bottom of the microdrive and each 30G to prevent slippage.

11. Once all the 30G tubes have been installed into the microdrive body, pull the 5.5mil wire from the top so that only ~2mm is protruding from the bottom.
12. Use the Dremel with a diamond-tip blade to cut off excess 30G, making flush with the bottom surface of each cannula (**Fig. 2.5 [G]**).
13. Using forceps, push 5.5mil wire from the top of the 30G to poke through the newly cut surface at the bottom of the cannula. If unable to move, use a hypodermic needle to poke the bottom of the cannula to separate the 5.5mil from the 30G.
14. Pull 5.5 mil wire from the bottom so that only a ~2mm is protruding from the top of 30G. Using a diamond-tip Dremel blade, cut the 30G 2mm above the head of the microdrive body (**Fig. 2.5 [H]**).
15. Push the 5.5 mil wire through the 30G from bottom to ream out the newly cut end of 30G. Ensure that 5.5 mil can travel up and down the 30G.
16. Use a camera mounted on surgery scope to take a closeup picture of the bottom of the cannula, then one at a time, push a 5.5mil wire through the bottom of the cannula, and note which number n-trode corresponds to each 30G hole on the bottom of the cannula.
17. For each n-trode drive, mark the lower 2mm of the inner 23G with a sharpie to note the upper limit of travel. Thread inner 23G of each shuttle onto a 30G emanating from the top of the microdrive. Screw the 0-80 rod of the shuttle into the center hole of each microdrive body shuttle position. Use pliers to insert outer 23G into outer hole.
18. Screw each shuttle down the threaded rod until resistance is felt. This is where the inner 23G reaches its limit towards the bottom of the microdrive body. Mark this bottom limit on the inner 23G with a marker.
19. If any shuttles touch each other when lowered, remove offending shuttles and shave to make thinner, then reinsert onto microdrive.
20. For each shuttle, remove 5.5mil wire from 30G, then cut 3cm piece of polyimide and insert into inner 23G, and down into the 30G, leaving 2-3mm to stick out of the top.

- 21.** Cut a 1 x 1mm piece of lab tape. Make a slit halfway through to the center of the tape. Place the tape around the exposed polyimide. This will prevent it from falling further into the 30G while loading the n-trode and will avoid having to use glue at this stage.
- 22.** For each n-trode, trim untwisted ends to the same length, ~4mm above where they are fused. Thread the knotted end of the n-trode through a non-plated hole on the EIB, aimed at the corresponding shuttle. Use a 1mm piece of foam to fill the non-plated hole to hold the n-trodes in place.
- 23.** Guide the twisted end of the n-trode into the polyimide and lower until it comes out of the bottom, leaving enough slack at the top to allow the shuttle full travel.
- 24.** Use forceps to pin each of the electrode wires into the corresponding plated EIB vias. Press pins firmly to ensure connection.
- 25.** Load remaining drives with n-trodes and continue pinning all electrodes to EIB. Check for any cut wires and redo if needed.
- 26.** With all shuttles at the top of their travel, trim n-trodes coming out of cannula to the same length.
- 27.** Check the connectivity of the n-trodes. Replace any electrode with a pre-plating resistance > 6 MOhm.
- 28.** Glue n-trodes to polyimide, then remove the tape from polyimide and glue polyimide to the 23G.
- 29.** Apply glue to the interface of the pin/electrode/EIB to hold in place.
- 30.** ETO sterilize microdrive. This may take a couple of days.
- 31.** Lower one n-trode to the desired length, noting where on the n-trode it was protruding from the cannula when the shuttle was fully retracted. Cut the n-trode at this point with serrated scissors at a 45-degree angle. Repeat for remaining n-trodes.
- 32.** Install cone and cap housing to microdrive while not actively working on microdrive, and again immediately before surgery.

2.5 Environmental Monitoring and Behavioral Control

2.5.1 Position Tracking Diode Assembly

Context

The purpose of the diode assembly is to facilitate position tracking of the animal from a ceiling-mounted camera in low-light conditions with potential occlusion from wires and suspension system. Previously, the animal was tracked from a light ring that was constructed from bending plastic and taping copper as metal traces to which LEDs were soldered. There was also a second cluster of lights on a 'tail' component that protruded behind the animal's head. Common issues with this design were that the tail often led to the animal bumping into walls or having a startle response from the looming stimulus. Additionally, there was no standardization to the size, height, or placement of LEDs, which could affect speed, head-direction, and position generalizations across experiments. Additionally, because the light ring had been attached directly to pre-amplifiers, each wall collision would potentially damage the head-stage or introduce a noise artifact. Key improvements presented here include the design of a printed circuit board for the light ring and a 3D printed casing that coupled to the microdrive housing cone. These improvements standardized the tracking light and reduced risk to head-stage electronics.

Procedure

1. The head-stage has a 3-pin female Mill-max connector, with the outermost pins to route power and ground for the tracking array. Using a ~2" insulated two-wire cable, construct a jumper by soldering a 3 x 1 male Mill-max on one end and a 2 x 2 male Mill-max on the other side. On the side with 3 x 1 Mill-max, do not solder the middle pin to a wire. On the 2 x 2 side, solder two pins to each wire (**Fig. 2.6 [A]**).

2. Solder female 2 x 2 Mill-max to PCB ring (**Fig. 2.6 [B]**). Solder adjacent pads together as shown (**Fig. 2.6 [B]**).
3. Solder five red (toward the back of the animal) and five green (toward the front of the animal) surface mount LED's on PCB ring at diode symbol (**Fig. 2.6 [C]**). Orient the anode away from the ring center. Use a multimeter to confirm polarity. Note that many LED's come with a green stripe corresponding to the anode.
4. Solder a resistor next to each LED installed (**Fig. 2.6 [C]**).
5. Check completed ring light with a 5V DC power supply (**Fig. 2.6 [D]**). Confirm that less than ~20 μ A current is being drawn to power the light. Exceeding this may cause damage to head-stage.
6. Use superglue or transparent epoxy to insulate any exposed traces or pads.
7. Install PCB ring into 3D printed housing and adhere nuts to mating point (**Fig. 2.6 [E-F]**).

2.5.2 Reward Port

Context

Previous reward wells suffered from several issues. First, the interface was not compatible with modern electrophysiological systems. Second, liquid reward often accrued in the well. This led to animals occasionally receiving reward on inaccurate trials by collecting the reward leftover from previous correct trials. Third, the zone of detection was positioned such that animals triggered reward delivery when they would step on the reward well when they were exploring beyond the edge of the track. Finally, older designs did not have a built-in sensor cue delivery system to aid in memory tasks. The method presented here improves upon these limitations with a novel reward-port design with a draining trough, a constrained trigger zone, and integrated electronics for modern electrophysiological systems.

Procedure

1. The reward port will arrive with the back panel attached to the front of the port. Separate rear panel by cutting through attachment pegs with clippers. Smooth remaining peg fragments with sandpaper.
2. Install the hex nuts into their sockets (**Fig. 2.7 [A]**). The nuts should be held in place by friction, and not fall out on their own. Ensure that screws align with nut.
3. Snap the RJ45 connector through the backside of the PCB, aligning to the set of 12 holes. Solder the metal RJ45 pins to the PCB in place (**Fig. 2.7 [B]**).
4. Solder the resistors to the labeled pads (**Fig. 2.7 [B]**; R1: 1.02 kOhm; R2: 10 kOhm).
5. *Optional*. Install LED on the trough-facing side of PCB to use as a controllable sensory cue, along with resistor R3 (resistor dependent on LED selected).
6. Wrap the cylindrical heads of PT and IR LED with electrical tape; only the rounded tip should remain exposed. This prevents unwanted light scatter and adds a tighter fit to the reward port to prevent liquid entry to the electronics.
7. Cover the PT and IR LED pins with heat-shrink and heat with heat gun.
8. With reward port's trough facing away, insert the head of the IR LED into the left side of the port, PT into the right side. With the ground pin on the bottom bend the pins at 90 degrees into the side grooves of the reward port. Remove heat-shrink that protrudes into the PCB seat.
9. Thread the PCB onto the IR LED and PT pins so that the PCB rests on the back of the reward port. The RJ45 jack should be aligned with the bottom opening of the port. Screw the PCB to the reward port. Then solder the pins to the PCB and snip any part of the soldered pins that protrude beyond the solder joint (**Fig. 2,7 [B-C]**). Cover the back of the PCB with electrical tape to insulate from back housing.

10. Slide the back panel onto the back of the reward port and screw in place on the side holes.
11. Secure the reward port to the behavioral track using the port legs (**Fig. 2.7 [D]**).
12. Some users have experienced lick-artifact in electrophysiological recordings. One possible solution has been to add a grounding wire from the behavioral track to the reward liquid using an alligator clipped to the track with a wire in contact with the liquid (**Fig. 2.7 [E]**). Other users have found success leaving the reward wells in a desiccator when not in use. Others have found success, ensuring that the PCB components are well insulated and not making contact with the reward port.
13. Some 3D printed materials, and printers, are too fragile for many mating cycles of the 3D printed tubing screws threads. Some users have opted to add off-the-shelf Luer lock plastic components to the 3D-printed tubing holes using super glue or dental cement. Others have used an adaptor that very seldomly needs to be removed, thereby moving the mating cycle stress to the easily replaceable adapter. (**Fig. 2.7 [E]**).

2.6 Discussion

Electrophysiology in freely moving animals has been limited by technical bottlenecks related to scaling up the recording sites and the complexity involved in simultaneously targeting multiple brain regions. Previous investigations in our lab have been hindered by time-consuming microdrive fabrication, a skill that trainees had to master before recordings could begin. It was our attempt here to increase reproducibility and standardization by using computer aided design and modern manufacturing technologies to reduce variability and increase likelihood of interpretable experiments. Our toolbox has now been tested by many users with various requirements, and succeeds using an integrated design approach, where the sensor circuit board was embedded within the reward port body, the modular cannula and EIB mated with the microdrive body, and the ring circuit board coupled to the microdrive housing through an adapter. We show validation of our toolbox with recordings from the established results of spatial selectivity and phase precession, along with indistinguishable learning performance between implanted and non-implanted animals.

The remaining drawback to our approach is the reliance on hand-pinning electrode wires to the electrode interface board and the use of custom milled nuts. Future work can address this shortcoming by utilizing off the shelf components or employ a different mechanism of linear translation. Connectorization may also be improved upon by printing flexible circuit traces that connect the head-stage to individual electrode shuttles, easing the path to process automation.

Future improvements to the reward port include the integration of additional sensors or close-up video capture, in order to further enrich the environmental monitoring; a mini ~100 frames/second

camera could be integrated within the reward port housing. Altogether, these tools represent a coordinated effort across software design programs and manufacturing processes to facilitate research required for impactful research into our cognitive processes.

2.7 Figures

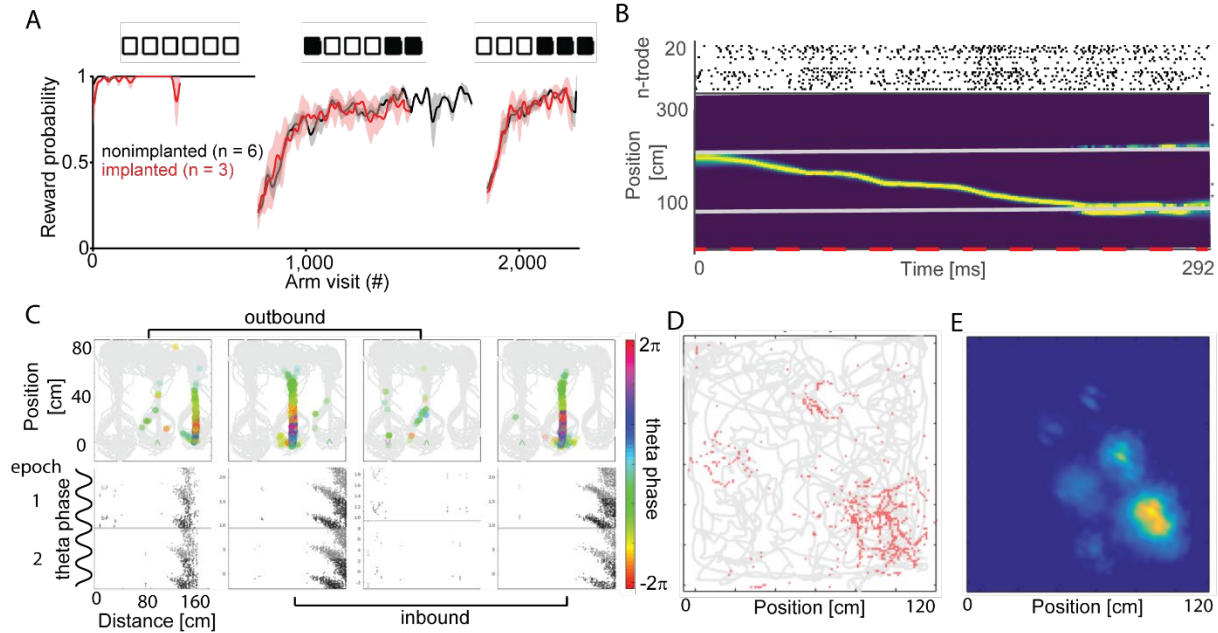


Figure 2.1 | Validation of Microdrive Implant

(A) Microdrive-Implanted and nonimplanted animals learn similarly on an automated 6-arm variant of the W-track spatial alternation task over contingency changes. In the leftmost contingency, animals are rewarded for visiting any port (errors occur when they go down the arm, but do not poke in the reward well). In the next contingency, animals were rewarded for visiting the third arm ('home') in between alternations to the 2nd and 4th arms (3-2-3-4-3...). The next contingency has the 2nd arm as the 'home' and the animal must alternate outbound trials to the 1st and 3rd arms (2-1-2-3-2...), is exploration where the animals get rewarded wherever they go. **(B)** Spatial decoding of multiunit from dorsal hippocampal area CA1 on a 3 arm W-track task during a locally detected sharp wave ripple event. Top shows spikes from each n-trode by row. Middle is decoded posterior of linearized position. The three panels within this posterior plot are the three W arms stacked center, right, left arms from bottom to top, with the reward port locations at the bottom of each. The animal's current position is at the center reward port and is demarcated with a dashed red line. **(C)** Example of theta-phase precession from a CA1 recording site. Top row shows 2D trajectory-type separated animal position (gray) and spike locations colored by phase of hippocampal theta. Bottom shows first and second W-maze epoch of the session stacked vertically, for the corresponding trajectory-type. **(D)** Example of unit recorded in medial entorhinal cortex showing grid-like firing pattern. Raw spike positions are in red and animal position is shown as a gray path. **(E)** 2D autocorrelation of unit shown in **D**, highlighting the periodic nature of the firing pattern.

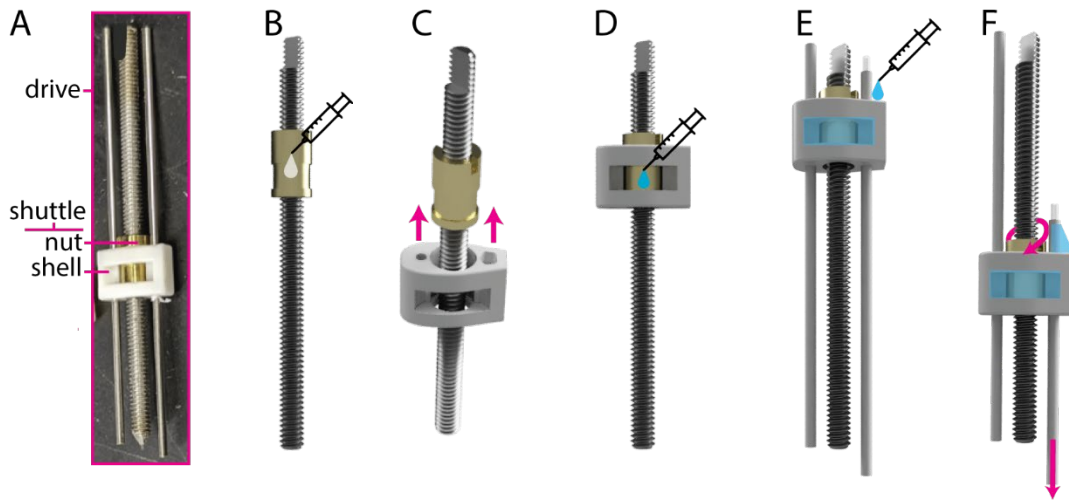


Figure 2.2 | Fabrication of the N-Trode Drive

(A) Image of drive showing the terminology used in the protocol. **(B)** Nut is screwed on to the rod and thin machine lubricant is applied around the outside of the nut. **(C)** Shuttle shell is pushed up to encase the nut. **(D)** With the nut's lower lip sitting below the exposed side window of shell, Metabond is applied through the window and left to cure. After curing, the nut is twisted free of the Metabond, but will remain encased in place within the shell, completing the shuttle. **(E)** The side of the top inner 23G tube is glued to the top of the shuttle shell, **(F)** creating the mechanism for rotational to linear thrust bearing.

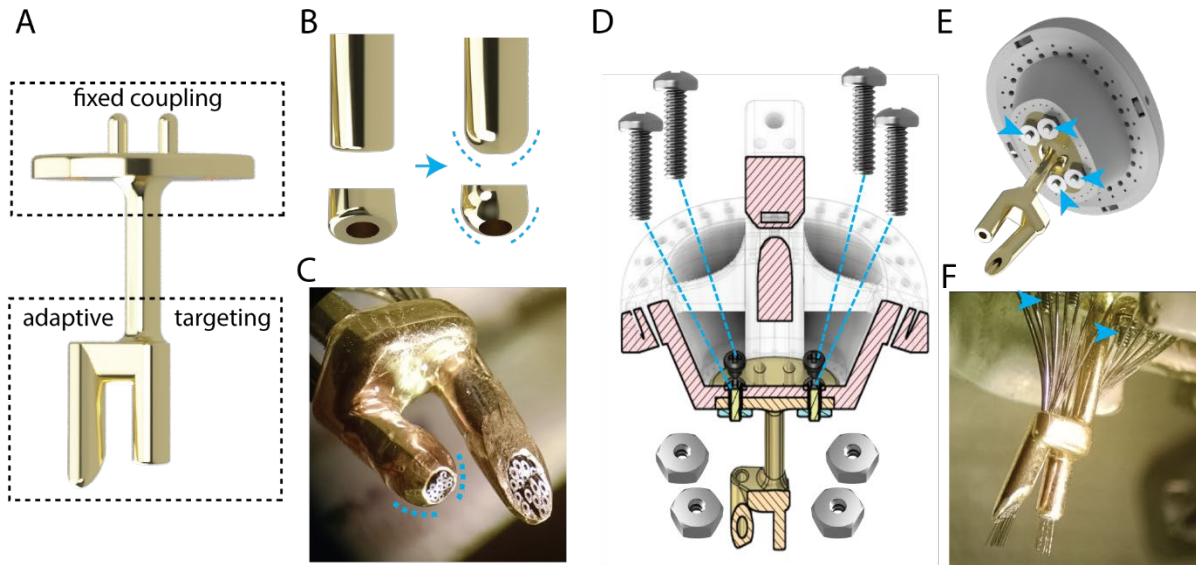


Figure 2.3 | Modular Guide-Cannula

(A) Guide-cannula featuring a fixed coupling base and customizable targeting cannulae. (B) Chamfering the cannulae tip. (C) Cannula that has been beveled. (D) Sectioned schematic of the microdrive showing the cannula mating with the microdrive body using 4 screws and nuts. (E) Underside view of cannula mated with microdrive body. (F) Image showing cannula of completed microdrive with tubing and n-trodes emerging from the bottom.

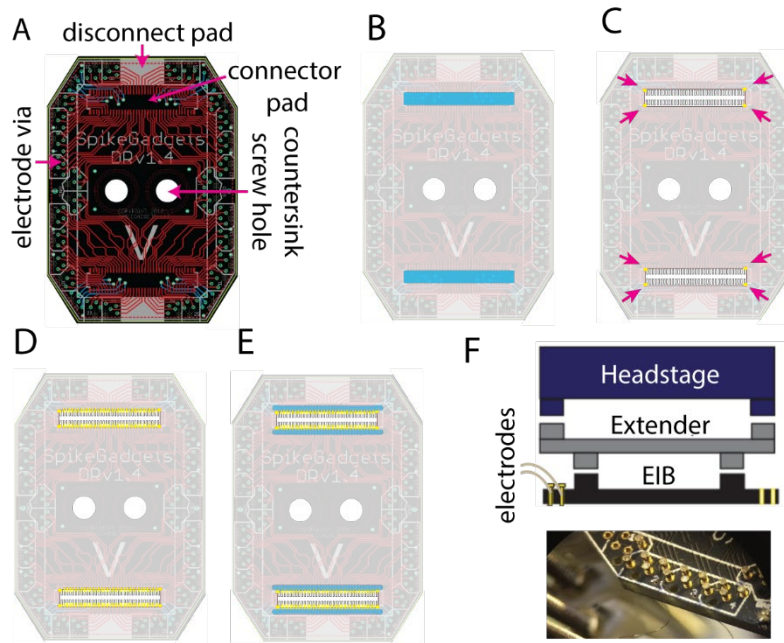


Figure 2.4 | Populating Electrode Interface Boards

(A) Electrode interface board featuring pads for leveraged disconnection and countersink holes to mate with microdrive body. **(B)** Blue region highlights where thick layer of superglue should be applied on the EIB. **(C)** pink arrows and yellow marks show where to solder the ground pins to the connector. **(C)** yellow lines show where to connect all the connector feet to the EIB pads. **(D)** Blue region shows where to apply thin layer of superglue to reinforce solder joints. **(F)** Gold pins are used to attach the electrode to the EIB. A side profile of the extender board is also show attached with head-stage

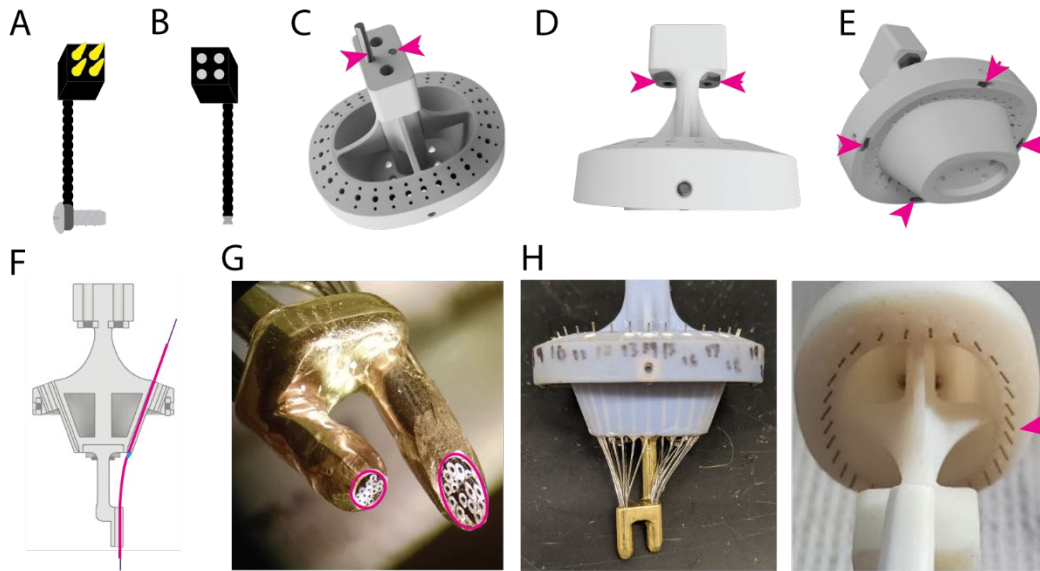


Figure 2.5 | Microdrive Assembly

(A) Skull attached component of the ground-wire. Male Mill-max connector with braided cable and soldered to a bone screw. (B) The microdrive-attached component of the ground-wire. Female Mill-max connector with braided cable. Bare end will be soldered to EIB ground. (C) Arrows show insertion of threaded rod into the neck of microdrive. (D) Arrows show nuts in microdrive neck. (E) Nuts are secured in the side holes as attachment points for housing. (F) Section through microdrive shows metal tubing for a single n-trode. (G) Metal tubing is cut as to be flush with the bottom of the cannula. (H) Metal tubing is trimmed at the top of the microdrive.

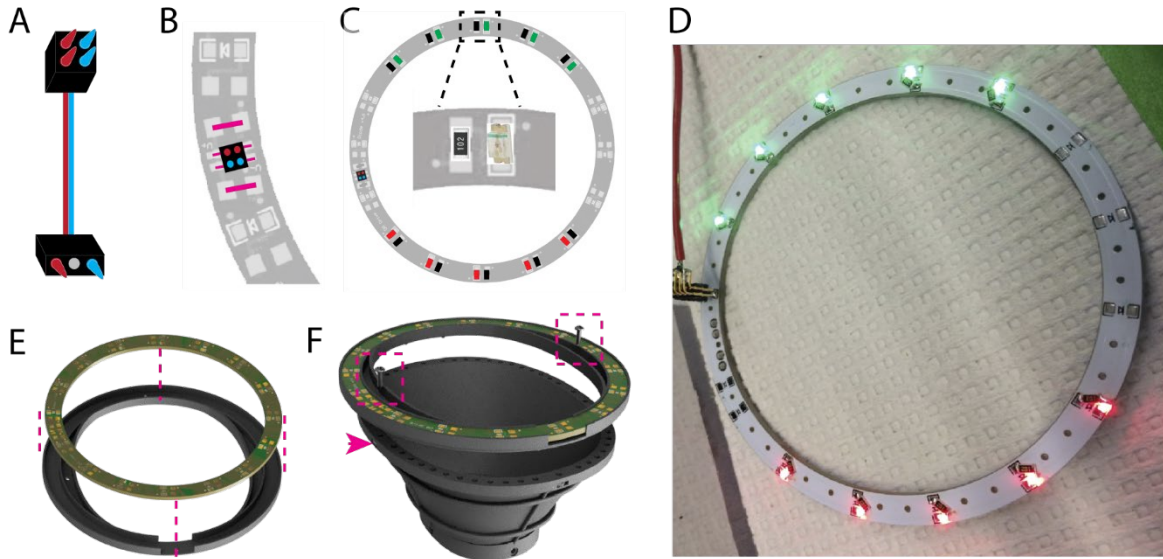


Figure 2.6 | Position tracking diode array

(A) Jumper cable connecting the diode array to the head-stage. (B) Female Mill-max soldered to the diode ring. The adjacent pads are shorted together as shown in pink. (C) Surface mount resistors and LEDs populate the diode ring. (D) Test the diode array to ensure proper current draw. (E) Diode array mates with 3D-printed adapter. (F) Adapter mates with microdrive housing.

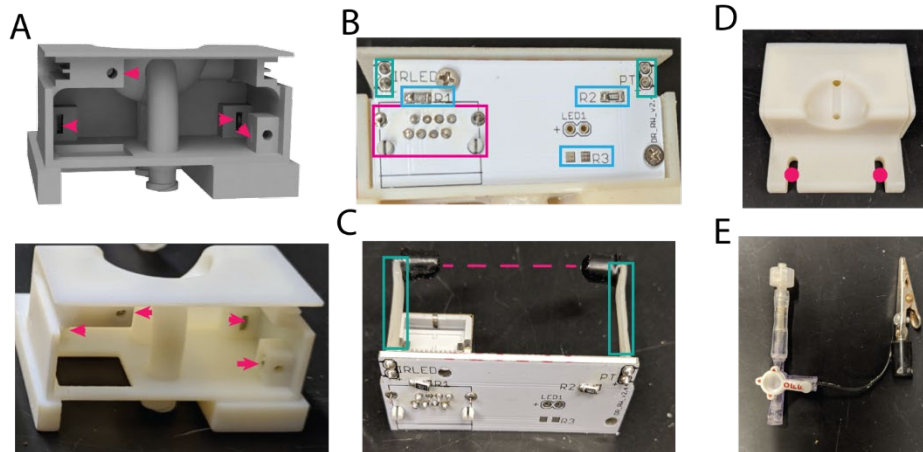


Figure 2.7 | Entry Detection and Reward Delivery Port

(A) Exposed back view of reward port demonstrating insertion points in pink for hex nuts with model (top) and completed real (bottom) view. **(B)** Pink rectangle highlights RJ45 pins snapped into place and soldered to PCB. Blue rectangles show resistor pads. Green rectangles show IR LED and PT pins soldered to the PCB and trimmed. **(C)** Completed PCB showing the face-to-face positioning of IR LED, and PT in pink. The heat-shrink on the pins are highlighted by the green rectangles. The reward port is omitted in order to visualize components. **(D)** Front view of completed reward port showing position of screws for attaching port to behavioral track. **(E)** Tubing adapter to reduce mating cycles with reward port, and to allow grounding with an alligator clip.

2.8 References

- Aharoni, D., Khakh, B. S., Silva, A. J., & Golshani, P. (2019). All the light that we can see: A new era in miniaturized microscopy. *Nature Methods*, *16*(1), 11.
- Andermann, M. L., Gilfoy, N. B., Goldey, G. J., Sachdev, R. N., Wolfel, M., McCormick, D. A., . . . Levene, M. J. (2013). Chronic cellular imaging of entire cortical columns in awake mice using microprisms. *Neuron*, *80*(4), 900-913. doi:10.1016/j.neuron.2013.07.052
- Blair, H. (2015). OvalDrive36: A chronically implantable microdrive system for brain-wide single-unit recording, optogenetic stimulation, and cyclic voltammetry in behaving rats. In.
- Ghosh, K. K., Burns, L. D., Cocker, E. D., Nimmerjahn, A., Ziv, Y., Gamal, A. E., & Schnitzer, M. J. (2011). Miniaturized integration of a fluorescence microscope. *Nat Methods*. doi:10.1038/nmeth.1694
- nmeth.1694 [pii]
- Halo-18 Microdrive . Neuralynx.
- Kastner, D., Miller, E., Yang, Z., Roumis, D., Liu, D., Frank, L., & Dayan, P. (2019). *Dynamic preferences account for inter-animal variability during the continual learning of a cognitive task*.
- Voigts, J., Newman, J. P., Wilson, M. A., & Harnett, M. T. (2019). *An easy-to-assemble, robust, and lightweight drive implant for chronic tetrode recordings in freely moving animals*. Cold Spring Harbor Laboratory. Retrieved from <https://dx.doi.org/10.1101/746651>
- Voigts, J., Siegle, J. H., Pritchett, D. L., & Moore, C. I. (2013). The flexDrive: An ultra-light implant for optical control and highly parallel chronic recording of neuronal ensembles in freely moving mice. *Frontiers in systems neuroscience*.
- Yamamoto, J., & Wilson, M. A. (2008). Large-scale chronically implantable precision motorized microdrive array for freely behaving animals. *Journal of Neurophysiology*, *100*(4), 2430-2440.

Chapter 3 : Conclusion and Discussion

3.1. Significance of Memory Reactivation Synchronization with Rhythmic Movement

Previous evidence suggested that whisking and sniffing may act to stereotypically fragment the stream of exploratory sensory processes ([Halpern, 1983](#); [Kepecs, Uchida, & Mainen, 2006](#); [Kleinfeld et al., 2006](#); [J. D. Moore, 2013](#); [Nicolelis et al., 1995](#); [Tort, Brankačk, & Draguhn, 2018](#)). Recent work demonstrated that the respiration phase was synchronized with sharp-wave ripple (SWR) occurrence ([Karalis & Sirota, 2018](#); [Y. Liu et al., 2017](#)), motivating the question if other rhythmic orofacial oscillations may influence hippocampal activity. Crucial evidence has linked licking with increasing spike-timing precision over the course of learning and across the sensorimotor-reward brain regions ([Ranier Gutierrez et al., 2010](#)). And although there are direct projections between these regions and the hippocampal formation, it remained unclear whether quasiperiodic licking input during reward-based learning could influence SWR-replay.

To this picture, our novel findings contribute the alignment of SWR-replay with the licking phase at the reward port of a spatial alternation task, implicating coordination of sensorimotor-reward networks with memory processing. Our study is the first to examine the orofacial modulation of SWR occurrence in freely behaving animals learning a memory task. These findings suggest that feed-forward and feed-back processes may be exploiting cross-frequency coupling to minimize energy expenditure or gate the encoding and integration of ongoing behavior with the implementation of prior learning.

A potential reason for the previous scarcity of attention on this issue was the technical and integrative complexity of these experiments. As presently depicted, such experiments require multi-domain specialization to develop customized tools for sufficient chronic sampling of units across multiple recording sites from animals freely behaving during a learning task, while simultaneously monitoring port entry events. These developments form the primary technological

advance of this dissertation and is freely available to the research community as an open-source novel electrophysiological and behavior toolbox. Demonstrated by the successful adoption of these tools in diverse experiments, these tools advance enhance research capability and reduce the harm to animals by working to reduce experimental variability.

Altogether our efforts represent an advancement in understanding how the orofacial movement for active sampling and reward ingestion can synchronize with mechanisms of association formation. In addition to licking being a behavior used to monitor animal models of disorders such as mental illness ([Galistu et al., 2011](#); [Hartfield et al., 2003](#); [Schepisi et al., 2014](#)) and aging ([Zhang et al., 2008](#)), our results could facilitate future work to address critical questions in compulsive consumption of diet-induced obesity, eating disorders, and alcohol ([Barkley-Levenson & Crabbe, 2012, 2015](#); [Robinson & McCool, 2015](#)) or drug addiction ([Eastwood et al., 2014](#)).

Our results suggest that more considerable attention be paid to head movements during periods of reduced locomotive velocity, which are often categorized as ‘immobile.’ This terminology of the spatial memory-task behavioral state is used as a convenient simplification; however, given the pervasive impact on memory networks currently presented, the appropriate experimental design must be employed to avoid misinterpretation of neural activity. Understanding how oromotor activity interacts with memory replay is critical to our knowledge of how the internal state interacts with externalized behavior. A remaining question is whether the licking movement influences hippocampal activity through sensory afference or motor efference.

3.2 Reafference and Corollary Discharge Underlying Replay-Movement Synchrony

What are the likely pathways linking oromotor rhythmicity and hippocampal modulation? A study in humans implicated the olfactory reafferent rhythm in the modulation of hippocampal delta oscillations (0.5– 4 Hz) ([Zelano, 2016](#)), with hippocampal delta activity elsewhere being shown to entrain the occurrence of SWRs ([Axmacher et al., 2008](#)). Two other studies in rodents have implicated respiration in the entrainment of SWR occurrence, one during sleep ([Karalis & Sirota, 2018](#)), and the other during awake head fixation ([Y. Liu et al., 2017](#)). Interestingly, these studies come to somewhat opposing conclusions as to the anatomical pathway of influence. In the sleep study, SWR synchronization remains following an olfactory afferent disruption, which leads the authors to conclude that the respiratory corollary discharge emanating from the brainstem likely plays the modulatory scaffold for hippocampal output. The study in the awake, head-fixed state found a reduction in SWR entrainment after the suppression of olfactory reafference, leading them to conclude an olfactory reafference as being the primary SWR orchestrator. What could explain the discrepancy between these studies?

First, the method of disruption of sensory activity differed, and therefore the nature of manipulated activity likely changed. The awake study used a bilateral injection of viral vector construct, which expressed designer receptors exclusively activated by designer drugs, allowing for temporary suppression of respiration-locked sensory projections onto the olfactory bulb. In contrast, the sleep study used methimazole injection, which ablates olfactory epithelium that hosts the mechanoreceptor-expressing sensory neurons ([Bergman, Ostergren, Gustafson, & Brittebo, 2002](#); [Grosmaître, Santarelli, Tan, Luo, & Ma, 2007](#)), effectively depriving the olfactory bulb of respiratory input.

Second, although the awake state study had animals head-fixed in place, the animals were still in opposing states of arousal with different sensorimotor contextual complexity. Notably, the functional specialization of SWRs in sleep vs. awake states differs in multiple characteristics ([Roumis & Frank, 2015](#)), which may be indicative of the varying weight of influence of sensory vs. motor activity. The evidence of respiratory pathway of impact on the hippocampus appears to be a dual mechanism of entrainment, emerging from both olfactory reafferent and respiratory corollary discharge emitted by the brainstem ([Karalis & Sirota, 2018](#)), with dynamic degrees of reliance depending on state and context.

These studies provide insight into a potential pathway for licking influence on the hippocampus, because, during licking bouts, the slower breathing oscillation is cross-frequency coupled with the faster licking oscillation ([Welzl & Bureš, 1977](#)). Additionally, respiration and licking have separately been shown to entrain overlapping networks in the frontal cortex, nucleus accumbens, and amygdala ([Ranier Gutierrez et al., 2010](#); [Karalis & Sirota, 2018](#)), and they both are controlled by overlapping brainstem pacemaker circuits. Although there is a coordination of rhythmic oromotor behaviors by shared brainstem circuitry, the pathway underlying the present results must additionally take into consideration the gustatory network that licking primarily engages. As noted, a previous study found licking modulation in multiple regions ([Ranier Gutierrez et al., 2010](#)) including the insular cortex which is involved in interoception ([Accolla & Carleton, 2008](#); [Katz et al., 2001](#); [Livneh et al., 2020](#)), and the reward-action network consisting of the orbitofrontal cortex ([E. T. Rolls, 2007](#); [Tremblay & Schultz, 1999](#)), amygdala ([Pecina & Berridge, 2005](#); [Schoenbaum et al., 1998](#)), and nucleus accumbens ([Mogenson et al., 1980](#)). The amygdala, insula, and cortex all project to the nucleus accumbens, forming an integration point for oromotor evaluation. The confluence of lick-induced spike synchrony across multiple targets of hippocampal input and output suggests many pathways of possible influence.

3.3 Active sensing is associated with effective processing

Neural activity and environment control behavior. Predictable timing of neural reactivation relative to the phase of an externally manifested action implies the existence of a consciously triggered global clock that can hierarchically orchestrate spike timing and thereby affect synaptic modification. From an ethological perspective, a voluntary movement that is shown to synchronize the activity of memory and taste-reward networks will impact how information flows in the brain and therefore have the potential to change reward-driven behavior and affect the survival of the organism.

In addition to effecting change in synaptic networks, extensive evidence exists that active sensing involving expectation and volition changes the sensory response in licking ([Mayrhofer et al., 2019](#); [Wilkins & Bernstein, 2006](#)), somatosensory ([Krupa et al., 2004](#)), auditory ([Eliades & Wang, 2008](#)), and olfactory ([Fuentes et al., 2008](#)) modalities. This is consistent with the increased delay of identification in experiments employing passive reward delivery via an intraoral cannula ([Katz et al., 2001](#)), compared to active sensing state ([Poulet & Petersen, 2008](#)). Additionally, evidence shows that sniffing-induced theta oscillations enhance discrimination by ensuring spike time precision in the olfactory system ([Schaefer et al., 2006](#)).

From these findings, it's clear that learning induces a significant functional reorganization of neural activity throughout significant components of the taste–reward and memory networks. We speculate that cross-frequency coupling between ~8 Hz licking oscillations in both the motor and sensory circuits interact with hippocampal SWRs through cross-frequency coupling. This may thereby serve as a mechanism to transfer information from sensorimotor brain networks operating

at behavioral timescales to the fast processing required for practical neural computation and synaptic plasticity, thus integrating taste-reward signaling with memory processing.

3.4 Speculative Role of Synchrony Between Oromotor Phase and Memory Reactivation

Does oromotor entrainment influence tasks relate to hippocampal function? Recording from intracranial EEG in humans, it has been shown that LFP in the hippocampus, amygdala, and piriform cortex are all entrained to respiration, and that performance on a memory recall task is sensitive to the phase of nasal breathing when the stimulus is initially presented ([Zelano, 2016](#)). Complementary to our claim that rhythmic licking bouts are privileged periods regarding the efficiency of reactivated information flow, these results show that in humans, the efficacy of encoding sensory stimuli is predicted by an externally identifiable phase of orofacial behavior.

Foundationally, a study in rodents discovered that proficiency in solving reinforcement-based associative cue learning required licking-induced synchrony across neural ensembles of the frontal cortex, insular cortex, nucleus accumbens, and amygdala ([Ranier Gutierrez et al., 2010](#)). This is consistent with other reports of licking-related activity in these regions ([R. Gutierrez et al., 2006](#); [Nishijo et al., 1998](#); [T. Yamamoto et al., 1988](#)). Additionally, the authors attributed the reduction in spike timing variability over learning to lick-coherency, as the cue-selective neurons that most effectively discriminated stimulus identity were selectively synchronized activity with licking. Moreover, it was found that for most lick-synchronized neurons, phase-locking was epoch-specific, showing that neural activity was content-specific, and not merely an exhaust fume of oromotor behavior.

Relevant to learning, neural activity in many regions have been shown to couple with hippocampal activity bursts like SWRs, including associative cortices ([R. Gutierrez et al., 2006](#); [Jadhav et al.,](#)

[2016](#); [Peyrache et al., 2009a](#); [Wang & Ikemoto, 2016](#); [Wierzynski et al., 2009](#); [Wilber et al., 2017](#)), primary sensory cortices ([Ji & Wilson, 2007](#); [Rothschild et al., 2017](#); [Sirota et al., 2003](#)), ventral striatum ([Lansink et al., 2008](#)), ventral tegmental area ([Gomperts et al., 2015](#)), basolateral amygdala([Girardeau et al., 2017](#)), and thalamic nuclei([Lara-Vásquez et al., 2016](#); [Yang et al., 2019](#)). We speculate that hippocampal SWRs are part of the directed teaching signal employed during learning, acting to engrave association between coincident neural activity orchestrated by active sensing.

Integrating prior evidence of widespread taste-reward network lick-locking with present results depicting the lick-phase alignment on hippocampal activity, we speculate that SWR-related synaptic change is differentially induced during, and because of, active sensing. We suggest that licking-induced synchrony of SWR's represents a convergence of the sensory association system with memory retrieval and formation system. And perhaps that after learning, the role of rhythmic behavior, through minimization of variability during ongoing sensorimotor state transition, supplants the SWR function of long-range information transmission across the gustatory-association network.

3.5 References

- Accolla, R., & Carleton, A. (2008). Internal body state influences topographical plasticity of sensory representations in the. In *rat gustatory cortex. Proc Natl Acad Sci U S A* 105 (pp. 4010-4015).
- Axmacher, N., Elger, C. E., & Fell, J. (2008). Ripples in the medial temporal lobe are relevant for human memory consolidation. *Brain*, 131(Pt 7), 1806-1817. doi:10.1093/brain/awn103
- Barkley-Levenson, A. M., & Crabbe, J. C. (2012). Ethanol drinking microstructure of a high drinking in the dark selected mouse line. *Alcohol Clin Exp Res*, 36, 1330-1339.
- Barkley-Levenson, A. M., & Crabbe, J. C. (2015). Distinct ethanol drinking microstructures in two replicate lines of mice selected for drinking to intoxication. *Genes Brain Behav*, 14, 398-410.
- Bergman, U., Ostergren, A., Gustafson, A. L., & Brittebo, B. (2002). Differential effects of olfactory toxicants on olfactory regeneration. *Archives of toxicology*, 76, 104-112.
- Eastwood, E. C., Barkley-Levenson, A. M., & Phillips, T. J. (2014). Methamphetamine drinking microstructure in mice bred to drink high or low amounts of methamphetamine. *Behav Brain Res*, 272, 111-120.
- Eliades, S. J., & Wang, X. (2008). Neural substrates of vocalization feedback monitoring in primate auditory cortex. *Nature*, 453(7198), 1102-1106. doi:10.1038/nature06910
- Fuentes, R. A., Aguilar, M. I., Aylwin, M. L., & Maldonado, P. E. (2008). Neuronal activity of mitral-tufted cells in awake rats during passive and active odorant stimulation. *J Neurophysiol*, 100, 422-430.
- Galistu, A., Modde, C., Pireddu, M. C., Franconi, F., Serra, G., & D'Aquila, P. S. (2011). Clozapine increases reward evaluation but not overall ingestive behaviour in rats licking for sucrose. *Psychopharmacology (Berl)*, 216, 411-420.
- Girardeau, G., Inema, I., & Buzsaki, G. (2017). Reactivations of emotional memory in the hippocampus-amygdala system during sleep. *Nat Neurosci*, 20(11), 1634-1642. doi:10.1038/nn.4637

- Gomperts, S. N., Kloosterman, F., & Wilson, M. A. (2015). VTA neurons coordinate with the hippocampal reactivation of spatial experience. *Elife*, *4*. doi:10.7554/eLife.05360
- Grosmaître, X., Santarelli, L. C., Tan, J., Luo, M., & Ma, M. (2007). Dual functions of mammalian olfactory sensory neurons as odor detectors and mechanical sensors. *Nature neuroscience*, *10*, 348-354.
- Gutierrez, R., Carmena, J. M., Nicolelis, M. A., & Simon, S. A. (2006). Orbitofrontal ensemble activity monitors licking and distinguishes among natural rewards. *J Neurophysiol*, *95*(119–133).
- Gutierrez, R., Simon, S. A., & Nicolelis, M. A. (2010). Licking-induced synchrony in the taste–reward circuit improves cue discrimination during learning. *Journal of Neuroscience*, *30*(1), 287-303.
- Halpern, B. P. (1983). Tasting and smelling as active, exploratory sensory processes. *Am J Otolaryngol*, *4*(246–249).
- Hartfield, A. W., Moore, N. A., & Clifton, P. G. (2003). Effects of clozapine, olanzapine and haloperidol on the microstructure of ingestive behaviour in the rat. *Psychopharmacology (Berl)*, *167*, 115-122.
- Jadhav, S. P., Rothschild, G., Roumis, D. K., & Frank, L. M. (2016). Coordinated Excitation and Inhibition of Prefrontal Ensembles during Awake Hippocampal Sharp-Wave Ripple Events. *Neuron*, *90*(1), 113-127. doi:10.1016/j.neuron.2016.02.010
- Ji, D., & Wilson, M. A. (2007). Coordinated memory replay in the visual cortex and hippocampus during sleep. *Nat Neurosci*, *10*(1), 100-107.
- Karalis, N., & Sirota, A. (2018). Breathing coordinates limbic network dynamics underlying memory consolidation. *bioRxiv*, 392530. doi:10.1101/392530
- Katz, D. B., Simon, S. A., & Nicolelis, M. A. (2001). Dynamic and multimodal responses of gustatory cortical neurons in awake rats. *J Neurosci*, *21*, 4478-4489.
- Kepecs, A., Uchida, N., & Mainen, Z. F. (2006). The sniff as a unit of olfactory processing. *Chem Senses*, *31*, 167-179.

- Kleinfeld, D., Ahissar, E., & Diamond, M. E. (2006). Active sensation: insights from the rodent vibrissa sensorimotor system. *Curr Opin Neurobiol*, *16*(4), 435-444. doi:10.1016/j.conb.2006.06.009
- Krupa, D. J., Wiest, M. C., Shuler, M. G., Laubach, M., & Nicolelis, M. A. (2004). Layer-specific somatosensory cortical activation during active tactile discrimination. *Science*, *304*(5679), 1989-1992. doi:10.1126/science.1093318
- Lansink, C. S., Goltstein, P. M., Lankelma, J. V., Joosten, R. N., McNaughton, B. L., & Pennartz, C. M. (2008). Preferential reactivation of motivationally relevant information in the ventral striatum. *J. Neurosci.*, *28*(25), 6372-6382. doi:10.1523/JNEUROSCI.1054-08.2008
- Lara-Vásquez, A., Espinosa, N., Durán, E., Stockle, M., & Fuentealba, P. (2016). Midline thalamic neurons are differentially engaged during hippocampus network oscillations. *Sci Rep*, *6*(1), 1-16.
- Liu, Y., McAfee, S. S., & Heck, D. H. (2017). Hippocampal sharp-wave ripples in awake mice are entrained by respiration. *Sci Rep*, *7*(1), 8950. doi:10.1038/s41598-017-09511-8
- Livneh, Y., Sugden, A. U., Madara, J. C., Essner, R. A., Flores, V. I., Sugden, L. A., . . . Andermann, M. L. (2020). Estimation of Current and Future Physiological States in Insular Cortex. *Neuron*.
- Mayrhofer, J. M., El-Boustani, S., Foustoukos, G., Auffret, M., Tamura, K., & Petersen, C. C. H. (2019). Distinct Contributions of Whisker Sensory Cortex and Tongue-Jaw Motor Cortex in a Goal-Directed Sensorimotor Transformation. *Neuron*. doi:10.1016/j.neuron.2019.07.008
- Mogenson, G. J., Jones, D. L., & Yim, C. Y. (1980). From motivation to action: functional interface between the limbic system and the motor system. *Prog Neurobiol*, *14*(69–97).
- Moore, J. D. (2013). Hierarchy of orofacial rhythms revealed through whisking and breathing. *Nature*, *497*, 205-210.
- Nicolelis, M. A., Baccala, L. A., Lin, R., & Chapin, J. K. (1995). Sensorimotor encoding by synchronous neural ensemble activity at multiple levels of the somatosensory system. *Science*, *268*(5215), 1353-1358.

- Nishijo, H., Uwano, T., Tamura, R., & Ono, T. (1998). Gustatory and multimodal neuronal responses in the amygdala during licking and discrimination of sensory stimuli in awake rats. *J Neurophysiol*, *79*, 21-36.
- Pecina, S., & Berridge, K. C. (2005). Hedonic hot spot in nucleus accumbens shell: where do μ -opioids cause increased hedonic impact of sweetness? *J Neurosci*, *25*, 11777-11786.
- Peyrache, A., Khamassi, M., Benchenane, K., Wiener, S. I., & Battaglia, F. P. (2009a). Replay of rule-learning related neural patterns in the prefrontal cortex during sleep. *Nat. Neurosci.*, *12*(7), 919-926.
- Poulet, J. F., & Petersen, C. C. (2008). Internal brain state regulates membrane potential synchrony in barrel cortex of behaving mice. *Nature*, *454*(7206), 881-885. doi:10.1038/nature07150
- Robinson, S. L., & McCool, B. A. (2015). Microstructural analysis of rat ethanol and water drinking patterns using a modified operant self-administration model. *Physiol Behav*, *149*, 119-130.
- Rolls, E. T. (2007). Sensory processing in the brain related to the control. In *of food intake. Proc Nutr Soc* *66* (Vol. 96).
- Rothschild, G., Eban, E., & Frank, L. M. (2017). A cortical-hippocampal-cortical loop of information processing during memory consolidation. *Nat Neurosci*, *20*(2), 251-259. doi:10.1038/nn.4457
- Roumis, D. K., & Frank, L. M. (2015). Hippocampal sharp-wave ripples in waking and sleeping states. *Curr Opin Neurobiol*, *35*, 6-12. doi:10.1016/j.conb.2015.05.001
- Schaefer, A. T., Angelo, K., Spors, H., & Margrie, T. W. (2006). Neuronal oscillations enhance stimulus discrimination by ensuring action potential precision. *PLoS Biol*, *4*, 163.
- Schepisi, C., Cianci, S., Bedse, G., Fu, J., Gaetani, S., & Nencini, P. (2014). Differences in the structure of drinking, cart expression and dopamine turnover between polydipsic and non polydipsic rats in the quinpirole model of psychotic polydipsia. *Psychopharmacology (Berl)*, *231*(19), 3889-3897.

- Schoenbaum, G., Chiba, A. A., & Gallagher, M. (1998). Orbitofrontal cortex and basolateral amygdala encode expected outcomes during learning. *Nat Neurosci*, *1*(2), 155-159.
- Sirota, A., Csicsvari, J., Buhl, D., & Buzsaki, G. (2003). Communication between neocortex and hippocampus during sleep in rodents. *Proc Natl Acad Sci USA*, *100*(4), 2065--2069.
- Tort, A. B., Brankačk, J., & Draguhn, A. (2018). Respirationentrained brain rhythms are global but often overlooked. *Trends in Neurosciences*, *41*, 186-197.
- Tremblay, L., & Schultz, W. (1999). Relative reward preference in primate orbitofrontal cortex. *Nature*, *398*(6729), 704-708.
- Wang, D. V., & Ikemoto, S. (2016). Coordinated Interaction between Hippocampal Sharp-Wave Ripples and Anterior Cingulate Unit Activity. *J Neurosci*, *36*(41), 10663-10672.
doi:10.1523/JNEUROSCI.1042-16.2016
- Welzl, H., & Bureš, J. (1977). Lick-synchronized breathing in rats. *Physiology & behavior*, *18*(4), 751-753.
- Wierzynski, C. M., Lubenov, E. V., Gu, M., & Siapas, A. G. (2009). State-dependent spike-timing relationships between hippocampal and prefrontal circuits during sleep. *Neuron*, *61*(4), 587-596.
- Wilber, A. A., Skelin, I., Wu, W., & McNaughton, B. L. (2017). Laminar Organization of Encoding and Memory Reactivation in the Parietal Cortex. *Neuron*, *95*(6), 1406-1419 e1405.
doi:10.1016/j.neuron.2017.08.033
- Wilkins, E. E., & Bernstein, I. L. (2006). Conditioning method determines patterns of c-fos expression following novel taste-illness pairing. *Behav Brain Res*, *169*, 93-97.
- Yamamoto, T., Matsuo, R., Kiyomitsu, Y., & Kitamura, R. (1988). Sensory inputs from the oral region to the cerebral cortex in behaving rats: an analysis of unit responses in cortical somatosensory and taste areas during ingestive behavior. *J Neurophysiol*, *60*, 1303-1321.

Yang, M., Logothetis, N. K., & Eschenko, O. (2019). Occurrence of hippocampal ripples is associated with activity suppression in the mediodorsal thalamic nucleus. *Journal of Neuroscience*, 39(3), 434-444.

Zelano, C. (2016). Nasal respiration entrains human limbic oscillations and modulates cognitive function. *Journal of Neuroscience*, 36, 12448-12467.

Zhang, H., Bethel, C. S., Smittkamp, S. E., & Stanford, J. A. (2008). Age-related changes in orolingual motor function in F344 vs F344/BN rats. *Physiol Behav*, 93(3), 461-466.

Appendix : Hippocampal Sharp-Wave Ripples in Waking and Sleeping States

Authors: Roumis, D. K., & Frank, L. M.

Published: 2015. *Curr Opin Neurobiol*, 35, 6-12. doi:10.1016/j.conb.2015.05.001

Abstract

Waking and sleeping states are privileged periods for distinct mnemonic processes. In waking behavior, rapid retrieval of previous experience aids memory-guided decision making. In sleep, a gradual series of reactivated associations supports consolidation of episodes into memory networks. Synchronized bursts of hippocampal place cells during events called sharp-wave ripples communicate associated neural patterns across distributed circuits in both waking and sleeping states. Differences between sleep and awake sharp-wave ripples, and in particular the accuracy of recapitulated experience, highlight their state-dependent roles in memory processes.

Introduction

The ebb and flow of waking and sleeping states imposes structure and periodicity on all mammalian life. In addition to the state of awareness, neural states that accompany waking and sleeping differ drastically in several dimensions, including the level of neuromodulators, widespread synchronization, and responsiveness to input from external stimuli ([Diekelmann & Born, 2010a](#)). These features dissociate the neural context of waking and sleeping states and manifest in distinct memory processing ([Barnes & Wilson, 2014](#); [Diekelmann, Buchel, Born, & Rasch, 2011](#); [A. Rolls et al., 2013](#)). While awake, rapidly retrieved memories influence prediction, deliberation, and evaluation. Often, a decision must be made following only a short period of deliberation, suggesting a need for rapid and precise memory retrieval. In sleep, fresh memories are gradually strengthened, transformed, and integrated into the ensemble of amassed knowledge in the process of system-level consolidation ([Dumay & Gareth Gaskell, 2012](#); [Inostroza & Born, 2013](#)). Here, the need for rapidity and precision may be relaxed, and indeed a high fidelity representation may not be optimal for building more generalized representations.

Memory reactivation, serving both retrieval and consolidation, entails repetition of previously experienced episodic associations. Reactivation is commonly detected in the context of patterns of activity in spatially selective cells in subregions of the hippocampus ([Carr et al., 2011](#)). The hippocampus is essential for all aspects of spatial memory, including encoding, consolidation, and retrieval ([O'Keefe & Nadel, 1978](#); [Riedel et al., 1999](#)). Hippocampal pyramidal neurons that are active during a given experience are often referred to as 'place cells' because a large fraction of them fire in a location-dependent manner - preferring certain 'place fields' as animals explore space. Plasticity mechanisms associate cells with neighboring place fields, enhancing neighbor coactivity following their activation during exploration ([O'Neill et al., 2008](#)). During a pause in active exploration or while asleep, bursts (100-200 ms) of place cell activity occur

within distinct high-frequency (150-250 Hz) fluctuations in the hippocampal local field potential, called sharp-wave ripples (SWRs; **Fig. A.1 [A]**; ([Buzsaki, 1986](#))). Sequences of simultaneously recorded place cells, whose collective place field assemblies reflect trajectories through space, are often reactivated in a time-compressed cascade during hippocampal SWRs (**Fig. A.1[A-B]**). The timescale of SWRs aligns with the optimal window for inducing synaptic plasticity, and therefore could influence the encoding of memory traces in synaptic weights ([Buzsaki, 1989](#); [Marr, 1971](#)).

SWRs have garnered significant attention as a common phenomenon for broadcasting mnemonic messages, in both waking and sleeping states ([Carr et al., 2011](#); [O'Neill, Pleydell-Bouverie, Dupret, & Csicsvari, 2010](#)). However, the processing demands of waking and sleep are distinct, and differences in sleep and awake SWR replay events may support these distinct functions. Here we review recent developments addressing this issue and discuss the hypotheses that SWR replay during the waking state serves to mediate awake memory retrieval ([Carr et al., 2011](#)) and update navigational planning with respect to current perceptual input, whereas SWR replay during sleep is fundamentally geared to gradually consolidate a memory trace into a broader framework of existing memories.

The Role of Awake SWR Replay

The vicarious representations of spatial paths extending beyond an animal's current position could be an efficient component for deliberating and evaluating possible routes to reach a goal ([Carr et al., 2011](#); [Johnson, 2007](#); [Pfeiffer & Foster, 2013](#); [Yu & Frank, 2015](#)). In a causal test of a role for awake SWR events, Jadhav et al. ([Jadhav, 2012](#)) found that waking SWR activity was necessary for navigational memory-guided decision making in rats. The authors employed a spatial alternation task with a 'W' shaped maze on which the animals were rewarded at each arm's end for navigating in the following order: outbound-left, inbound-center, outbound-right,

inbound-center, and so on (**Fig. A.1 [C]**). Brief pulses of electrical stimulation, delivered immediately upon awake SWR onset, selectively disrupted SWRs and lead to a highly significant impairment in performance of the outbound alternation rule, which depends on integrating immediate past experience with the task rule. Parallel results came from a study in which awake SWR detection during learning triggered a bright light which led to an impairment in trace eyeblink conditioning in rabbits, likely because the light disrupted neocortical activity associated with SWRs ([Nokia, Mikkonen, Penttonen, & Wikgren, 2012](#)).

Subsequent studies have begun to identify a relationship between the content of SWRs and behavior ([Dupret, O'Neill, Pleydell-Bouverie, & Csicsvari, 2010](#); [Singer, Carr, Karlsson, & Frank, 2013](#)). Using the 'W' maze spatial alternation task (**Fig. A.1 [C]**), Singer and colleagues ([Singer et al., 2013](#)) found a greater degree of coordination in the pairwise firing of place cells in the waking state during SWRs that preceded a correct outbound decision, compared to an incorrect decision, on a trial-by-trial basis. This suggests that failure to reactivate the appropriate assembly representing possible future paths may lead to errors in navigational decision making. Interestingly, they did not find a consistent bias for the reactivated trajectory representation to reflect the subsequent navigational choice of the animal. This latter finding is in line with recent arguments positioning hippocampal replay as primarily communicating possible trajectory options for downstream circuits to evaluate ([Johnson, 2007](#); [Wikenheiser & Redish, 2015](#); [Yu & Frank, 2015](#)). In contrast, another study, employing an 'open field' foraging task, did detect a bias for the content of awake replay events to represent space in the general direction of the subsequent behavior – although there were still many replay events sweeping toward alternate locations. The relative hippocampal involvement in prediction, deliberation, and evaluation is likely influenced by task, learning stage, and environment.

Finally, we note that awake replay occurs in both the forward direction, consistent with the animal's experience, as well as in the reverse direction, with the relative prevalence and control of these sequences likely reflecting different processes ([Csicsvari, 2007](#); [Davidson, 2009](#); [Diba, 2007](#); [Foster, 2006](#); [Gupta, 2010](#); [Wikenheiser & Redish, 2013](#)). For instance, reverse replay in the waking state commonly occurs when the animal has arrived at a goal location, potentially supporting on-line reinforcement learning ([Carr et al., 2011](#); [Davidson, 2009](#); [Diba, 2007](#); [Foster, 2006](#)). Forward replay in the waking state is more prevalent in anticipation of a trajectory, when deliberation of future paths and spatial working memory is critical ([Carr et al., 2011](#); [Diba, 2007](#)). The task-location specificity of forward and reverse awake replay suggests an actively controlled retrieval system related to ongoing behavior.

The Role of Sleep SWR Replay

In contrast to the role of memory retrieval for active planning, replay in sleep is a component of system consolidation, which is thought to involve a quantitative and qualitative transformation of representations, stabilizing, decontextualizing, and integrating associations into distributed hippocampal-cortical circuits according to the statistical structure of experienced episodes ([Frankland & Bontempi, 2005](#); [Inostroza & Born, 2013](#); [Lesburquerque et al., 2011](#); [McClelland, McNaughton, & O'Reilly, 1995](#); [Tse et al., 2011](#); [Winocur, Moscovitch, & Bontempi, 2010](#)).

Consistently, evidence indicates that sleep promotes mnemonic flexibility in inference tasks that are enriched by the inductive capacity to link remote fragments of episodic representations ([Coutanche, Gianessi, Chanales, Willison, & Thompson-Schill, 2013](#); [Durrant, Taylor, Cairney, & Lewis, 2011](#); [Ellenbogen, Hu, Payne, Titone, & Walker, 2007](#); [Tse et al., 2007](#); [Verleger, Rose, Wagner, Yordanova, & Kolev, 2013](#); [Wagner, Gais, Haider, Verleger, & Born, 2004](#)).

Memory stabilization and integration in sleep is thought to require reactivation of awake neural patterns, serving to direct synaptic modifications across hippocampal-neocortical networks

([Buzsaki, 1996](#); [Diekelmann & Born, 2010b](#); [McClelland et al., 1995](#); [Sutherland & McNaughton, 2000](#)). Hippocampal SWR replay and cortical reactivation primarily occurs during periods of slow-wave sleep (SWS) ([Ji & Wilson, 2007](#); [Peyrache et al., 2009a](#); [Wierzynski et al., 2009](#)). Evidence of a direct link between SWR-related replay in sleep and memory processes has been provided by a number of studies employing a spatial memory task ([de Lavilleon, Lacroix, Rondi-Reig, & Benchenane, 2015](#); [Dupret et al., 2010](#); [Girardeau, 2009](#); [Nakashiba, Buhl, McHugh, & Tonegawa, 2009](#)). If SWR replay assemblies percolate mnemonic messages across distributed circuits, a significant swath of the brain's activity should be temporally aligned with SWRs. Such evidence was recently reported in a study showing globally coordinated response patterns from monkey whole-brain functional magnetic resonance imaging at the time of hippocampal SWRs while the subjects alternated between sleeping and waking ([Logothetis, 2012](#)).

Additionally, SWR sequences in the sleeping state have been shown to favor the forward direction, maintaining the overall temporal structure of the animals' actual experience ([Kudrimoti, Barnes, & McNaughton, 1999](#); [Lee, 2002](#); [Nadasdy, Hirase, Czurko, Csicsvari, & Buzsaki, 1999](#); [Skaggs & McNaughton, 1996](#); [Wikenheiser & Redish, 2013](#)). In order to infer future events based on previous exposure to a particular instance, preserving the appropriate overall temporal order of episodic fragments may be a crucial feature in the face of decontextualization processes. Fittingly, sleep has been shown to selectively strengthen the forwardly learned associations of word or picture sequences during post-sleep waking retrieval ([Drosopoulos, Windau, Wagner, & Born, 2007](#); [Griessenberger et al., 2012](#)).

The Fidelity of Replay

A critical feature of awake SWRs is the fidelity of recapitulated experience, as accurate portraits of established trajectories are crucial for rapid memory-driven behavioral performance. Karlsson and Frank ([Karlsson, 2009](#)) recorded from principal neurons in hippocampal areas CA1 and

CA3 while rats performed the W-track alternation task (**Fig. A.1 [C]**) flanked by 'sleep-box' sessions. Strikingly, their analyses reveal that awake SWRs contained overall higher fidelity recapitulations of previously experienced traversals through place fields than SWRs recorded in sleep-like states (**Fig. A.2**).

Furthermore, recent evidence couples fidelity of replay with an additional level of coherence across hippocampal areas within and across hemispheres. Carr et al. ([Carr et al., 2012](#)) found that increased synchrony of 'slow' gamma oscillations (20-50 Hz) across CA3 and CA1 regions was predictive of replay fidelity in the waking state, suggestive of an internal clocking mechanism to coordinate sequential reactivation across the hippocampal network. In contrast, spiking during SWRs in sleep-like states was less modulated by slow gamma with no clear relationship between gamma synchrony and the fidelity of replay.

Beyond the coupling of hippocampal slow gamma oscillations in the waking state, sleep SWRs are temporally coordinated with oscillating 'Up' and 'Down' states of widespread activation and suppression of cortical activity, respectively ([Diekelmann & Born, 2010b](#); [Peyrache, Battaglia, & Destexhe, 2011](#); [Phillips et al., 2012](#); [Siapas & Wilson, 1998](#); [Sirota et al., 2003](#)). These oscillations are linked to the retention and integration of new learning into existing knowledge structures ([Marshall, Helgadottir, M€olle, & Born, 2006](#); [Tamminen, Lambon Ralph, & Lewis, 2013](#)). Synchronized interaction between the hippocampus and prefrontal cortex (PFC), one of the major sites of hippocampal output, is critical for system consolidation ([Preston & Eichenbaum, 2013](#)), occurs largely coincident with SWRs during SWS ([Benchenane, 2010](#); [Wierzynski et al., 2009](#)), and specifically includes reactivated cortical patterns of awake experiences ([Euston, Tatsuno, & McNaughton, 2007](#); [Peyrache et al., 2009a](#)). Recording in the PFC, Peyrache et al. ([Peyrache et al., 2009a](#)) found that the temporal dynamics of reactivation strength, or the accuracy with which population activity in sleep corresponded to waking

experience, peaked immediately preceding a transition from Down to Up states, which is temporally aligned with a prevalence of SWRs ([Battaglia, Sutherland, & McNaughton, 2004](#); [Peyrache et al., 2009a](#)). Given that hippocampal SWRs can occur during both Up and Down states ([Battaglia et al., 2004](#); [Isomura, 2006](#)), this raises an intriguing possibility that the phase of certain cortical oscillations are linked with the relative fidelity of replay transmission in the hippocampal-cortical axis. For instance, widespread activation or suppression of cortical activity, respectively associated with Up or Down states, could either influence the cortical receptivity to input patterns from the hippocampus, or variably infuse noise into an ensuing hippocampal replay assembly. Additionally, recent work demonstrated that the medial entorhinal cortex, part of the main input and output structure between the hippocampus and neocortex, contains persistent Up states that can span multiple quantized neocortical Up/Down states and influence the activity levels of the hippocampus, potentially gating the form of transmission across the hippocampal-neocortical axis around the time of SWR replay ([Hahn, McFarland, Berberich, Sakmann, & Mehta, 2012](#)).

A Role for 'Noisy' Replay

It seems intuitive that high fidelity replay would promote effective decision-making during waking, but how could lower fidelity, 'noisy' recapitulations of experience serve the mnemonic functions of sleep? Importantly, sleep allows the brain to consolidate sparse data and store the statistics of the environment into a semantic memory system, allowing for inductive predictions about the future. Inspired by computational linguistics, Battaglia and Pennartz ([Battaglia & Pennartz, 2011](#)) advance an illustrative approach of how memory networks, trained by 'noisy' episodic replay, could become schematized and generative, constructing episodes based on past experience and allowing for prediction in the face of uncertainty. In this way, the comparatively more random organization of sleep SWR replay may be a feature rather than a

bug, serving to fulfill the transformational consolidation process and supporting the capacity to build rich schemata from only a limited number of episodic associations.

Recent evidence is consistent with the idea that adding 'noise' to the relevant neural circuits during sleep consolidation alters the specificity, but not necessarily the strength, of learning.

Barnes and Wilson ([Barnes & Wilson, 2014](#)) conditioned electrical stimulation in the rat olfactory bulb (OB) with a foot-shock, an established paradigm for subsequently eliciting the rat's natural fear response to the conditioned olfactomimetic stimulation. However, in intervening SWS bouts between conditioning and testing, they stimulated a naive (not previously conditioned) OB site, likely eliciting a very different activity pattern than that which was conditioned. Surprisingly, this manipulation, which consisted of introducing novel and seemingly irrelevant activity during the period of memory consolidation, did not decrease the strength of the trained memory association. Instead, this manipulation led to memory generalization, as observed by fear response to previously unpaired odors. Together, these studies suggest that the level of interference during periods of consolidation can influence the precision of memory expression, and furthermore predicts that over-rigidity in sleep replay, relative to awake, may impair the ability to flexibly use past memory in a novel context.

Conclusion

SWRs may be a common neurophysiological phenomenon for broadcasting mnemonic messages in both waking and sleeping states, the importance of which is underscored by recently documented impairments of sequence reactivation in models of schizophrenia ([Phillips et al., 2012](#); [Suh, Foster, Davoudi, Wilson, & Tonegawa, 2013](#)), dementia ([Cheng & Ji, 2013](#); [Witton et al., 2014](#)), and aging ([Gerrard, Burke, McNaughton, & Barnes, 2008](#)). Causal manipulations lend strong support to this role for SWRs, but elucidation of their intrinsic features is necessary to understand the mechanisms supporting distinctive memory processes. Awake

SWRs proceed both forward and reverse, entail a more veridical account of experience, and can predict future behavior. Sleep SWRs mainly unfold in the forward direction, are generally more noisy depictions of past actions, and are tightly coordinated with cortical oscillations. Together, the evidence supports the hypotheses that SWR replay during the waking state serves to support retrieval and planning, whereas SWR replay during sleep is geared to gradually consolidate a memory trace into a broader framework of existing memories.

Figures

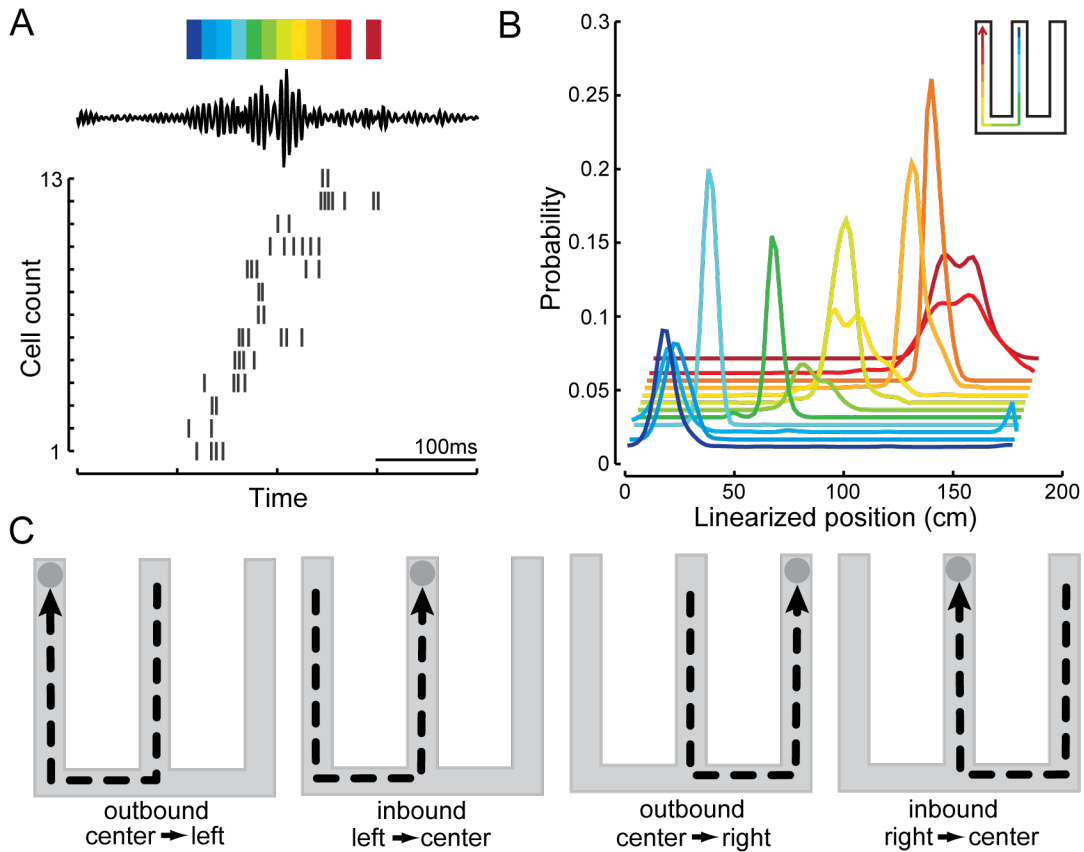


Figure A.1 | SWR Reactivation of Spatial Sequences

(A) Sequential spiking from place cells during an awake SWR. Bottom, rows depicting the spiking of individual place cells in CA1 or CA3 activated during the SWR. Top, the filtered local field potential signal (150–250 Hz) from one tetrode with the color bar showing the separation of each 15-ms decoded bin. (B) Probability distributions of decoded locations for the spiking in each associated colored bin in a. Inset shows a cartoon of the replayed trajectory. (C) Schematic depicting the rewarded behavioral sequence of the ‘W’ track task. Adapted with permission from ref. ([Carr, Karlsson, & Frank, 2012](#)).

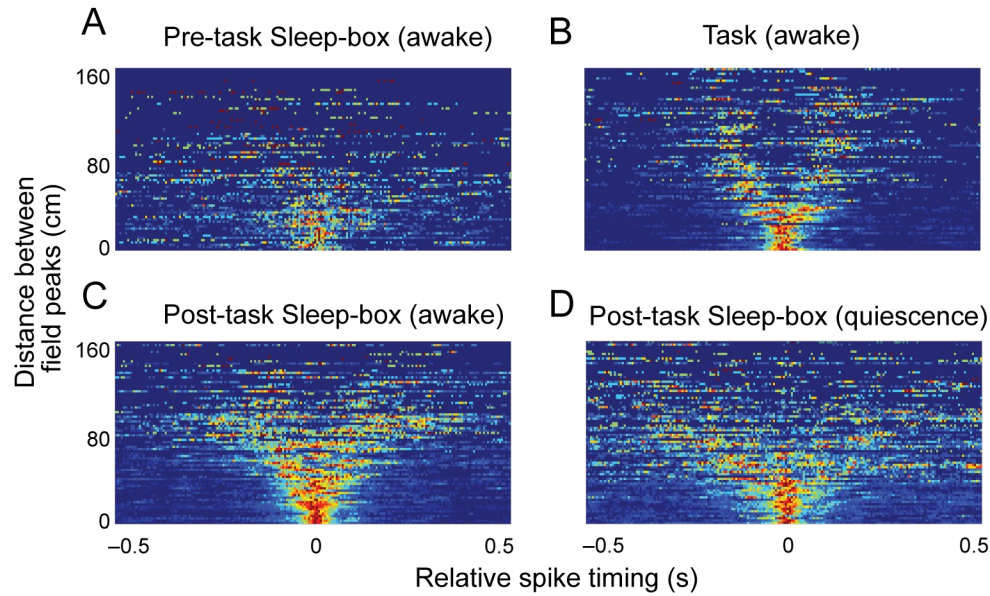


Figure A.2 | The quality of SWR replay of remote task trajectories is higher during awake than quiescent periods

Karlsson and Frank ([Karlsson, 2009](#)) calculated the extent to which the linear spatial distance between the peaks of place field pairs belonging to a remote ‘W’ environment predicted the relative timing of their SWR spikes for all place cell pairs. The normalized cross-correlation histograms of all the pairs is shown in order of their place field distances, with the signature of the degree to which the place-field distances are linked to their SWR timing being represented by the emergent ‘V’ shape centered at 0-ms latency. **(A)** Awake SWRs during the first sleep-box session of the day, prior to the daily exposure of the ‘W’ track task ($R^2 = 0.025$). **(B)** Awake SWR replay during task performance shows the most robust remote replay ($R^2 = 0.1736$; see ref. [55] for further explanation of behavioral paradigm). **(C)** SWRs during waking bouts in the post-task sleep-box, after exposure to the ‘W’ maze task ($R^2 = 0.1164$). **(D)** SWRs during quiescent, sleep-like states in the sleep-box, after exposure to the ‘W’ maze task ($R^2 = 0.0693$). R^2 values were computed by taking the correlation of the distance between place field peaks and the absolute value of the relative spike timing measure. Adapted with permission from ref. ([Karlsson, 2009](#)).

References

- Barnes, D. C., & Wilson, D. A. (2014). Slow-wave sleep-imposed replay modulates both strength and precision of memory. *J Neurosci*, *34*(15), 5134-5142. doi:10.1523/JNEUROSCI.5274-13.2014
- Battaglia, F. P., & Pennartz, C. M. (2011). The construction of semantic memory: grammar-based representations learned from relational episodic information. *Front Comput Neurosci*, *5*, 36. doi:10.3389/fncom.2011.00036
- Battaglia, F. P., Sutherland, G. R., & McNaughton, B. L. (2004). Hippocampal sharp wave bursts coincide with neocortical "up-state" transitions. *Learn Mem*, *11*(6), 697-704. doi:10.1101/lm.73504
- Benchenane, K. (2010). Coherent Theta Oscillations and Reorganization of Spike Timing in the Hippocampal- Prefrontal Network upon Learning. *Neuron*, *66*, 921-936.
- Buzsaki, G. (1986). Hippocampal Sharp Waves - Their Origin and Significance. *Brain Res*, *398*(2), 242-252. doi:Doi 10.1016/0006-8993(86)91483-6
- Buzsaki, G. (1989). Two-stage model of memory trace formation: a role for "noisy" brain states. *Neuroscience*, *31*(3), 551-570.
- Buzsaki, G. (1996). The hippocampo-neocortical dialogue. *Cereb.Cortex.*, *6*(2), 81-92.
- Carr, M. F., Jadhav, S. P., & Frank, L. M. (2011). Hippocampal replay in the awake state: a potential substrate for memory consolidation and retrieval. *Nat Neurosci*, *14*(2), 147-153.
- Carr, M. F., Karlsson, M. P., & Frank, L. M. (2012). Transient slow gamma synchrony underlies hippocampal memory replay. *Neuron*, *75*(4), 700-713.
- Cheng, J., & Ji, D. (2013). Rigid firing sequences undermine spatial memory codes in a neurodegenerative mouse model. *Elife*, *2*, e00647. doi:10.7554/eLife.00647
- Coutanche, M. N., Gianessi, C. A., Chanales, A. J., Willison, K. W., & Thompson-Schill, S. L. (2013). The role of sleep in forming a memory representation of a two-dimensional space. *Hippocampus*, *23*(12), 1189-1197. doi:10.1002/hipo.22157

- Csicsvari, J. (2007). Place-selective firing contributes to the reverse-order reactivation of CA1 pyramidal cells during sharp waves in open-field exploration. *Eur. J. Neurosci.*, *26*, 704-716.
doi:10.1111/j.1460-9568.2007.05684.x
- Davidson, T. J. (2009). Hippocampal replay of extended experience. *Neuron*, *63*, 497-507.
doi:10.1016/j.neuron.2009.07.027
- de Lavilleon, G., Lacroix, M. M., Rondi-Reig, L., & Benchenane, K. (2015). Explicit memory creation during sleep demonstrates a causal role of place cells in navigation. *Nat Neurosci*, *18*(4), 493-495.
doi:10.1038/nn.3970
- Diba, K. (2007). Forward and reverse hippocampal place-cell sequences during ripples. *Nat. Neurosci.*, *10*, 1241-1242. doi:10.1038/nn1961
- Diekelmann, S., & Born, J. (2010a). The memory function of sleep. *Nat Rev Neurosci*, *11*(2), 114-126.
doi:10.1038/nrn2762
- Diekelmann, S., & Born, J. (2010b). Slow-wave sleep takes the leading role in memory reorganization. *Nat.Rev.Neurosci.*, *11*(3), 218.
- Diekelmann, S., Buchel, C., Born, J., & Rasch, B. (2011). Labile or stable: opposing consequences for memory when reactivated during waking and sleep. *Nature neuroscience*, *14*(3), 381-386.
doi:10.1038/nn.2744
- Drosopoulos, S., Windau, E., Wagner, U., & Born, J. (2007). Sleep enforces the temporal order in memory. *PLoS One*, *2*(4), e376. doi:10.1371/journal.pone.0000376
- Dumay, N., & Gareth Gaskell, M. (2012). Overnight lexical consolidation revealed by speech segmentation. *Cognition*, *123*(1), 119-132. doi:10.1016/j.cognition.2011.12.009
- Dupret, D., O'Neill, J., Pleydell-Bouverie, B., & Csicsvari, J. (2010). The reorganization and reactivation of hippocampal maps predict spatial memory performance. *Nat Neurosci*, *13*, 995-1002.

- Durrant, S. J., Taylor, C., Cairney, S., & Lewis, P. A. (2011). Sleep-dependent consolidation of statistical learning. *Neuropsychologia*, *49*(5), 1322-1331. doi:10.1016/j.neuropsychologia.2011.02.015
- Ellenbogen, J. M., Hu, P. T., Payne, J. D., Titone, D., & Walker, M. P. (2007). Human relational memory requires time and sleep. *Proc Natl Acad Sci U S A*, *104*(18), 7723-7728.
doi:10.1073/pnas.0700094104
- Euston, D. R., Tatsuno, M., & McNaughton, B. L. (2007). Fast-forward playback of recent memory sequences in prefrontal cortex during sleep. *Science*, *318*(5853), 1147-1150.
- Foster, D. J. (2006). Reverse replay of behavioural sequences in hippocampal place cells during the awake state. *Nature*, *440*, 680-683. doi:10.1038/nature04587
- Frankland, P. W., & Bontempi, B. (2005). The organization of recent and remote memories. *Nat Rev Neurosci*, *6*(2), 119-130. doi:10.1038/nrn1607
- Gerrard, J. L., Burke, S. N., McNaughton, B. L., & Barnes, C. A. (2008). Sequence reactivation in the hippocampus is impaired in aged rats. *J Neurosci*, *28*(31), 7883-7890.
doi:10.1523/JNEUROSCI.1265-08.2008
- Girardeau, G. (2009). Selective suppression of hippocampal ripples impairs spatial memory. *Nature neuroscience*, *12*, 1222-1223.
- Griessenberger, H., Hoedlmoser, K., Heib, D. P., Lechinger, J., Klimesch, W., & Schabus, M. (2012). Consolidation of temporal order in episodic memories. *Biol Psychol*, *91*(1), 150-155.
doi:10.1016/j.biopsycho.2012.05.012
- Gupta, A. S. (2010). Hippocampal replay is not a simple function of experience. *Neuron*, *65*, 695-705.
doi:10.1016/j.neuron.2010.01.034
- Hahn, T. T., McFarland, J. M., Berberich, S., Sakmann, B., & Mehta, M. R. (2012). Spontaneous persistent activity in entorhinal cortex modulates cortico-hippocampal interaction in vivo. *Nat Neurosci*, *15*(11), 1531-1538. doi:10.1038/nn.3236

- Inostroza, M., & Born, J. (2013). Sleep for Preserving and Transforming Episodic Memory. <http://dx.doi.org/10.1146/annurev-neuro-062012-170429>. doi:10.1146/annurev-neuro-062012-170429
- Isomura, Y. (2006). Integration and Segregation of Activity in Entorhinal-Hippocampal Subregions by Neocortical Slow Oscillations. *Neuron*, *52*, 871-882.
- Jadhav, S. P. (2012). Awake hippocampal sharp-wave ripples support spatial memory. *Science*, *336*, 1454-1458. doi:10.1126/science.1217230
- Ji, D., & Wilson, M. A. (2007). Coordinated memory replay in the visual cortex and hippocampus during sleep. *Nat Neurosci*, *10*(1), 100-107.
- Johnson, A. (2007). Neural ensembles in CA3 transiently encode paths forward of the animal at a decision point. *J. Neurosci.*, *27*, 12176-12189. doi:10.1523/JNEUROSCI.3761-07.2007
- Karlsson, M. P. (2009). Awake replay of remote experiences in the hippocampus. *Nat. Neurosci.*, *12*, 913-918. doi:10.1038/nn.2344
- Kudrimoti, H. S., Barnes, C. A., & McNaughton, B. L. (1999). Reactivation of hippocampal cell assemblies: effects of behavioral state, experience, and EEG dynamics. *J Neurosci*, *19*(10), 4090-4101.
- Lee, A. K. (2002). Memory of sequential experience in the hippocampus during slow wave sleep. *Neuron*, *36*, 1183-1194. doi:10.1016/S0896-6273(02)01096-6
- Lesburgueres, E., Gobbo, O. L., Alaux-Cantin, S., Hambucken, A., Trifilieff, P., & Bontempi, B. (2011). Early tagging of cortical networks is required for the formation of enduring associative memory. *Science*, *331*(6019), 924-928. doi:10.1126/science.1196164
- Logothetis, N. K. (2012). Hippocampal-cortical interaction during periods of subcortical silence. *Nature*, *491*, 547-553.
- Marr, D. (1971). Simple memory: a theory for archicortex. *Philos Trans R Soc Lond B Biol Sci*, *262*(841), 23-81.

- Marshall, L., Helgadottir, H., M€olle, M., & Born, J. (2006). Boosting slow oscillations during sleep potentiates memory. *Nature*, *444*, 610-613.
- McClelland, J. L., McNaughton, B. L., & O'Reilly, R. C. (1995). Why there are complementary learning systems in the hippocampus and neocortex: Insights from the successes and failures of connectionist models of learning and memory. *Psychol Rev*, *102*, 419-457.
- Nadasdy, Z., Hirase, H., Czurko, A., Csicsvari, J., & Buzsaki, G. (1999). Replay and time compression of recurring spike sequences in the hippocampus. *J Neurosci*, *19*(21), 9497-9507.
- Nakashiba, T., Buhl, D. L., McHugh, T. J., & Tonegawa, S. (2009). Hippocampal CA3 output is crucial for ripple-associated reactivation and consolidation of memory. *Neuron*, *62*(6), 781-787.
doi:10.1016/j.neuron.2009.05.013
- Nokia, M. S., Mikkonen, J. E., Penttonen, M., & Wikgren, J. (2012). Disrupting neural activity related to awake-state sharp wave-ripple complexes prevents hippocampal learning. *Front Behav Neurosci*, *6*, 84. doi:10.3389/fnbeh.2012.00084
- O'Keefe, J., & Nadel, L. (1978). *The hippocampus as a cognitive map*. London: Oxford University Press.
- O'Neill, J., Pleydell-Bouverie, B., Dupret, D., & Csicsvari, J. (2010). Play it again: reactivation of waking experience and memory. *Trends in Neurosciences*, *33*(5), 220-229.
doi:10.1016/j.tins.2010.01.006
- O'Neill, J., Senior, T. J., Allen, K., Huxter, J. R., & Csicsvari, J. (2008). Reactivation of experience-dependent cell assembly patterns in the hippocampus. *Nat Neurosci*, *11*(2), 209-215.
doi:10.1038/nn2037
- Peyrache, A., Battaglia, F. P., & Destexhe, A. (2011). Inhibition recruitment in prefrontal cortex during sleep spindles and gating of hippocampal inputs. *Proc Natl Acad Sci U S A*, *108*(41), 17207-17212. doi:1103612108 [pii]
10.1073/pnas.1103612108

- Peyrache, A., Khamassi, M., Benchenane, K., Wiener, S. I., & Battaglia, F. P. (2009a). Replay of rule-learning related neural patterns in the prefrontal cortex during sleep. *Nat. Neurosci.*, *12*(7), 919-926.
- Pfeiffer, B. E., & Foster, D. J. (2013). Hippocampal place-cell sequences depict future paths to remembered goals. *Nature*, *497*(7447), 74-79.
- Phillips, K. G., Bartsch, U., McCarthy, A. P., Edgar, D. M., Tricklebank, M. D., Wafford, K. A., & Jones, M. W. (2012). Decoupling of sleep-dependent cortical and hippocampal interactions in a neurodevelopmental model of schizophrenia. *Neuron*, *76*(3), 526-533.
doi:10.1016/j.neuron.2012.09.016
- Preston, A. R., & Eichenbaum, H. (2013). Interplay of hippocampus and prefrontal cortex in memory. *Curr Biol*, *23*(17), R764-773. doi:10.1016/j.cub.2013.05.041
- Riedel, G., Micheau, J., Lam, A. G., Roloff, E. L., Martin, S. J., Bridge, H., . . . Morris, R. G. (1999). Reversible neural inactivation reveals hippocampal participation in several memory processes. *Nat. Neurosci.*, *2*(10), 898-905.
- Rolls, A., Makam, M., Kroeger, D., Colas, D., de Lecea, L., & Craig Heller, H. (2013). Sleep to forget: interference of fear memories during sleep. *Mol. Psychiatry*, *18*(11), 1166-1170.
doi:10.1038/mp.2013.121
- Siapas, A. G., & Wilson, M. A. (1998). Coordinated interactions between hippocampal ripples and cortical spindles during slow-wave sleep. *Neuron*, *21*(5), 1123-1128.
- Singer, A. C., Carr, M. F., Karlsson, M. P., & Frank, L. M. (2013). Hippocampal SWR Activity Predicts Correct Decisions during the Initial Learning of an Alternation Task. *Neuron*, *77*(6), 1163-1173.
doi:10.1016/j.neuron.2013.01.027
- Sirota, A., Csicsvari, J., Buhl, D., & Buzsaki, G. (2003). Communication between neocortex and hippocampus during sleep in rodents. *Proc Natl Acad Sci USA*, *100*(4), 2065--2069.

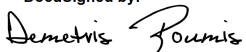
- Skaggs, W. E., & McNaughton, B. L. (1996). Replay of neuronal firing sequences in rat hippocampus during sleep following spatial experience. *Science*, *271*(5257), 1870-1873.
- Suh, J., Foster, D. J., Davoudi, H., Wilson, M. A., & Tonegawa, S. (2013). Impaired hippocampal ripple-associated replay in a mouse model of schizophrenia. *Neuron*, *80*(2), 484-493.
doi:10.1016/j.neuron.2013.09.014
- Sutherland, G. R., & McNaughton, B. (2000). Memory trace reactivation in hippocampal and neocortical neuronal ensembles. *Curr.Opin.Neurobiol.*, *10*(2), 180-186.
- Tamminen, J., Lambon Ralph, M. A., & Lewis, P. A. (2013). The role of sleep spindles and slow-wave activity in integrating new information in semantic memory. *J Neurosci*, *33*(39), 15376-15381.
doi:10.1523/jneurosci.5093-12.2013
- Tse, D., Langston, R. F., Kakeyama, M., Bethus, I., Spooner, P. A., Wood, E. R., . . . Morris, R. G. (2007). Schemas and memory consolidation. *Science.*, *316*(5821), 76-82.
- Tse, D., Takeuchi, T., Kakeyama, M., Kajii, Y., Okuno, H., Tohyama, C., . . . Morris, R. G. (2011). Schema-dependent gene activation and memory encoding in neocortex. *Science*, *333*(6044), 891-895.
doi:science.1205274 [pii]
10.1126/science.1205274
- Verleger, R., Rose, M., Wagner, U., Yordanova, J., & Kolev, V. (2013). Insights into sleep's role for insight: Studies with the number reduction task. *Adv Cogn Psychol*, *9*(4), 160-172. doi:10.2478/v10053-008-0143-8
- Wagner, U., Gais, S., Haider, H., Verleger, R., & Born, J. (2004). Sleep inspires insight. *Nature.*, *427*(6972), 352-355.
- Wierzynski, C. M., Lubenov, E. V., Gu, M., & Siapas, A. G. (2009). State-dependent spike-timing relationships between hippocampal and prefrontal circuits during sleep. *Neuron*, *61*(4), 587-596.

- Wikenheiser, A. M., & Redish, A. D. (2013). The balance of forward and backward hippocampal sequences shifts across behavioral states. *Hippocampus*, *23*(1), 22-29. doi:10.1002/hipo.22049
- Wikenheiser, A. M., & Redish, A. D. (2015). Decoding the cognitive map: ensemble hippocampal sequences and decision making. *Current opinion in neurobiology*, *32*(32), 8–15. doi:10.1016/j.conb.2014.10.002
- Winocur, G., Moscovitch, M., & Bontempi, B. (2010). Memory formation and long-term retention in humans and animals: convergence towards a transformation account of hippocampal-neocortical interactions. *Neuropsychologia*, *48*(8), 2339-2356. doi:10.1016/j.neuropsychologia.2010.04.016
- Witton, J., Staniaszek, L. E., Bartsch, U., Randall, A. D., Jones, M. W., & Brown, J. T. (2014). Disrupted hippocampal sharp-wave ripple-associated spike dynamics in a transgenic mouse model of dementia. *J Physiol*. doi:10.1113/jphysiol.2014.282889
- Yu, J. Y., & Frank, L. M. (2015). Hippocampal-cortical interaction in decision making. *Neurobiol Learn Mem*, *117C*, 34-41. doi:10.1016/j.nlm.2014.02.002

Publishing Agreement

It is the policy of the University to encourage open access and broad distribution of all theses, dissertations, and manuscripts. The Graduate Division will facilitate the distribution of UCSF theses, dissertations, and manuscripts to the UCSF Library for open access and distribution. UCSF will make such theses, dissertations, and manuscripts accessible to the public and will take reasonable steps to preserve these works in perpetuity.

I hereby grant the non-exclusive, perpetual right to The Regents of the University of California to reproduce, publicly display, distribute, preserve, and publish copies of my thesis, dissertation, or manuscript in any form or media, now existing or later derived, including access online for teaching, research, and public service purposes.

DocuSigned by:

4594AE1F9DC945B... Author Signature

3/15/2020
Date